Title: Disease Bundling or Specimen Bundling? Cost- and Capacity-Efficient Strategies for Multi-disease Testing with Genetic Assays

Authors:

Douglas R. Bish: Professor, Department of Information Systems, Statistics, and Management Science, University of Alabama, Tuscaloosa, Alabama, 35487, United States, email: *drbish@ua.edu*

Ebru K. Bish: Professor, Department of Information Systems, Statistics, and Management Science, University of Alabama, Tuscaloosa, Alabama, 35487, United States, email: *ekbish@ua.edu*

Hussein El Hajj: Assistant Professor, Department of Information Systems and Analytics, Santa Clara University, Santa Clara, California, 95053, United States, email: *helhajj@scu.edu*

Disease Bundling or Specimen Bundling? Cost- and Capacity-Efficient Strategies for Multi-disease Testing with Genetic Assays

Douglas R. Bish[1], Ebru K. Bish[1]*, Hussein El Hajj[2]

1. Department of Information Systems, Statistics, and Management Science, University of Alabama, Tuscaloosa, AL 35487, United States

2. Department of Information Systems and Analytics, Santa Clara University, Santa Clara, CA 95053, United States

June 15, 2022; Revised: December 10, 2022; March 26, 2023; June 15, 2023

Abstract

Problem definition: Infectious disease screening can be expensive and capacity-constrained. We develop cost- and capacity-efficient testing designs for multi-disease screening, considering: **(1)** *multiplexing* (disease bundling), where one assay detects multiple diseases using the same specimen (e.g., nasal swabs, blood); and **(2)** *pooling* (specimen bundling), where one assay is used on specimens from multiple subjects, bundled in a testing pool. A testing design specifies an *assay portfolio* (mix of single-disease/multiplex assays) and a *testing method* (pooling/individual testing per assay).

Methodology/results: We develop novel models for the nonlinear, combinatorial multi-disease testing design problem: a deterministic model, and a distribution-free, robust variation, which both generate *Pareto* frontiers for cost- and capacity-efficient designs. We characterize structural properties of optimal designs, formulate the deterministic counterpart of the robust model, and conduct a case study of respiratory diseases (including COVID-19) with overlapping clinical presentation.

Managerial implications: Key drivers of optimal designs include the assay cost function, the tester's preference towards cost- versus capacity-efficiency, prevalence/co-infection rates, and, for the robust model, prevalence uncertainty. When an optimal design uses multiple assays, it does so in conjunction with pooling, and uses individual testing for at most one assay. While prevalence uncertainty can be a design hurdle, especially for emerging or seasonal diseases, the integration of multiplexing and pooling, and the ordered partition property of optimal designs (under certain co-infection structures), serve to make the design more structurally robust to uncertainty. The robust model further increases

*Corresponding Author: *ekbish@cba.ua.edu*

robustness, and is also practical as it needs only an uncertainty set around each disease prevalence. Our Pareto designs demonstrate the cost- versus capacity trade-off, and show that multiplexing-only or pooling-only designs need not be on the Pareto frontier. Our case study illustrates the benefits of optimally integrated designs over current practices, and indicates a low price of robustness.
Keywords: Testing design, public health screening, multiplex assay, pooled testing, assay portfolio, partition problem

1 Introduction and Motivation

Infectious disease screening improves health outcomes by identifying disease-positive subjects and their underlying pathogen. Pathogen detection is done through in-vitro laboratory testing on a specimen (e.g., nasal swab, blood) collected from the subject, and is especially important for diseases that manifest with overlapping symptoms, but require different treatment. Examples include: respiratory diseases; sexually-transmitted diseases; transfusion-transmittable diseases; gastrointestinal diseases; blood infections and sepsis. Consider respiratory diseases, a common cause of medical visits and hospitalizations [22, 80]; treatment may differ depending on the virus causing the disease, e.g., influenza, respiratory syncytial virus, COVID-19; or there may be no treatment at all, e.g., the common cold, but only testing can distinguish one pathogen from another [18]. Further, not knowing whether the pathogen is bacterial can result in antibiotic overuse [40, 70], contributing to the growing problem of antibiotic resistance [60]. We use the terms disease and pathogen interchangeably, and refer to a specific disease/pathogen by the most common name.

A widely used assay is the Polymerase Chain Reaction (PCR) assay, a highly sensitive and specific genetic assay that detects a pathogen's DNA (or RNA) [16, 38]. Upon collection, specimens are sent to a testing laboratory, where they are prepared, and a small sample of each specimen is placed in a PCR assay (i.e., a commercial testing kit that consists of a small vial with reagents), which, in turn, is placed in a PCR machine. PCR machines have capacities that range from 1 to several hundred assays per run (96 and 384 are common capacities, e.g., [51]). Each run typically requires 1-4 hours (depending on the machine) to complete; the run-time, along with the capacity, determines the machine's throughput. During a run, a unique section of the pathogen's DNA, if present, is amplified using reagents such as polymerase, DNA nucleotides, and pathogen-specific primers; and pathogen-specific probes emit a signal (e.g., a fluorescence) if the pathogen is detected in the specimen. Disease screening via PCR is expensive, and can be capacity-restricted. Screening is often performed in state public health, hospital, blood donation agency, or commercial laboratories, which can test hundreds, or more, specimens per week for multiple diseases. Thus, it is essential for screening efforts to be cost- and capacity-efficient. In this light, we study a novel testing design problem that utilizes two *bundling* strategies to make screening more cost- and capacity-efficient:

Multiplexing (Disease Bundling): One multiplex assay can detect multiple diseases using the same specimen, as opposed to single-disease (*singleton*) assays. Multiplex assays are available for many disease groups, including, for example, respiratory, sexually-transmitted, transfusion-transmittable, and gastrointestinal diseases, e.g., [10]. For instance, commercially available multiplex assays for respiratory diseases bundle two to 33 pathogens [9, 10, 24, 44, 52, 61, 76]; the Alabama Department of Public Health uses a 20-plex assay to screen for respiratory pathogens, including COVID-19 [8].

Pooling (Specimen Bundling): Under pooling, specimens from multiple subjects are bundled (i.e., pooled) and tested with one assay. Dorfman pooling [30] is the most common pooling method in practice, and is the method considered in this paper; we describe it here for a singleton assay: if the pooled test outcome is negative, then all subjects in the pool are declared negative for the disease; otherwise, each subject is re-tested individually via the same type of assay, and is classified as negative or positive based on their individual test outcome. Because only a small sample of the specimen is needed for each test, each specimen has sufficient material for multiple tests. Examples of pooling (mostly for singleton assays) range from transfusion-transmittable (e.g., West Nile virus, *B. microti*, Zika virus), to respiratory (e.g., influenza), to sexually-transmitted diseases, and many others, e.g., [2, 4, 12, 64, 78, 82, 84]. More recently, the CDC and the FDA have provided guidance for pooling for COVID-19 [17, 37].

Multiplex PCR assays are widely available, and pooling with PCR is commonly used, as PCR is conducive to both bundling strategies for the following reasons: (1) From a *cost perspective*, many of the reagents are not disease-specific (e.g., the polymerase and the DNA nucleotides), and the required amount of these reagents is fairly insensitive to the number of diseases in the assay. The disease-specific reagents (e.g., the primers and the probes) are relatively inexpensive compared to the other reagents. Thus multiplexing reduces the testing cost per disease over the corresponding singleton assays, leading to a concave cost structure in the number of diseases bundled. (2) From a *technology perspective*, due to amplification, PCR can detect minute quantities of the pathogen's genetic material, and thus is not very susceptible to dilution, preserving its high sensitivity with pooling, e.g., [66]. (3) From a *testing capacity* perspective, multiplexing leads to a more efficient use of the limited testing capacity, improving both the throughput and turn-around times. Pooling also reduces the number of tests required (hence the testing cost and the capacity used) for low prevalence diseases, e.g., [4].

When multiplexing and pooling are used separately for a given set of diseases (the disease selection problem, while of great interest, is beyond the scope of this paper), the cost- and capacity-efficiency objectives coincide, and the best nonintegrated design is straightforward: (i) for *multiplexing-only*, bundle all the diseases into one multiplex to take advantage of the concave nature of the assay cost in the number of diseases bundled; and (ii) for *pooling-only*, pool each singleton assay if the disease prevalence is below a threshold. When integrating multiplexing and pooling, however, the design problem becomes nonlinear and combinatorial, due to the interdependent decisions of an *assay portfolio* (the mix and composition of singleton and multiplex assays) and a *testing method* (individual testing or pooling for each assay). Integrated multiplexing and pooling is not commonly used, although practical examples exist. We illustrate this integrated testing design through the American Red Cross' use of a 3-plex assay for hepatitis B, C, and HIV in Dorfman pools of 16 [2]: A specimen of each blood donation is sent to a testing laboratory, where samples from 16 specimens (each from a different donor) are pooled and tested

with one 3-plex assay for hepatitis B, C, and HIV. If the pooled test is negative for all three diseases, then the 16 donations are declared negative for all three diseases. Otherwise (the pool tests positive for at least one of the three diseases), then each specimen (via another small sample) is individually re-tested using the same 3-plex assay. Donations are then classified as negative or positive for each disease based on their individual test outcome. There are no guidelines on when, and how, these strategies should be integrated. This knowledge gap partially explains why integrated strategies are uncommon. We narrow the knowledge gap with the following methodological contributions and managerial insights:

Methodological contributions: (1) Development of novel multi-disease testing design models for this nonlinear, partition-type combinatorial problem: a deterministic model, and a distribution-free, robust variation, which both generate Pareto frontiers for cost- and capacity-efficient designs; **(2)** Development of the deterministic counterpart of the robust model (Theorem A.1, Corollary A.1); **(3)** Characterization of structural properties of optimal testing designs as a function of key problem parameters (Theorems 1-4); and establishing the optimality of ordered partitions for certain co-infection structures (Theorem 5), leading to a polynomial-time algorithm (Corollary 1).

Managerial contributions and insights: (1) Key drivers of optimal designs include the assay cost function, the tester's preference towards cost- versus capacity- efficiency, prevalence/co-infection rates, and, for the robust model, prevalence uncertainty. Given a disease set, the most capacity-efficient design bundles all diseases into one multiplex, and uses pooling only if the combined disease prevalence is below a threshold (Theorem 2), but this is not necessarily the most cost-effective design (Theorem 3). Once a combination of cost- and capacity-efficiency is considered, the structure of an optimal design becomes complex (Theorems 1, 4). Now a portfolio of multiplex and/or singleton assays can be optimal as long as pooling is used; in this case, individual testing can be used by at most one assay. Further, as co-infection rates rise, multiplexing becomes more favorable (Lemma 1). These properties highlight the interdependence between multiplexing and pooling; **(2)** Designs that integrate multiplexing and pooling are more structurally robust to variations in prevalence estimates than pooling alone, because the pooling performance becomes a function of the assay prevalence (i.e., combined prevalences of the diseases in the assay), rather than the individual disease prevalences. Further, when ordered partitions are optimal (under certain co-infection structures, Theorem 5), the design becomes more robust; **(3)** The robustness of the design can be further improved through a robust model, which is also practical, as it only needs an uncertainty set around each disease prevalence. These last two insights are especially promising for seasonal (e.g., respiratory diseases) or emerging diseases (e.g., COVID-19), for which prevalence rates are difficult to estimate; **(4)** The Pareto designs allow the tester to choose a design based on their cost and capacity priorities; **(5)** Our case study of 18 respiratory diseases illustrates that Pareto designs improve upon cost- and/or capacity-efficiency of multiplexing-only or pooling-only benchmarks by as

much as 40%. This is despite the fact that the respiratory disease group is a relatively difficult group for testing design, compared to other disease groups, as some respiratory diseases exhibit high seasonality, high uncertainty (partially caused by COVID-19), and relatively high prevalences. Further, the price of robustness is low in our case study.

These findings underscore the value of integrated multiplexing and pooling optimization, a unique feature of our model. The use of cost- and capacity-efficient testing designs could further allow expanded screening, to cover larger populations or more diseases, providing a win-win situation for both public health practitioners (e.g., state public health laboratories, healthcare providers) and patients.

The remainder of the paper is organized as follows. §2 provides a review of the literature; and §3 provides the notation and formulates the testing design problem. §4 and §5 establish properties of optimal designs and derive strategy insight. §6 illustrates the value of optimal designs through a case study based on publicly available data; and §7 concludes with research limitations and future research suggestions. Mathematical proofs and some case study results are relegated to the Online Appendix.

2 Literature Review

This paper is related to research on pooling and multiplexing. While the literature in each area is large, the literature that studies their integration from a cost- and capacity-efficiency perspective is limited. Our review of each area is not exhaustive, but rather representative of the related research, so as to position our work in the literature.

We focus on PCR assays. Alternative testing technologies for pathogen identification include antigen assays and cell cultures [1, 28, 41, 42, 56, 68]. Antigen assays tend to be less expensive, but also less sensitive, than PCR; further, PCR can identify a larger set of pathogens, because not all viral pathogens have antigen assays. On the other hand, testing via cell cultures is highly accurate (like PCR), but more expensive, with much longer turn-around times. As a result, PCR (and more recently, multiplex PCR) assays are becoming increasingly common.

Regarding pooling, Dorfman pooling was first proposed in the 1940's for syphilis screening in military inductees [30]. Since then, many variations of Dorfman pooling, as well as other pooling schemes, have been extensively studied, mostly for a singleton assay, to minimize the per subject expected number of tests. While minimizing this metric improves both the cost- and capacity-efficiency for a singleton assay, these metrics diverge for multiple diseases, due to different costs of multiplex and singleton assays; this is one of the departures of our work from this literature. It is well-known that pooling reduces the expected number of tests over individual testing when disease prevalence is sufficiently low, and an optimal pool size has been analytically characterized for various pooling schemes, see [4, 11, 54, 67] for reviews of the pooling literature, and the references therein.

Considering PCR multiplexing, three main research streams are of interest: **(1)** Efficacy studies,

many of which establish that multiplexing generally preserves the high sensitivity and specificity of their counterpart singleton PCR assays, e.g., [52]. **(2)** Design studies, which focus on compatibility from a biochemical perspective, e.g., how to design primers for different pathogens that work well together (i.e., without interference) when combined in an assay, e.g., [73, 86]. **(3)** Cost-effectiveness studies: Large multiplex assays typically offer higher operational efficiencies over their multiple singleton assay counterparts (see §6). Thus, much of this literature explores the benefits of multiplexing in comparison to current practices, or in clinical settings, mainly in terms of whether the pathogen identification improves treatments and reduces costs. For example, a major benefit of pathogen identification is reduction in unnecessary antibiotic use [40, 70], along with reduction in inpatient stay [75]. Multiplexing has been shown to be cost-effective for many disease groups and populations, e.g., [5, 72, 81], including respiratory diseases, e.g., [77], see also the survey paper that compares assay performance, and clinical (e.g., mortality rate, inpatient stay, unnecessary antibiotic use) and economic (e.g., hospitalization cost) impacts of various FDA-approved multiplex assays for different disease groups (bloodstream, respiratory, gastrointestinal, central nervous system), based on previously published studies [74].

In summary, much of the multiplexing literature studies existing commercial assays, and does not delve into assay design; and the biochemical assay design research is complementary to the operational design problem that we study: we start, as an input, with a set of pathogens, with reagents compatible for multiplexing, and construct multiplex and/or singleton assays for these pathogens so as to maximize the operational efficiencies. Importantly, we show that, while it is feasible to bundle all these diseases in one multiplex, this strategy is not necessarily optimal when considering pooling.

The operations/biostatistics literature that studies the design of multiplexing and pooling strategies from an efficiency perspective is limited. [79] considers Dorfman pooling (with pool sizes determined via enumeration) for a 2-plex for *Chlamydia trachomatis* and *Neisseria gonorrhoeae* (both sexually-transmitted diseases); their numerical study shows that this 2-plex with pooling reduces the number of tests over both its counterpart with individual testing, and two singletons with pooling. [46, 47] extend this work to other pooling schemes for the two-disease setting. Thus, all three papers [46, 47, 79] consider only the two-disease setting, where the 2-plex is the only multiplex, and do not delve into assay portfolio design; they also consider the expected number of tests – which is equivalent to the testing cost only when the 2-plex and the singleton assays have the same cost, which is not necessarily true (see §1); and these papers do not provide analytical methods for optimal pool size determination. From a clinical perspective, [59] shares results from the implementation of a 2-plex PCR for *Chlamydia trachomatis* and *Neisseria gonorrhoeae*, both with Dorfman pooling (in pools of five), and with individual testing, at two clinics, and shows that pooling reduces the number of tests by 50.3% over individual testing, while achieving high efficacy. [83] studies the cost-effectiveness of three Dorfman pool sizes (6, 24, 48)

for the hepatitis B, C, and HIV 3-plex over current blood screening practices in different countries; as a practical example, this 3-plex is used by the American Red Cross in Dorfman pools of 16 [2]. From a methodological perspective, our problem is also related to the partition problem, discussed subsequently.

3 The Notation, Decision Problem, and Model

3.1 The Notation and the Decision Problem

We denote all vectors in boldface. $N = \{1, 2, \cdots, n\}$ denotes the disease set for testing, arranged in non-increasing order of disease prevalence. Co-infections are possible, and unless otherwise stated, we make no assumptions on the co-infection structure, that is, each pair of diseases in set N can be positively or negatively correlated, or independent.

We study both deterministic and robust versions of the multi-disease testing design problem for genetic assays, considering multiplexing and Dorfman pooling (hereafter, "pooling") strategies. While the deterministic model is the first step in the study of this novel problem, the robust model, i.e., under prevalence uncertainty, provides a realistic extension, especially for emerging or seasonal diseases, which typically exhibit high uncertainty, e.g., [4, 31, 67]. The objective is to minimize a *convex combination* of the two key dimensions of testing design: the expected testing cost and capacity requirement (i.e., expected number of tests), or a robust version of it, with the relative weights dictated by parameter $\lambda \in [0, 1]$. The set of optimal designs ($\forall \lambda \in [0, 1]$) provides the *Pareto designs*, including the cost and test minimizing special cases (the latter is the primary objective studied in the pooling literature, §2).

A testing design corresponds to:

(i) An **assay portfolio**, represented by a *partition* of set N into mutually exclusive and exhaustive disease subsets, such that the diseases in each subset are bundled into one assay. Let $\boldsymbol{S} = (S^k)_{k=1,\cdots,q}$, for some $q = 1, 2, \cdots, n$, denote a partition of set N: $S^k \cap S^l = \emptyset$, $k, l = 1, \cdots, q : k \neq l$, $\cup_{k=1}^{q} S^k = N$, with $s^k = |S^k|$ denoting the size of assay S^k. Then, $s^k = 1$ corresponds to a *singleton*; and $s^k \geq 2$ corresponds to a *multiplex*, or an s^k*-plex*, for the diseases in S^k.

(ii) A **testing method** for each assay, i.e., pooling or individual testing, and if pooling, then the pool size, denoted by $t \in Z^+$. Let $\boldsymbol{t} = (t^k)_{k=1,\cdots,q}$ denote the pool size vector. Then, if $t^k = 1$, assay S^k is tested individually, and if $t^k \geq 2$, assay S^k is tested via pooling, with pool size t^k.

In general, we use the superscript k for assay index, the subscript i for disease index, and drop the indices when clear from context, e.g., we use set S when referring to an assay, and a vector of sets $\boldsymbol{S}$ when referring to a partition of set N, that is, to an assay portfolio.

Each assay produces a binary outcome for each disease that it tests, e.g., an s-plex produces an s-dimensional binary test outcome vector, with a positive/negative outcome indicating the presence/absence of the corresponding disease. We assume that all assays have perfect sensitivity and specificity (reasonable for genetic assays). In pooling, if the outcome vector for the pooled test is nega-

tive for all the diseases in the assay, then all subjects in the pool are declared negative for those diseases; otherwise (the pool tests positive for at least one disease in the assay), each subject is re-tested individually via the *same* type of assay, and is classified as negative or positive for each disease based on their individual test outcome vector. Assay sensitivity may reduce for large pools due to dilution. While dilution is not pronounced for genetic assays (due to the amplification of the genetic material from the specimens), we follow the common practice, and restrict pool sizes to a *pool size limit*, $\overline{M}$, e.g., [4, 66].

Assumption ($\boldsymbol{A}$)**.** *The assay cost function for an s-plex,* $c(s), s \in Z^+$*, is concave non-decreasing in* s*, with* $c(1) = \gamma\ (> 0)$*, and* $c(s) \leq \gamma \times s,\ s \in Z^+$*, that is, bounded from above by a linear function.*

A concave functional form is realistic for genetic assays, because many of their reagents are not disease-specific, and the disease-specific primers and probes are less expensive, and also similar to each other (mainly consisting of simple strands of DNA), hence have similar cost, see §1. We define the *composite cost function*, $\tilde{c}(s, \lambda) \equiv \lambda\ c(s) + 1 - \lambda,\ s \in Z^+, \lambda \in [0, 1]$.

We express all performance metrics per testing subject. Let $T(S, t)$ and $C(S, t)$ respectively denote the per subject expected number of tests ("expected tests") and the per subject expected testing cost for assay S and pool size t, where

$$C(S, t) = c(s) \times T(S, t). \tag{1}$$

Then, the per subject expected total testing cost ("total cost") for assay portfolio $\boldsymbol{S}$, pool size vector $\boldsymbol{t}$, and $\lambda \in [0, 1]$, denoted by $TC(\boldsymbol{S}, \boldsymbol{t}, \lambda)$, is a convex combination of the expected testing cost and tests:

$$TC(\boldsymbol{S}, \boldsymbol{t}, \lambda) = \lambda \sum_k C(S^k, t^k) + (1 - \lambda) \sum_k T(S^k, t^k) = \sum_k \tilde{c}(s^k, \lambda) \times T(S^k, t^k). \tag{2}$$

We use $T_D(S, t)$ to denote the the per subject expected tests under pooling with pool size $t \in Z^+, t \geq 2$.

Because co-infections are possible, each subject is either free of all diseases in set N, or infected by one, or more, diseases in this set. To represent all infection possibilities of a subject, let $N(l), l = 1, 2, \cdots, n$, denote the set of all l-tuples of set N, i.e., the set of all $\binom{n}{l}$ ordered elements (arranged in increasing disease index), each with l diseases. For example, $N(1) = N, N(2) = \{ij : i, j \in N, i < j\}, N(3) = \{ijr : i, j, r \in N, i < j < r\}$, and so on. Thus indices $0, i, ij, ijr, \cdots, 12...n$, respectively denote the cases of no-infection, infection i only, infections i and j only, infections i, j, and r only, and so on.

For the deterministic prevalence model (see §3.2 for extension to stochastic prevalences), the deterministic joint prevalence vector ("joint vector"), $\boldsymbol{p} = [p_0, (p_i)_{i \in N}, (p_{ij})_{ij \in N(2)}, (p_{ijr})_{ijr \in N(3)}, \cdots, p_{12...n}]$, denotes the probability that a random subject is in each of the 2^n infection categories, that is, with p_0 denoting the no-infection probability, $p_i, i \in N(1)$, denoting all mono-infection probabilities, and the other elements denoting all possible co-infection probabilities, where:

$$p_0 + \sum_{i \in N} p_i + \sum_{ij \in N(2)} p_{ij} + \sum_{ijr \in N(3)} p_{ijr} + ... + p_{12...n} = 1. \tag{3}$$

We define A_i^+ as the event that a random subject is infected with disease $i \in N$ (and may be co-infected

with some other diseases in set $N \setminus \{i\}$).

Definition 1. *For assay $S \subseteq N$, assay prevalence, $\pi(S)$, is the probability that a random subject is infected by at least one disease in assay S (and may be co-infected with other diseases in set $N \setminus S$):*

$$\pi(S) = Pr(\cup_{i\in S} A_i^+) = \sum_{i\in S} p_i \quad + \sum_{ij\in N(2):i\in S \text{ or } j\in S} p_{ij} + \sum_{ijr\in N(3):i\in S \text{ or } j\in S \text{ or } r\in S} p_{ijr} \; + \cdots + p_{12\ldots n}. \quad (4)$$

The marginal prevalence of each disease, denoted $\pi_i, i \in N$, and the overall prevalence of the disease set, denoted $\pi(N)$, are given by:

$$\pi_i = Pr(A_i^+) = p_i + \sum_{j:ij\in N(2)} p_{ij} + \sum_{j:ji\in N(2)} p_{ji} + \sum_{jr:ijr\in N(3)} p_{ijr} + \sum_{jr:jir\in N(3)} p_{jir} + \sum_{jr:jri\in N(3)} p_{jri} + \cdots + p_{12\cdots n}, i \in N, \quad (5)$$

$$\pi(N) = Pr(\cup_{i\in N} A_i^+) = \sum_{i\in N} p_i + \sum_{ij\in N(2)} p_{ij} + \sum_{ijr\in N(3)} p_{ijr} + \ldots + p_{12\ldots n} = 1 - p_0, \quad (6)$$

where $\boldsymbol{\pi} = (\pi_i)_{i\in N}$ is the marginal prevalence vector ("marginal vector").

The following relationship trivially holds due to co-infections and the disease indexing:

$$\pi_n \le \pi_{n-1} \le \cdots \le \pi_1 \le \pi(N) \le \sum_{i\in N} \pi_i. \quad (7)$$

Regarding the per subject expected tests function, for assay S, one test suffices for individual testing ($t = 1$), while for pooling with pool size $t \ge 2$, one pooled test is conducted for all t subjects, which, if positive for at least one disease in assay S, is followed by an individual re-test for each of the t subjects in the pool. Thus, we can write, e.g., [4]:

$$T(S,t) = \begin{cases} T_D(S,t) = \frac{1}{t} + 1 - \big(1 - \pi(S)\big)^t & , \quad \text{if } t \ge 2 \\ 1 & , \quad \text{if } t = 1 \end{cases}. \quad (8)$$

3.2 Model Formulations

To formulate the multi-disease testing design problem, we represent a partition (assay portfolio) $\boldsymbol{S}$ by the binary decision variable vector $\boldsymbol{x} = (\boldsymbol{x}^k)_{k=1,\cdots,n}$, where each $\boldsymbol{x}^k = (x_i^k)_{i\in N}$, $\forall k$, that is, $x_i^k = 1$ if disease i is included in assay S^k, and 0 otherwise, hence $\pi(S^k) = \pi(\boldsymbol{x}^k), \forall k$.

Deterministic Multi-Disease Testing Design Problem (TD):

$$\begin{aligned} \underset{\boldsymbol{x},\boldsymbol{t}}{\text{minimize}} \quad & TC(\boldsymbol{x},\boldsymbol{t},\lambda) = \lambda \sum_{k=1}^{n} C(\boldsymbol{x}^k, t^k) + (1-\lambda) \sum_{k=1}^{n} T(\boldsymbol{x}^k, t^k) \\ & = \sum_{k=1}^{n} \tilde{c}\Big(\sum_{i\in N} x_i^k, \lambda\Big) \times \min\left\{1, \; \frac{1}{t^k} + 1 - \Big(1 - \pi(\boldsymbol{x}^k)\Big)^{t^k}\right\} \quad (9) \\ \text{subject to} \quad & \sum_{k=1}^{n} x_i^k = 1, \qquad i \in N \quad (10) \\ & t^k \le \overline{M}, \qquad k = 1, \cdots, n \quad (11) \\ & t^k \ge 0, \text{ integer}, \qquad k = 1, \cdots, n, \quad (12) \\ & x_i^k \text{ binary}, \qquad i \in N, \; k = 1, \cdots, n. \quad (13) \end{aligned}$$

Objective (9) minimizes a convex combination of the expected testing cost and expected tests, with weights dictated by parameter $\lambda \in [0,1]$; thus by varying λ, the model generates the Pareto designs, including the cost and test minimizing special cases. (10) ensures that each disease is tested by an assay; (11) restricts pool sizes to the pool size limit; (12)-(13) are logical constraints on integer decision variables. There is symmetry among solutions, and symmetry breaking constraints can be added.

We now formulate the robust testing design problem under stochastic prevalences. To this end, we denote random variables in upper-case and their realizations in lower-case letters; use $\Omega(.)$ to denote an uncertainty set; and use ";" for probabilistic conditioning. Let $\boldsymbol{P}$ denote the continuous random joint vector, which implies, via Eq. (5), a continuous random marginal vector, $\boldsymbol{\Pi} = (\Pi_i)_{i \in N}$, with respective realizations $\boldsymbol{p}$ and $\boldsymbol{\pi}$ (converging to the notation for the deterministic problem).

Robust Multi-Disease Testing Design Problem (R-TD):

$$\begin{aligned} \underset{\boldsymbol{x},\ \boldsymbol{t}}{\text{minimize}} \quad & \max_{\boldsymbol{p} \in \Omega(\boldsymbol{P})} \left\{ \lambda \sum_{k=1}^{n} C(\boldsymbol{x}^k, t^k; \boldsymbol{p}) + (1-\lambda) \sum_{k=1}^{n} T(\boldsymbol{x}^k, t^k; \boldsymbol{p}) \right\} \\ \text{subject to} \quad & (10), (11), (12), (13). \end{aligned} \tag{14}$$

It is difficult to accurately estimate the distribution of the marginal vector $\boldsymbol{\Pi}$ (at disease prevalence level), let alone the distribution of the joint vector $\boldsymbol{P}$ (at mono- and co-infection probability level). Therefore, we adopt a *distribution-free* approach, and construct an interval type uncertainty set, e.g., [31, 32, 71], for each random marginal prevalence, $\Pi_i, i \in N$, which then implies an equivalent uncertainty set on $\boldsymbol{P}$ (Remark A.1). The former is relatively easier to construct, e.g., the lower and upper limits of a statistical confidence interval (CI) on each disease prevalence can be used, as we do in the case study. (While not practical due to the large number of co-infections, one can also start with an uncertainty set on $\boldsymbol{P}$.)

The joint optimization of multiplexing and pooling, the cost- and capacity-based objective, and the robust model are our main modeling departures from the literature (§1- §2), leading to a combinatorial problem: **TD**, with a non-linear objective and a partition-type decision, is NP-hard in general [21]; and **R-TD**, with a mini-max objective, is even harder.

In particular, our decision problem is related to partitioning a set of objects, each with a certain attribute, into a variable number of mutually exclusive and exhaustive groups, to minimize the total cost of the partition. Within this large body of this literature, the most relevant works include [21], which shows the optimality of an ordered partition for a cost function that is concave in the attribute sum, and [3], which extends this result to a cost function that depends on the group size, and the average or the maximum attribute in the group. The ordered partition property leads to an equivalent Shortest Path-based formulation that can be solved in polynomial time [3, 21], see §5.2. [3] also provides the necessary conditions for the optimality of a monotone partition, i.e., an ordered partition for which objects with smaller attributes are placed in smaller groups (this property does not hold in our setting).

The aforementioned results require the concavity of the total cost function in the attribute sum - in our setting, concavity in the sum of marginal disease prevalences, which does not necessarily hold for our problem (see Eqs. (2), (4), (8)), except for a special case with no co-infections (§5.2). Others extend the necessary conditions for the optimality of an ordered partition to different cost functions that do not apply to our setting, e.g., [48, 49]. A mini-max variation of the partition problem, when restricted to ordered partitions, is also studied, e.g., [62, 69], which, in our setting, corresponds to the ordered partition that minimizes the highest cost per assay for a given prevalence vector. This is in contrast with our robust model, which minimizes the highest total cost (i.e., for all assays) over all possible prevalence vectors in an uncertainty set. In the absence of the ordered partition property, the partition problem remains NP-hard; and the literature develops various heuristics and exact algorithms, such as genetic algorithms [57]; linear relaxation-based methods, e.g., dual heuristics, volume algorithms [7, 13, 23, 39]; implicit enumeration and search trees; simplex, hybrid primal, and symmetric subgradient cutting plane methods; and column generation [6]. We refer the interested reader to [6, 7, 39, 58] for detailed overviews.

4 Structural Properties of Optimal Testing Designs

§4.1 provides preliminaries on testing method optimization; and §4.2 integrates assay portfolio optimization into testing design in a multi-disease setting, a unique feature of our model.

4.1 Preliminaries: Optimal Testing Method - Pooling versus Individual Testing

Given an assay portfolio $\boldsymbol{S}$, the testing design problem reduces to testing method optimization (pooling versus individual testing for each assay), and the single-disease results from the literature extend in a straightforward manner to our multi-disease setting. We use t^*_D to denote the optimal Dorfman pool size, i.e., in the domain $t \in Z^+, t \geq 2$, and t^* to denote the (global) optimal pool size, i.e., in the domain $t \in Z^+, t \geq 1$ (including the individual testing option, $t = 1$). To make the dependence of $T(.)$ and $t^*(.)$ on $\pi(S)$ explicit, in places we use $\pi(S)$ as an argument, e.g., $t^*(\pi(S))$.

Property 1. *[From [4]]. Consider a single disease with prevalence π. The optimal integer pool size, $t^*_D(\pi)$, that minimizes the expected tests function under Dorfman pooling, i.e.,* $\text{minimize}_{t\in Z^+, t\geq 2}\, T_D(\pi, t)$, *is the solution to:*

$$t^*_D(\pi) = \min\Big\{argmin_{t\in\{\lfloor t_{frac}\rfloor, \lceil t_{frac}\rceil,\ \overline{M}\}}\{T_D(\pi,t)\}, \overline{M}\Big\}, \quad \textit{where}\ \ t_{frac} = \frac{2}{\ln(1-\pi)} W_0\Big(-\frac{1}{2}\big(-\ln(1-\pi)\big)^{1/2}\Big),$$

where $W_0(\cdot)$ denotes the principle branch (i.e., the largest solution) of the Lambert function $W(x)$, defined by, $x = W(x)e^{W(x)}, \forall x \in \mathbb{R}$ [25].

Property 1 trivially extends to a multiplex, and a threshold for when pooling is optimal over individual testing can be derived for integer pool sizes, extending a similar result for continuous pool sizes, e.g., [4].

Property 2. *For any assay $S \subseteq N$, the optimal integer pool size, $t^*_D(\pi(S))$, can be derived by Property 1, by letting $\pi = \pi(S)$. Further:*

1. $T(\pi(S), t_D^*(\pi(S))) \leq T(\pi(S), 1) = 1$ *only if* $\pi(S) \leq \underline{p} = 1 - \sqrt[3]{\frac{1}{3}} \approx 0.31$, *where the pooling threshold* $\underline{p}$ *is independent of assay size* s, *that is,*

$$t^*(\pi(S)) = \begin{cases} t_D^*(\pi(S)), & \text{if } \pi(S) \leq \underline{p} \\ 1, & \text{otherwise} \end{cases}, \quad \text{leading to:} \quad T(\pi(S), t^*(\pi(S))) = \begin{cases} T_D(\pi(S), t_D^*(\pi(S))), & \text{if } \pi(S) \leq \underline{p} \\ 1, & \text{otherwise} \end{cases}.$$

2. *[From [4, 34]]* $T(\pi(S), t^*(\pi(S))) = T_D(\pi(S), t_D^*(\pi(S)))$ *is strictly concave increasing in* $\pi(S) \in [0, \underline{p}]$, *and* $T(\pi(S), t^*(\pi(S))) = 1$ *for* $\pi(S) \in [\underline{p}, 1]$.

As Property 2 indicates, for a given assay portfolio $\boldsymbol{S}$, an optimal testing method can be determined *independently* for each assay in the portfolio. In the remainder of the paper, we consider that all assay portfolios use the optimal testing method delineated in Properties 1-2.

4.2 Optimal Testing Designs

For the robust formulation **R-TD**, under an interval type uncertainty set for the marginal vector (Remark A.1), we are able to characterize the worst-case solution (Theorem A.1 and Corollary A.1). These results lead to the deterministic counterpart for **R-TD**, which corresponds to a specific instance of **TD**, as outlined in the following remark.

Remark 1. *1. By Theorem A.1, the deterministic counterpart of* **R-TD** *has the following objective function:*

$$\underset{\boldsymbol{x},\, \boldsymbol{t}}{\text{minimize}} \ \sum_{k=1}^{n} \tilde{c}\left(\sum_{i \in N} x_i^k, \lambda \right) \ \times \min \left\{ 1, \ \frac{1}{t^k} + 1 - \left(1 - \min \left\{ 1, \sum_{i \in N} \overline{\pi}_i x_i^k \right\} \right)^{t^k} \right\}.$$

2. *Noting the equivalent objective of* **TD** *in (9), i.e., a function of assay prevalences only, the deterministic counterpart of* **R-TD** *reduces to an instance of* **TD** *with specific assay prevalences:* $\pi(S) = \min\left\{1, \sum_{i \in S} \overline{\pi}_i\right\}$, $\forall S \subseteq N$. *This equivalence indicates that the structural properties for* **TD** *(Theorems 1-4) continue to hold for* **R-TD**, *with* $\pi(S) = \min\left\{1, \sum_{i \in S} \overline{\pi}_i\right\}$, $\forall S \subseteq N$.

3. *Further, for the special case where* $\sum_{i \in N} \overline{\pi}_i \leq 1$, *the deterministic counterpart of* **R-TD** *also reduces to* **TD** *with the specific* $\boldsymbol{p}$ *provided in Corollary A.1.*

Importantly, the deterministic counterpart of **R-TD** requires only an upper limit on each disease prevalence, $\overline{\pi}_i, i \in N$. From an implementation point, this is highly desirable, and such upper limits can be derived, for example, from statistical CIs for disease prevalences. In general, the higher the uncertainty around a disease prevalence, the higher its upper limit will be, increasing the conservatism of the robust solution, which will be studied in §6.

Next, we characterize the optimal testing designs for **TD** and derive insight. (By Theorem A.1, Corollary A.1, and Remark 1, the structural results extend to **R-TD**.) To this end, we provide a series of definitions, which allow us to decompose the set of all possible testing designs into a number of

mutually exclusive and exhaustive design classes, based on how the disease set is partitioned and the testing methods used (see Table 1 for a mapping of all possible design classes and strategies).

Definition 2. *A partition* $\boldsymbol{S} = (S^k)_{k=1,\cdots,q}$ *is a q-partition, $q = 1, 2, \cdots, n$, if it consists of exactly q assays; and an ordered q-partition if* $S^1 = \{1, \cdots, s^1\}, S^2 = \{s^1 + 1, \cdots, s^1 + s^2\}, \cdots, S^q = \{\sum_{k=1}^{q-1} s^k + 1, \cdots, n\}$*, for some cardinality vector* $\boldsymbol{s} = (s^k)_{k=1,\cdots,q} : \sum_{k=1}^{q} s^k = n$*, that is, the disease set is partitioned into q assays following a non-increasing order of disease prevalences, $\pi_i, i \in N$.*

Definition 3. *Consider a q-partitioned testing design* $(\boldsymbol{S}, \boldsymbol{t})$*, for any* $q = 1, 2, \cdots, n$*:*

1. *If all q assays utilize pooling ($\boldsymbol{t} \geq \mathbf{2}$), it is a Dorfman design; if all q assays utilize individual testing ($\boldsymbol{t} = \mathbf{1}$), it is an individual-testing design; and if some assays utilize pooling while others utilize individual testing ($\boldsymbol{t} : \exists k, l = 1, \cdots, q : t^k = 1,\ t^l \geq 2$), it is a mixed-testing design.*
2. *If at least one multiplex is used ($q = 1, \cdots, n-1$), it is an mx design; otherwise ($q = n$), it is an all-singleton design.*

We use the notation $D^{(q)}$*,* $I^{(q)}$*,* $q = 1, \cdots, n$*, and* $M^{(q)}$*,* $q = 2, \cdots, n$*, to denote the optimal testing design when constrained to be within the q-partitioned Dorfman, individual-testing, and mixed-testing design classes, respectively. (The* $M^{(1)}$ *design, i.e., one assay with a mix of pooling and individual testing, is not possible.)*

Table 1: The mapping between all design classes and strategies

Strategy	**Design Class**
only multiplexing (no pooling)	$I^{(q)}, q = 1, \cdots, n-1$
only pooling (no multiplexing)	$D^{(n)}$ and $M^{(n)}$
both multiplexing and pooling	$D^{(q)}, q = 1, \cdots, n-1$, and $M^{(q)}, q = 2, \cdots, n-1$
no multiplexing and no pooling	$I^{(n)}$

Definition 4. *Design class A dominates design class B, denoted* $A \preceq B$*, if the total cost of an optimal* **TD** *solution within design class A is less than or equal to that for design class B.*

We are ready to provide structural properties of optimal designs; in case of multiple optimal designs, the results characterize one of the optimal designs. To put our results into perspective, we first provide the optimal design when multiplexing and pooling strategies are optimized separately (which will serve as benchmarks in the case study of §6), representing the current modeling of these strategies in the literature (§2); in this case the cost- and capacity-efficiency objectives coincide.

Remark 2. *1.* **Multiplexing-only** *($\boldsymbol{t} = \mathbf{1}$): For an individual-testing design, the optimal assay portfolio is to bundle all diseases into one multiplex (see Assumption ($\boldsymbol{A}$)), that is, an* $I^{(1)}$ *design.*

2. **Pooling-only** *($\boldsymbol{S} = (\{i\})_{i \in N}$): For an all-singleton design, the optimal testing method for each assay follows the pooling threshold policy (Properties 1-2), that is, each singleton is pooled only if the prevalence of its disease is sufficiently low, that is,* $I^{(n)}$*,* $D^{(n)}$*, or* $M^{(n)}$ *design.*

When multiplexing and pooling are optimized jointly (i.e., **TD**), a main departure from the literature, the interplay between multiplexing and pooling impacts the design, and the optimal designs in Remark 2 are no longer necessarily optimal.

Theorem 1. *Consider* **TD**. *We have that,* $I^{(1)} \preceq I^{(q)}, \forall q = 2, \cdots, n$; *and an optimal* $M^{(q)}, q = 2, \cdots, n-1$, *design is such that only one assay is individually tested, and* $q-1$ *assays are pooled,* $\forall \lambda \in [0, 1]$. *Further, an optimal design class can be characterized as follows for any* $\lambda \in [0, 1]$*:*

1. *If* $\pi(N) \leq \underline{p}$, *then* $D^{(q)}$, *i.e., Dorfman, for some* $q = 1, \cdots, n$.
2. *If* $\pi_1 \leq \underline{p} < \pi(N)$, *then either* $I^{(1)}$, *or* $D^{(q)}$ *for some* $q = 2, \cdots, n$, *or* $M^{(q)}$ *for some* $q = 2, \cdots, n-1$.
3. *If* $\pi_n \geq \underline{p}$, *then* $I^{(1)}$, *i.e., n-plex individual-testing.*
4. *Otherwise (if* $\exists i \in \{1, \cdots, n-1\} : \pi_{i+1} < \underline{p} < \pi_i$ *), then either* $I^{(1)}$, *or* $M^{(q)}$ *for some* $q = 2, \cdots, n-i+1$.

Thus, the joint optimization of multiplexing and pooling implies testing designs that span the entire spectrum of design classes (see Table 1), demonstrating the richness of this decision problem. Now the optimal design is driven by the tension between reducing the expected number of tests versus the expected testing cost, hence the capacity versus cost trade-off. In particular, the expected tests function under pooling (at optimal pool sizes) is concave increasing in assay prevalence (Property 2), favoring multiplexing. On the other hand, the expected testing cost is the product of the assay cost function and the expected tests function (Eq. (1)), both of which are concave increasing as more diseases are bundled (as this also increases the assay prevalence), but the expected testing cost is not necessarily concave in the number of bundled diseases. To see the intuition, observe that the bundling of more diseases raises the assay prevalence, thus increasing the (individual) re-test probability (Eq. (8)), but all individual re-tests use the same type of assay as the original assay, the cost of which is increasing in the number of bundled diseases. Further, if disease bundling raises an assay's prevalence too much, then the efficiency provided by pooling is lost. As a result of these tensions, an assay portfolio of multiplex and/or singleton assays can now be optimal *as long as at least one assay is pooled* (i.e., $M^{(q)}$ or $D^{(q)}$). Further, a portfolio of multiple assays and a combination of testing methods can be optimal (i.e., $M^{(q)}$) *as long as only one assay uses individual testing* (all other assays must be pooled). We also note that the integration of multiplexing and pooling makes the designs structurally robust to prevalence uncertainty, because it is the assay's prevalence (i.e., the combined prevalences of the diseases in the assay) that drives the pool size, and not the disaggregate disease prevalences; we quantitatively study this aspect in the case study.

Theorem 1 highlights the dependencies between multiplexing and pooling, hence the need for joint optimization. The next section discusses these dependencies in a more precise manner, through the main drivers of optimal designs.

5 Design Insight: Main Drivers of an Optimal Testing Design

We now analyze the two main drivers of optimal designs: the cost structure (§5.1), and the disease prevalence/co-infection structure (§5.2).

5.1 Impact of the Cost Structure

We first study how the optimal testing design changes as the assay cost function ($c(.)$) or the tester's preference towards cost versus test minimization (parameter λ) changes. Let $\tilde{C}$ denote the infinitely many composite cost functions, $\tilde{c}(s,\lambda) = \lambda\, c(s) + 1 - \lambda, \forall \lambda \in [0,1]$, for which the assay cost function $c(.)$ satisfies Assumption ($\boldsymbol{A}$). The marginal differences of any composite cost function in this set are non-negative and bounded by γ (i.e., $0 \leq \tilde{c}(s+1,\lambda) - \tilde{c}(s,\lambda) \leq \gamma, \forall s \in Z^+, \forall \tilde{c}(.) \in \tilde{C}$), and satisfy concavity. The following definition allows us to compare cost functions in terms of their marginal differences.

Definition 5. *We say that function $g(.)$ has higher differences relative to function $g'(.)$, written $g(.) \geq_{diff} g'(.)$, if $g(s+1) - g(s) \geq g'(s+1) - g'(s), \forall s \in Z^+$.*

Property 3. *Any composite cost function $\tilde{c}(s,\lambda) \in \tilde{C}$ attains lower differences as: (1) the assay cost function $c(s)$ attains lower differences, or (2) λ decreases.*

Remark 3. *Among the infinitely many composite cost functions $\tilde{c}(.) \in \tilde{C}$:*

1. *The smallest-difference function in set $\tilde{C}$ is attained when $\lambda = 0$ or $c(s) = \gamma, \forall s \in Z^+$ (i.e., constant assay cost). Under this function,* **TD** *objective reduces to test minimization.*
2. *The highest-difference function in set $\tilde{C}$ is attained when $\lambda = 1$ and $c(s) = \gamma \times s, \forall s \in Z^+$. Under this function,* **TD** *objective reduces to cost minimization with a linear assay cost.*

In what follows, we first characterize the optimal design for the smallest- and highest-difference composite cost functions described in Remark 3, which respectively reduce to test minimization and cost minimization (with linear assay cost), allowing us to gain insight into the tension between these objectives. The test minimization special case is also important for positioning our work within the pooling literature, which extensively studies this objective (§2).

Theorem 2. *Consider the smallest-difference composite cost function in set $\tilde{C}$, that is, with $\lambda = 0$ or $c(s) = \gamma, \forall s \in Z^+$. We have that, $I^{(1)} \preceq M^{(q)}$, $\forall q = 2, \cdots, n$.*
Further, if $\pi(N) \leq \underline{p}$, then $D^{(1)} \preceq D^{(2)} \preceq \cdots \preceq D^{(n)}$.
The optimal design class can be characterized as follows:

1. *If $\pi(N) \leq \underline{p}$, then $D^{(1)}$, i.e., n-plex Dorfman.*
2. *Otherwise (if $\pi(N) > \underline{p}$), then $I^{(1)}$, i.e., n-plex individual-testing.*

Theorem 3. *Consider the highest-difference composite cost function in set $\tilde{C}$, that is, with $\lambda = 1$ and $c(s) = \gamma \times s, \forall s \in Z^+$. We have:*

If $\pi(N) \leq \underline{p}$, *then* $D^{(n)} \preceq D^{(n-1)} \preceq \cdots \preceq D^{(1)}$.

If $\pi_1 \leq \underline{p} < \pi(N)$, *then* $D^{(n)} \preceq D^{(q)}, \forall q = 1, \cdots, n-1$.

The optimal design class can be characterized as follows:

1. *If* $\pi_1 \leq \underline{p}$, *then* $D^{(n)}$, *i.e., all-singleton Dorfman.*
2. *If* $\pi_n \geq \underline{p}$, *then any individual testing design,* $I^{(q)}$, *for any* $q = 1, \cdots, n$.
3. *Otherwise (if* $\exists i \in \{1, \cdots, n-1\} : \pi_{i+1} < \underline{p} < \pi_i$*), then any* $M^{(q)}$, *for* $q = n-i+1, \cdots, n$, *which uses any individual testing design for diseases in set* $\{1, 2, \cdots, i\}$, *and pooled testing and singleton assays for each disease in set* $\{i+1 \cdots, n\}$.

Table 2: Optimal design class based on the composite cost function $\tilde{c}(.)$ ($\underline{p} \approx 0.31$; mx: multiplex)

Composite Cost Function	Prevalence Range			
	$\pi(N) \leq \underline{p}$	$\pi(N) > \underline{p}$		
		$\pi_1 \leq \underline{p}$	$\pi_{i+1} < \underline{p} < \pi_i$, for some $i \in \{1, \cdots, n-1\}$	$\pi_n \geq \underline{p}$
general $\tilde{c}(.)$ (Theorem 1)	$D^{(q)}$ (some $q = 1, \cdots, n$) *pooling (mx possible)*	$I^{(1)}$ or $D^{(q)}$ (some $q = 2, \cdots, n$) or $M^{(q)}$ (some $q = 2, \cdots, n-1$) *mx and pooling both possible*	$I^{(1)}$ or $M^{(q)}$ (some $q = 2, \cdots, n-i+1$) *mx (pooling possible)*	$I^{(1)}$ *mx only*
Special Cases				
the smallest-difference $\tilde{c}(.)$ ($\lambda = 0$ or $c(s) = \gamma, \forall s \in Z^+$) (Theorem 2)	$D^{(1)}$ *both mx and pooling*	$I^{(1)}$ *mx only*		
the highest-difference $\tilde{c}(.)$ ($\lambda = 1$ and $c(s) = \gamma \times s, \forall s \in Z^+$) (Theorem 3)	$D^{(n)}$ *pooling only*	$D^{(n)}$ *pooling only*	Any $M^{(q)}$, $q = n-i+1, \cdots, n$ *pooling (mx possible)*	Any $I^{(q)}$, $q = 1, \cdots, n$ *no pooling (mx possible)*

Table 2 summarizes the properties of optimal designs for the general as well as the extreme cases (the smallest- and highest-difference composite cost functions), established in Theorems 1-3. We note that all prevalence regions in the table are relevant in practice, as it is possible for the overall prevalence to be below or above the 31% threshold, as our case study indicates (§6). In the extreme cases, multiplexing is in the form of "all-or-none," that is, either all diseases are bundled into one n-plex (1-mx design), or each disease is tested separately via its own singleton assay (all-singleton design). Such all-or-none type assay portfolios also represent the designs when multiplexing and pooling are considered separately (Remark 2). As Theorems 2-3 show, this all-or-none form is driven by the tension between reducing the expected tests versus the expected testing cost. In particular, when pooling is optimal (i.e., $\pi(N) \leq \underline{p}$), for the smallest-difference composite cost function (i.e., test minimization objective), one additional assay in a Dorfman design increases the expected tests (i.e., $D^{(1)} \preceq D^{(2)} \preceq \cdots \preceq D^{(n)}$); and for the highest-difference composite cost function (testing cost minimization objective), one fewer assay in a Dorfman design increases the expected testing cost (i.e., $D^{(n)} \preceq D^{(n-1)} \preceq \cdots \preceq D^{(1)}$). Table 2 also provides insight into the behaviour of robust designs as prevalence uncertainty rises: as the upper limit of the uncertainty set for a disease prevalence, used in the deterministic counterpart of **R-TD** (Remark 1), increases, the robust design moves from left to right through the columns of Table 2, and in the most conservative case, it defaults to the *multiplexing-only* ($I^{(1)}$) benchmark.

The tension between test versus cost minimization continues to drive an optimal design in general, when the composite cost function lies in between the two extremes. To demonstrate this tension clearly, we now focus on the case where the overall disease prevalence does not exceed the pooling threshold ($\pi(N) \leq \underline{p} \approx 0.31$), when pooling is always optimal. In this case, the optimal design is $D^{(1)}$ for the smallest-difference, and $D^{(n)}$ for the highest-difference, composite cost function (Theorems 2-3, Table 2). Then the next question is whether there exists a (unique) cost threshold function $\overline{\tilde{c}^q}(.)$, such that $D^{(q-1)} \preceq D^{(q)}$ ($D^{(q)} \preceq D^{(q-1)}$) for all composite cost functions with smaller (higher) differences than $\overline{\tilde{c}^q}(.)$. As Example 1 shows, such a threshold cost function does not exist.

Example 1. *Consider disease set $N = \{1, 2, 3, 4\}$, with equal marginal prevalences, and no co-infections: $\pi_i = 0.06, i \in N$, and $\pi(N) = \sum_{i \in N} \pi_i = 0.24 \leq \underline{p}$; and assay cost functions $c(.)$ and $c'(.)$ (with corresponding composite cost functions $\tilde{c}(.)$ and $\tilde{c}'(.)$) : $c(1) = 1, c(2) = 1.43, c(3) = 1.75, c(4) = 2.05$, and $c'(1) = c(1),\ c'(s) = c(s) - 0.10, s = 2, 3, 4$. By Definition 5, $c'(.) \leq_{diff} c(.)$, hence by Property 3, $\tilde{c}'(\lambda) \leq_{diff} \tilde{c}(\lambda), \forall \lambda \in [0, 1]$. However, at $\lambda = 1$, $D^{(1)}$ is optimal for $\tilde{c}(\lambda = 1)$, whereas $D^{(2)}$ is optimal for the smaller-difference function, $\tilde{c}'(\lambda = 1)$.*

As the following result indicates, such thresholds do exist on λ.

Theorem 4. *Consider that $\pi(N) \leq \underline{p}$. Then, $\exists\ \overline{\lambda}^{(q)} \leq 1, q = 1, \cdots, n-1$, such that the optimal design has the following structure:*

$$\textit{optimal design class: } \begin{cases} D^{(1)}, \text{ if } \lambda \in \left[0, \overline{\lambda}^{(1)}\right] \\ D^{(r)}, \text{ for some } r = 2, \cdots, q, \quad \text{if } \lambda \in \left(\max\left\{\overline{\lambda}^{(1)}, \overline{\lambda}^{(q-1)}\right\},\ \overline{\lambda}^{(q)}\right], \ q = 2, \cdots, n-1 \\ D^{(n)}, \text{ if } \lambda \in \left(\max\left\{\overline{\lambda}^{(1)}, \overline{\lambda}^{(n-1)}\right\}, 1\right] \end{cases}$$

Remark 4. *1. Among the optimality regions delineated in Theorem 4, only the $D^{(1)}$-optimal region, $[0, \overline{\lambda}^{(1)}]$, is guaranteed to be non-empty (see the $\lambda = 0$ case in Theorem 2). That is, it is possible that there is no $\lambda \in [0, 1]$ for which design $D^{(q)}, q = 2, \cdots, n$, is optimal. Further, the $D^{(n)}$-optimal region is guaranteed to be non-empty only for the linear assay cost function (see Theorem 3, Remark 3), otherwise it is possible for $\overline{\lambda}^{(n-1)} = 1$, hence $(\overline{\lambda}^{(n-1)}, 1]$ to be empty.*

2. When $\pi(N) \leq \underline{p}$, the optimal design is completely characterized for $n \leq 3$, and the number of assays is non-decreasing in λ:

For $n = 2$: $D^{(1)}, \forall \lambda \in [0, \overline{\lambda}^{(1)}]$; and $D^{(2)}, \forall \lambda \in (\overline{\lambda}^{(1)}, 1]$.

For $n = 3$: $D^{(1)}, \forall \lambda \in [0, \overline{\lambda}^{(1)}]$; $D^{(2)}, \forall \lambda \in (\overline{\lambda}^{(1)},\ \overline{\lambda}^{(2)}]$; and $D^{(3)}, \forall \lambda \in \left(\max\{\overline{\lambda}^{(1)}, \overline{\lambda}^{(2)}\}, 1\right]$.

In general, however, the number of assays in an optimal Dorfman design need not be monotone in λ, for example, for $n = 4$, the optimal design is $D^{(2)}$ or $D^{(3)}, \forall \lambda \in \left(\max\{\overline{\lambda}^{(1)}, \overline{\lambda}^{(2)}\},\ \overline{\lambda}^{(3)}\right]$, that is, it can potentially alternate between $D^{(2)}$ and $D^{(3)}$ in this region, although such a numerical example is lacking.

5.2 Impact of the Disease Prevalence and Co-infection Structure

In this section, we discuss how the disease prevalence/co-infection structure, relatedly the correlations among disease prevalences, impacts the optimal assay portfolio; and develop an exact, efficient algorithm for certain co-infection structures. We first make the link between the co-infection and correlation structure explicit, and introduce two special cases that will guide our analysis.

Remark 5. *Let $\boldsymbol{\xi} = (\xi_i)_{i\in N}$ denote a multivariate binary vector, which assumes a value of 1 if a random subject is infected with disease $i \in N$ (i.e., event A_i^+ occurs), and 0 otherwise, in accordance with the joint vector $\boldsymbol{p}$. The marginal distributions, $\xi_i \sim Bernoulli(\pi_i), i \in N$ [27].*

1. *The pairwise correlation coefficient, $\rho(\xi_i, \xi_j) = \frac{p_{ij}-\pi_i\pi_j}{\sqrt{\pi_i(1-\pi_i)\pi_j(1-\pi_j)}}, \forall ij \in N(2)$, is increasing in co-infection probability (p_{ij}), as long as the marginal prevalences (π_i, π_j) remain unchanged. ($\rho(\xi_i, \xi_j)$ may have a narrower range than $[-1, 1]$ unless $\pi_i = \pi_j$, e.g., [36].)*
2. *Consider two special co-infection structures:*
   (a) *No co-infections: Events $A_i^+, \forall i \in N$, are mutually exclusive. Then, assay prevalence (Eq. (4)) reduces to:*
   $$\pi(S) = \sum_{i\in S} \pi_i, \quad \forall S \subseteq N, \tag{15}$$
   and $\rho(\xi_i, \xi_j) < 0, \ \forall ij \in N(2)$.
   (b) *Independent diseases: Events $A_i^+, \forall i \in N$, are mutually independent. Then, assay prevalence (Eq. (4)) reduces to:*
   $$\pi(S) = \sum_{i\in S} \pi_i - \sum_{ij\in N(2):i,j\in S} \pi_i\pi_j + \sum_{ijr\in N(3):i,j,r\in S} \pi_i\pi_j\pi_r + \cdots + (-1)^{s+1} \prod_{i\in S} \pi_i, \quad \forall S \subseteq N, \tag{16}$$
   and $\rho(\xi_i, \xi_j) = 0, \forall ij \in N(2)$.

Definition 6. *We say that joint vector $\boldsymbol{p}'$ is more correlated than joint vector $\boldsymbol{p}$, if $p'_{i\cdots j} \geq p_{i\cdots j}, \forall i \cdots j \in N(l), l = 2, \cdots, n$, and their marginal vectors are equal, $\boldsymbol{\pi'} = \boldsymbol{\pi}$, that is, each co-infection probability in $\boldsymbol{p}'$ is at least as large as its counterpart in $\boldsymbol{p}$, while their marginal prevalences are equal.*

Lemma 1. *Consider $\pi(N) \leq \underline{p}$. The threshold $\overline{\lambda}^{(n-1)}$ is non-decreasing as $\boldsymbol{p}$ becomes more correlated.*

Thus, when pooling is optimal, as the prevalence vector becomes more correlated (i.e., some co-infection probabilities rise while disease prevalences remain the same, Definition 6), the λ-region where an all-singleton design ($D^{(n)}$) is optimal shrinks, that is, multiplexing becomes more favorable.

The optimal design is completely characterized for the smallest- and highest-difference composite cost functions (Theorems 2-3). For the remaining cases, however, the optimal design is either some form of Dorfman or mixed-testing design, $D^{(q)}$ or $M^{(q)}$, or n-plex individual-testing design, $I^{(1)}$ (Table 2). Hence, one must consider all possible partitions of the disease set N, and this general partition-type problem, with no assumed relationship among disease prevalences, is NP-hard [21]. The following result

shows that when disease prevalences are independent, or when there are no co-infections, there exists an optimal design that uses an ordered partition (Definition 2) for both Dorfman and mixed-testing designs. This result plays a key role in the development of an efficient, exact solution procedure for these special cases. (Dorfman designs with $q = 1$ and $q = n$ are excluded from the theorem, as their assay portfolio and testing method are completely fixed.)

Theorem 5. *Suppose all disease prevalences are independent, or there are no co-infections:*

1. *Within each q-partitioned Dorfman design class, $D^{(q)}$, $q = 2, \cdots, n-1$, there exists an optimal design that uses an ordered q-partition.*
2. *Within each q-partitioned mixed-testing design class, $M^{(q)}$, $q = 2, \cdots, n$, there exists an optimal design for which diseases $\{1, \cdots, n^I\}$ (i.e., the n^I diseases with the highest prevalences) are bundled into one multiplex assay, which is individually tested, and diseases $\{n^I + 1, \cdots, n\}$ are tested via pooling, following some ordered $q-1$-partition, for some $n^I, n^D \in Z^+ : n^I + n^D = n$.*

From a practical perspective, the optimality of an ordered partition indicates that small forecasting errors in disease prevalences may not have a large impact on an optimal design as long as disease ordering is mostly preserved. Intuitively, the ordered partition result holds because, for both independent diseases and no co-infections cases, an ordered 2-partition yields the highest (lowest) possible assay prevalence for one (the other) assay, among all 2-partitions with fixed assay sizes (hence fixed assay costs), and the expected tests function is concave in assay prevalence (Property 2). This reasoning extends to any q-partition, because it can be split into multiple 2-partitions. In particular, in the no co-infections case, the total cost function ($TC(.)$) becomes concave in the sum of disease prevalences, and the results by [21] and [3] apply to our setting. In general, however, the total cost function is not necessarily concave in the sum of disease prevalences (due to co-infections), but the ordered partition result continues to hold for independent diseases (Theorem 5). The following remark and example provide some insight on when the ordered partition result may/may not hold.

Remark 6. *Consider that the prevalence vector satisfies the transitivity property, that is, if $\pi_i \geq \pi_j$ for some $i, j \in N$, then $\pi(\{i, r\}) \geq \pi(\{j, r\}), \forall r \in N \setminus \{i, j\}$. The transitivity property is satisfied in both the independent diseases and the no co-infections cases.*

The transitivity property of the prevalence vector is necessary, but not sufficient, for the ordered partition result in Theorem 5 to hold, as the following example demonstrates.

Example 2. *Consider disease set, $N = \{1, 2, 3\}$, with joint vector, $\boldsymbol{p} = (p_0 = 0.79, p_1 = 0.05, p_2 = 0.05, p_3 = 0, p_{12} = 0.06, p_{13} = 0.05, p_{23} = 0, p_{123} = 0)$ (i.e., $A_3^+ \subseteq A_1^+$), and marginal prevalences, $\pi_1 = 0.16, \pi_2 = 0.11, \pi_3 = 0.05$, which satisfy the transitivity property (Remark 6). However, for $\lambda = 0.6$ and assay cost function $c(s) = s^{0.8}, s = 1, 2, 3$, the optimal design is a $D^{(2)}$ design with $S_1 = \{1, 3\}$ and $S_2 = \{2\}$, which is not an ordered partition.*

Theorem 5 leads to an efficient algorithm.

Corollary 1. *Suppose all disease prevalences are independent, or there are no co-infections:*

1. *The problem of finding an optimal partition of set N reduces to a Shortest Path Problem on an acyclic directed graph $G(V(N), E(N))$ with:*
   - *Vertex set $V(N) = N \cup \{n+1\}$, i.e., each disease in set N represents a vertex, and vertex $n+1$ represents a dummy vertex;*
   - *Edge set $E(N) = \{(i,j) : i < j, i, j \in V(N)\}$, where edge (i,j) represents an assay for diseases $i, i+1, \cdots, j-1$ (equivalently, $S = \{i, i+1, \cdots, j-1\}$, with size $s = j - i$), with edge weight $w_{i,j} = \tilde{c}(s, \lambda) \times T(S, t^*(S))$, i.e., the assay's expected cost at the optimal pool size.*
2. *Both the construction of graph $G(V(N), E(N))$ and solving the Shortest Path Problem (e.g., via a topological sorting algorithm [26]) have polynomial complexity, $O(n^2)$.*

Corollary 1 holds because each ordered q-partition of set N, $q = 1, \cdots, n$, is represented by a path from vertex 1 to vertex $n+1$ on $G(V(N), E(N))$. Thus, the set of all ordered partitions of set N corresponds to the set of all paths from vertex 1 to vertex $n+1$, and an optimal partition of set N corresponds to the shortest path from vertex 1 to vertex $n+1$. Thus, when disease prevalences are independent or there are no co-infections, an optimal testing design can be found in polynomial time. When there are co-infections and disease prevalences are not independent, the problem remains NP-hard; and some of the existing algorithms for the partition problem (§3.2) can be modified to solve our problem, which is outside the scope of this paper.

Remark 7. *When $\sum_{i \in N} \overline{\pi}_i \leq 1$, Theorem 5 and Corollary 1 continue to hold for the deterministic counterpart of the robust problem,* **R-TD***, which, in this case, is based on a deterministic joint vector $\boldsymbol{p}$ with no co-infections (Corollary A.1). Thus, there exists an optimal robust design that is ordered, which can be determined in polynomial time.*

6 A Case Study of Respiratory Diseases

Large multiplex assays are used for a variety of diseases (see §1). In this case study, we focus on respiratory diseases, which are challenging for the testing design problem: Some respiratory diseases exhibit seasonal prevalence fluctuations, which not only lead to high uncertainty, but also alter the disease ordering dynamically throughout the year; as a group, respiratory diseases have higher prevalences than other disease groups, making pooling less beneficial; and during our study period of 2018 to 2021, this group not only included an emerging disease (COVID-19), but also diseases that responded to COVID-19 mitigation measures, resulting in drastic changes in their prevalence during the study period. We present the study design in §6.1, the data and sources in §6.2, and a discussion of the results in §6.3.

6.1 Study Design

We consider 18 respiratory diseases (14 viral, 4 bacterial) that manifest with overlapping clinical presentation over a four-year period (2018 to 2021) that spans both pre- and post-COVID periods. Weekly prevalence data are available during the study period.

Optimal designs: Assay design is a tactical decision, as design changes require the acquisition of assays and modification of procedures. Consequently, we produce a family of *base Pareto designs* for each of 2018 (without COVID-19) and 2021 (with COVID-19), which include the **deterministic (mean-based)** and **robust** designs, using models **TD** and **R-TD**, respectively, based on the yearly means and the CI upper limits of disease prevalences, for $\lambda \in [0, 1]$, in increments of 0.05, illustrating the trade-offs between testing cost and capacity.

Performance evaluation: We evaluate the base designs using weekly data from 2018-2021, and, in our discussion, distinguish between two settings: **(1)** the *perfect-information* setting, where a design is evaluated using the data from which it is derived; in this setting the design must contend with the *weekly prevalence variations* that underscore the mean (or the CI upper limit) due to seasonality and/or other natural variations; and **(2)** the *imperfect-information* setting, where a design is evaluated using another year's data, such that the design must also contend with *forecast error* in the yearly mean. We compare the base designs with the two **benchmarks** from Remark 2: *multiplexing-only* ($I^{(1)}$) and *pooling-only* (the best of $I^{(n)}, D^{(n)}$, and $M^{(n)}$).

The total cost ($TC(.)$, Eq. (2)), which is a convex combination of the expected testing cost and number of tests, is an abstract construct. To better illustrate the trade-offs, we report the testing cost and the number of tests (evaluated based on actual data), for all $\lambda \in [0, 1]$. For reference, the $\lambda = 0$ and $\lambda = 1$ designs minimize the expected number of tests and testing cost, respectively. We also report, $\forall \lambda \in [0, 1]$, the *price of robustness ratio* (Table B.1, Appendix B), and

$$\textit{Value of joint optimization ratio (VoJ)}(\lambda)\ (\%) = \frac{[TC(I^{(1)},\ \lambda) - TC^{X}(\lambda)]}{TC(I^{(1)},\ \lambda)} \times 100,\ X \in \{\textbf{TD}, \textbf{R-TD}\},$$

i.e., in comparison to the multiplexing-only benchmark, which consistently outperforms the pooling-only benchmark in the case study (due to high prevalence rates) and represents current testing practices.

6.2 Data: Sources and Descriptive Statistics

Table 3 reports the mean prevalences for the 18 diseases for each year in the study period, along with the data sources. For the 14 viral diseases, this mean is the average of the weekly prevalences; for the four bacterial diseases (Mycoplasma pneumoniae, Bordetella parapertussis, Bordetella pertussis, and Chlamydophila pneumoniae) this data were not available, and we use the literature to estimate weekly prevalences. The diseases are indexed following a non-increasing order of their 2018 mean prevalences (thus COVID-19 is #18). This order does not necessarily coincide with the weekly orders throughout

2018, the mean-based orders for other years, nor the CI-based orders for 2018 to 2021.

Co-infection rates, needed for **TD**, are not reported in the data sources, hence we assume disease prevalences are independent, that is, co-infection rates are proportional to the corresponding disease prevalences. Further, for **R-TD**, based on our data, $\sum_{i \in N} \overline{\pi}_i \leq 1$ in each year of the study period. Thus, we determine the optimal **TD** and **R-TD** designs in polynomial time using Corollary 1, i.e., by determining the best ordered partition (Theorem 5).

TD designs are based on the yearly mean prevalences in Table 3. For **R-TD**, we use the 52 weekly prevalence data each year to construct a 95% CI for each disease prevalence based on the Wald's method [65], which serves as the uncertainty set for $\mathbf{\Pi}$ (Appendix B). Fig. 1 plots the overall prevalence and select disease prevalences for each week in the study period; and illustrates how disease prevalences, hence their ordering, fluctuate substantially throughout each year, with some diseases being highly seasonal. Therefore, even in the perfect-information setting, an optimal **TD** design, which is an ordered partition based on yearly means, is not necessarily optimal for any given week in the year.

Table 3: Disease index, name, yearly mean prevalences for 2018 to 2021, and data sources

Index	Disease	Yearly Mean				Data Source
		2018	2019	2020	2021	
1	Influenza A	0.1902	0.2932	0.0930	0.0055	[20]
2	Influenza B	0.0978	0.0887	0.0488	0.0001	[20]
3	Respiratory syncytial virus (RSV)	0.0599	0.0596	0.0207	0.0613	[19]
4	Human metapneumovirus	0.0315	0.0293	0.0149	0.0150	[19]
5	Respiratory adenovirus	0.0310	0.0368	0.0186	0.0284	[19]
6	Parainfluenza virus 3	0.0277	0.0273	0.0012	0.0340	[19]
7	CoVOC43	0.0096	0.0140	0.0023	0.0137	[19]
8	Parainfluenza virus 2	0.0093	0.0020	0.0005	0.0076	[19]
9	CoVNL63	0.0070	0.0081	0.0053	0.0069	[19]
10	CoVHKU1	0.0070	0.0062	0.0072	0.0003	[19]
11	Parainfluenza virus 4	0.0062	0.0054	0.0022	0.0048	[19]
12	Mycoplasma pneumoniae	0.0051	0.0049	0.0050	0.0050	[76]
13	Bordetella parapertussis	0.0021	0.0021	0.0021	0.0021	[63]
14	Parainfluenza virus 1	0.0019	0.0152	0.0016	0.0003	[19]
15	CoV229E	0.0015	0.0061	0.0007	0.0028	[19]
16	Bordetella pertussis	0.0004	0.0004	0.0004	0.0004	[76]
17	Chlamydophila pneumoniae	0.0003	0.0003	0.0003	0.0004	[76]
18	COVID-19	N/A	N/A	0.0450	0.0613	[15, 50]
$\pi(N)$	Overall prevalence	0.4042	0.4838	0.2421	0.2254	

Cost structure: PCR cost data from the literature, e.g., [76], confirms the concave nature of the assay cost function in the number of diseases bundled. This is expected for genetic assays (see §1), because each PCR assay uses: **(1)** common reagents and materials that are not pathogen-specific (e.g., the polymerase enzyme, DNA nucleotides, vials), the required amounts of which are fairly insensitive to the number of diseases in the assay; and **(2)** pathogen-specific reagents (e.g., the primers and probes) that depend on the number of diseases, but their structure (hence cost) is fairly similar for the different diseases. Consequently, we consider a fixed cost per assay, and a variable cost per disease bundled; this function satisfies Assumption ($\boldsymbol{A}$). The cost data for medical tests is often difficult to find. Based on

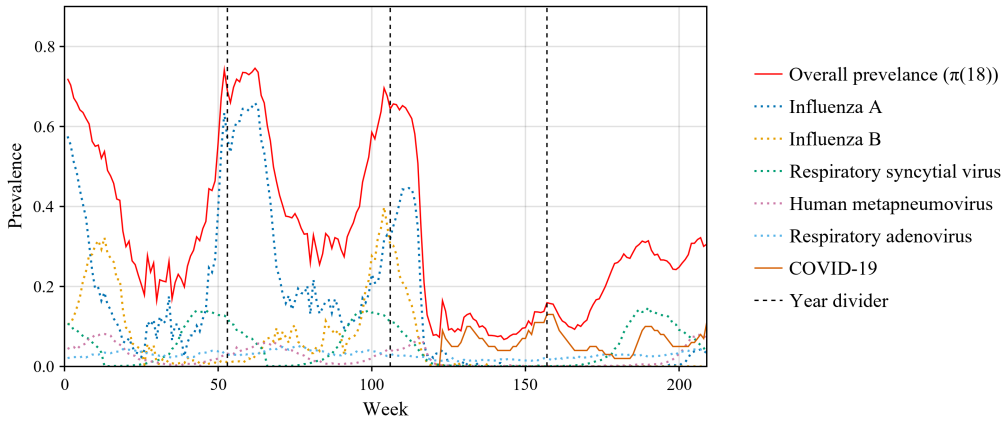

Figure 1: Overall prevalence, and select disease prevalences per week over 2018-2021

the limited data in [76], we fit various assay cost functions (Appendix B). We demonstrate our findings for the $c(s) = 25.54 + 4.46 \times s$ function, but sensitivity analysis for other cost functions indicates similar qualitative findings. Because the number of tests (per subject) is 1 for the $I^{(1)}$ benchmark, and the total cost is a convex combination of the testing cost and number of tests, we normalize the assay cost function so that $c(n) = 1$.

We consider a pool size limit, $\overline{M}$, of 32, which is common for PCR assays [11, 33, 85].

6.3 Case Study Findings

Key properties of optimal designs are established analytically (§4-5). In §6.3.1, we use the perfect-information setting to show additional properties; in §6.3.2, we compare optimal designs with benchmarks through the progression of the COVID-19 pandemic in the realistic, imperfect-information setting.

6.3.1 Properties of mean-based and robust designs (perfect-information setting)

To motivate our discussion, Tables 4-5 provide the **TD** and **R-TD** Pareto designs, along with the benchmarks designs, and their results, evaluated using 2018 (17 diseases) and 2021 (18 diseases, including COVID-19) weekly data, in terms of the actual testing cost and number of tests (mean, minimum, and maximum values over the 52 weeks), under the perfect-information settings, i.e., the 2018/2021-designs are evaluated using the 2018/2021 weekly data (under weekly variations but no forecast error). Fig. 2 plots the mean values for the testing cost and number of tests for each of the **TD** and **R-TD** designs, to visualize the Pareto frontier. Tables 4-5 also report the value of joint optimization ratios (VoJ, in terms of its range over λ), i.e., with respect to the 17-plex (for 2018) or the 18-plex (for 2021) $I^{(1)}$ benchmarks.

Mean-based versus robust designs: Mean-based designs and their robust counterparts are quite similar, despite the differences in their inputs, including different disease orderings (e.g., for 2018, the mean overall prevalence for **TD** is $\pi(N) = 0.4042$, whereas for **R-TD** it is 0.6079, i.e., the sum of the CI upper limits). *This underscores another benefit of* **TD***: by integrating multiplexing and pooling, the designs become structurally robust to variations in mean prevalences.* To see this, consider that pooling is the cause

Table 4: 2018 **TD** and **R-TD** designs, metrics, and VoJ based on 2018 data - without COVID-19 testing

Model ($n = 17$)	Range of λ values	Design Class	Assay Sizes	Pool Sizes	Perfect-information Setting: Testing Cost Mean (Min-Max)	Perfect-information Setting: Number of Tests Mean (Min-Max)	Perfect-information Setting: $VoJ(\lambda)$ (%) Range
TD	0.00-0.40	$I^{(1)}$	[17]	[1]	1.00 (1.00-1.00)	1.00 (1.00-1.00)	0.00-0.00
	0.45-0.55	$M^{(2)}$	[15, 2]	[1, 32]	0.93 (0.93-0.93)	1.05 (1.05-1.06)	0.11-1.35
	0.60-0.80	$M^{(2)}$	[12, 5]	[1, 13]	0.85 (0.84-0.89)	1.16 (1.13-1.24)	2.56-8.60
	0.85	$M^{(2)}$	[11, 6]	[1, 10]	0.84 (0.83-0.87)	1.21 (1.19-1.27)	10.21
	0.90	$M^{(3)}$	[8, 7, 2]	[1, 6, 32]	0.81 (0.76-0.97)	1.39 (1.29-1.67)	13.40
	0.95-1.00	$M^{(3)}$	[6, 6, 5]	[1, 5, 13]	0.79 (0.72-0.94)	1.55 (1.40-1.85)	16.70-21.50
	Disease Order:				1, 2, 3, 4, 5, 6, 7, 8, 9, 10, 11, 12, 13, 14, 15, 16, 17		
R-TD	0.00-0.40	$I^{(1)}$	[17]	[1]	1.00 (1.00-1.00)	1.00 (1.00-1.00)	0.00-0.00
	0.45-0.60	$M^{(2)}$	[15, 2]	[1, 32]	0.93 (0.93-0.93)	1.05 (1.05-1.06)	0.11-1.97
	0.65-0.80	$M^{(2)}$	[12, 5]	[1, 12]	0.85 (0.84-0.89)	1.16 (1.13-1.23)	4.03-8.57
	0.85-0.90	$M^{(2)}$	[11, 6]	[1, 9]	0.84 (0.83-0.87)	1.21 (1.19-1.26)	10.16-11.98
	0.95	$M^{(3)}$	[10, 5, 2]	[1, 8, 32]	0.83 (0.80-0.88)	1.31 (1.25-1.42)	14.75
	1.00	$M^{(3)}$	[7, 5, 5]	[1, 5, 12]	0.80 (0.74-0.96)	1.52 (1.39-1.84)	19.54
	Disease Order:				1, 2, 3, 4, 6, 5, 8, 7, 10, 9, 11, 12, 14, 13, 15, 16, 17		
Multiplexing-only	N/A	$I^{(1)}$	[17]	[1]	1.00	1.00	N/A
Pooling-only	N/A	$D^{(17)}$	17 singletons	3 to 32	1.24	4.20	N/A

Table 5: 2021 **TD** and **R-TD** designs, metrics, and VoJ based on 2021 data - with COVID-19 testing

Model ($n = 18$)	Range of λ values	Design Class	Assay Sizes	Pool Sizes	Perfect-information Setting: Testing Cost Mean (Min-Max)	Perfect-information Setting: Number of Tests Mean (Min-Max)	Perfect-information Setting: $VoJ(\lambda)$ (%) Range
TD	0.00-0.30	$D^{(1)}$	[18]	[3]	0.86 (0.59-1.02)	0.86 (0.59-1.02)	14.43-14.43
	0.35-0.70	$D^{(2)}$	[13, 5]	[3, 26]	0.71 (0.49-0.84)	0.93 (0.66-1.10)	14.65-22.44
	0.75	$D^{(2)}$	[11, 7]	[3, 13]	0.68 (0.48-0.82)	1.00 (0.71-1.21)	23.76
	0.80	$D^{(3)}$	[7, 6, 5]	[3, 7, 26]	0.63 (0.45-0.81)	1.21 (0.87-1.57)	25.77
	0.85-1.00	$D^{(3)}$	[6, 7, 5]	[3, 6, 26]	0.62 (0.45-0.80)	1.23 (0.89-1.57)	28.62-37.82
	Disease Order:				18, 3, 6, 4, 5, 8, 15, 9, 1, 12, 11, 10, 14, 16, 17, 13, 7, 2		
R-TD	0.00-0.30	$D^{(1)}$	[18]	[3]	0.86 (0.59-1.02)	0.86 (0.59-1.02)	14.43-14.43
	0.35-0.65	$D^{(2)}$	[13, 5]	[3, 26]	0.71 (0.49-0.84)	0.93 (0.66-1.10)	14.65-21.33
	0.70-0.75	$D^{(2)}$	[11, 7]	[3, 13]	0.68 (0.48-0.82)	1.00 (0.71-1.21)	22.14-23.76
	0.80-1.00	$D^{(3)}$	[6, 7, 5]	[3, 6, 26]	0.62 (0.45-0.80)	1.23 (0.89-1.57)	25.56-37.82
	Disease Order:				18, 3, 6, 5, 4, 7, 8, 9, 1, 12, 11, 15, 13, 16, 17, 10, 14, 2		
Multiplexing-only	N/A	$I^{(1)}$	[18]	[1]	1.00	1.00	N/A
Pooling-only	N/A	$D^{(18)}$	18 singletons	5 to 32	0.92	3.25	N/A

of weekly variability in the metrics; individual testing always uses one test, for all prevalences. Then: **(1)** through bundling of diseases in an assay, the assay's performance becomes a function of the assay prevalence (i.e., combined prevalences of the diseases in the assay), rather than the individual disease prevalences, which serves to increase its robustness under both weekly prevalence variations and forecast error; **(2)** the ordering of diseases within an assay is immaterial, it is only when ordering errors place the disease in the "wrong" assay do sub-optimalities arise; and **(3)** a particular pool size remains optimal for a range of prevalences, and beneficial for an even larger range. The performances of the mean-based and robust designs are even closer in 2021, due to a lower overall prevalence and lower CI upper limits (e.g., influenza had lower prevalences, and less pronounced seasonality, hence lower uncertainty). The

price of robustness is also low (Table B.1, Appendix B). Robust designs may even *lower* the actual cost (e.g., $\lambda = 0.70$ for 2021, Table 5 and Table B.1), because **TD** uses the expected costs based on yearly means, which may deviate from the actual costs due to weekly variations.

Comparison with benchmarks: The multiplexing-only ($I^{(1)}$) benchmark is on the Pareto frontier only for 2018 (not 2021), and only for $0 \leq \lambda \leq 0.4$ (Theorem 2, Fig. 2). For 2018 (Table 4), both **TD** and **R-TD** use multiple assays with mixed testing methods (pooling and individual testing) for all $\lambda \geq 0.45$; these designs have positive VoJ values, and show the trade-off between testing cost and number of tests. For 2021 (Table 5), which has a lower overall prevalence than 2018, every **TD** and **R-TD** design is a Dorfman design with multiplexing; and some of these Pareto designs improve upon both the testing cost and number of tests compared to the benchmarks. To better understand the practical impact of the trade-off between the testing cost and number of tests, remember that PCR machines can have large capacities (see §1), hence there are many settings in which they are run below capacity; and increasing the number of tests to reduce the testing cost in these settings can be an especially good trade-off.

Pooling alone does not provide as much benefit as the integrated mean-based or robust designs; the pooling-only benchmark is not on the Pareto frontier in either year. On the other hand, pooling of the n-plex ($D^{(1)}$) is not useful in 2018; for 2021, it can improve the 18-plex benchmark by 14.43% (i.e., $VoJ(\lambda = 0)$), compared to a VoJ of 37.82% attained through integrated multiplexing and pooling.

Design structures: Noting the mean overall prevalence of 0.4042 for 2018, and 0.2254 for 2021 (above and below the pooling threshold of 0.31, respectively), the optimal designs in Tables 4-5 are in agreement with Theorems 1-2. As λ increases, all designs move towards more assays: This is expected for the 2021-designs in light of Theorem 4 (as $\pi(18) = 0.2254 < 0.31$ for 2021), but, in the absence of this condition, we still see a similar trend for the 2018-designs. The first assay almost always bundles the most diseases (which have the highest prevalence), hence has the largest assay prevalence and the smallest pool size. This keeps the first assay's pool size constant as λ increases, allowing the other assays to use larger pools. The robust designs tend to have smaller pools than the mean-based designs due to the use of the CI upper limits.

Effect of seasonality: One challenge for testing design for respiratory diseases is seasonality. We explore the benefits of accounting for seasonality through the use of a separate **TD** design for the high versus low season, constructed and evaluated based on the 2018 data. We define the seasons based on the pooling threshold of 31%, as this implies when pooling is beneficial for the 17-plex: The *low season* spans the period for which the weekly overall prevalence remains below 31%, which, for 2018, was weeks 20-44, the remaining weeks represent the *high season*. The VoJ range over the 17-plex $I^{(1)}$ is, $[VoJ(\lambda = 0) = 0, VoJ(\lambda = 1) = 20.5\%]$ (Table 4) for original 2018 **TD** designs (without accounting for seasonality), and $[VoJ(\lambda = 0) = 5.3\%, VoJ(\lambda = 1) = 25.2\%]$ (Table B.2, Appendix B) with high- and low-season designs. Thus accounting for seasonality can further increase the benefits of optimal designs.

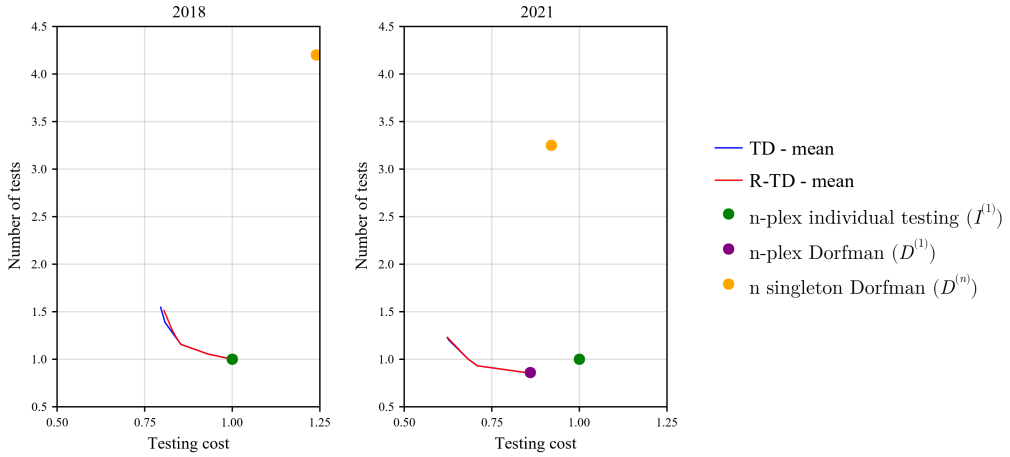

Figure 2: 2018 and 2021 perfect-information **TD** and **R-TD** designs and benchmarks

6.3.2 Testing design during the pandemic (imperfect-information designs)

The previous perfect-information setting provides a reference point on the potential benefits of joint optimization. Next, we study testing design in the realistic, imperfect-information setting, where prevalences are unknown at the time of testing design. One can integrate a sophisticated forecasting method (available in the literature for influenza and COVID-19) into our testing design models. While this is worthy of future investigation, a main finding from the study of the imperfect-information setting in this section is that *sophisticated forecasting methods may not be necessary to reap most of the benefits*. Integrating multiplexing and pooling already increases the robustness of optimal designs to forecast errors, see §6.3.1. As we shall see, the 2018-designs, or simple modifications of them to account for COVID-19 effects on influenza rates, work very well compared to the benchmarks.

2019-2021 (without COVID-19 testing): performance of 2018-designs

We first explore the performance of the 2018-designs for the 17 diseases (from Table 4, i.e., designs constructed using the 2018 data) on data from 2019 to 2021. While the disease ordering in 2018 does not match that in 2019, 2020, or 2021, these **TD** and **R-TD** imperfect-information designs continue to substantially outperform both benchmarks for the 2019-2021 period (Table B.3, Appendix B). For example, the $VoJ(\lambda = 1)$ values for mean-based and robust designs are 20.5% and 18.4% respectively, over the $I^{(1)}$ benchmark, in this period. These benefits are similar in scale to the 2018-designs under perfect information, continuing to show that both **TD** and **R-TD** are quite robust to forecast errors.

Next, we show that we can improve upon the performance of the 2018-designs, evaluated using 2021 data, via design modifications based on minimal information on the impact of COVID-19.

2021 (both with and without COVID-19 testing): performance of modified-2018-designs

Due to the pandemic, 2021 was quite an unusual year for respiratory diseases. The protective measures taken for COVID-19 also reduced the influenza rates, greatly perturbing the order of diseases from 2018.

This was apparent in November to December of 2020 (the beginning of the 2020/21 influenza season), during which the reported influenza rates were much lower than the historic averages, and such unusual influenza patterns were anticipated to continue into 2021. Thus, we now demonstrate how the testing designs for 2021 can be improved with simple forecasting: to this end, we simply set influenza A and B prevalences to their averages from November and December of 2020; for all other diseases, we continue to use the 2018 data. Using this *modified* 2018 data, we produce *modified-2018-designs* using **TD** and **R-TD**. First we produce testing designs for the 17 diseases (without COVID-19), then turn our attention to COVID-19. Forecasting an emerging, and evolving, disease is very difficult, and many COVID-19 forecasting methods in the literature turned out to be highly inaccurate. In the absence of a reliable COVID-19 forecast in 2021, we explore a simple strategy of adding COVID-19 into the first assay in the modified-2018-designs for **TD** and **R-TD**, thus bundling it with the most prevalent diseases in each design. Retrospectively, this can be accomplished using the modified-2018 data and a mean COVID-19 prevalence of 10%. With an actual 2021 COVID-19 mean of 6.1% (unknown at the time of testing design), it is sub-optimal, and represents an overestimation.

Table B.4 (Appendix B) report the results for the modified-2018-designs, and for comparison purposes, the 2021 perfect-information designs, both with and without COVID-19 testing, all evaluated using 2021 data. For each design with COVID-19 testing, Fig. 3 also depicts the weekly performance using 2021 data, in terms of the actual testing cost and the number of tests, and its mean performance over the year (in solid lines). The pooling-only benchmark is not depicted in Fig. 3, as it continues to be substantially dominated by all other designs. Finally, Table 6 reports the VoJ for the modified-2018 and perfect-information 2021 designs with respect to the $I^{(1)}$ benchmark based on the 2021 data.

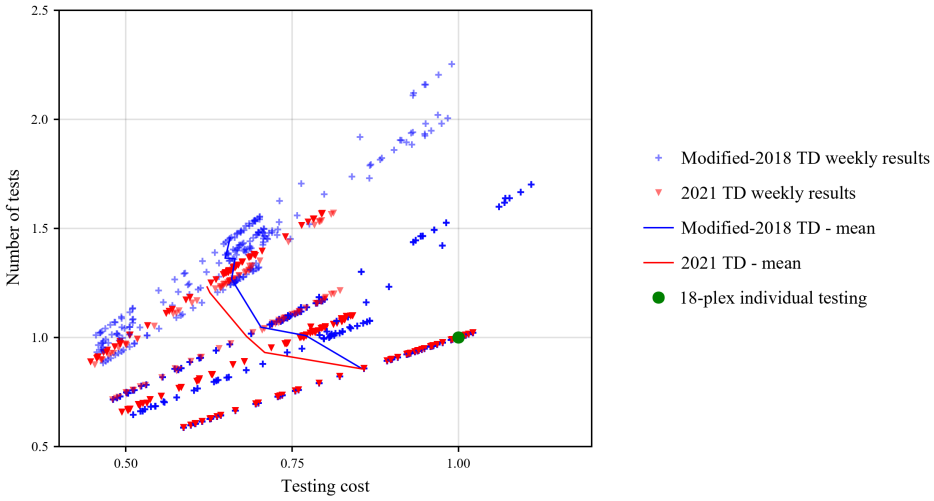

Figure 3: Modified-2018 versus 2021 **TD** designs and $I^{(1)}$ benchmark based on 2021 data

Perfect-information versus imperfect-information designs: The family of modified-2018 **TD** de-

signs performs very well in 2021, both with and without COVID-19 testing (Table B.4, Fig. 3); and their VoJ values are high and close to the 2021 perfect-information design values, which represent the maximum possible benefits under perfect information (Table 6). These findings continue to illustrate the structurally robust nature of **TD** designs under prevalence uncertainty.

Table 6: VoJ for modified-2018 and 2021 **TD** and **R-TD** designs based on 2021 data - with/without COVID-19 testing

		Without COVID-19						
Modified-2018 **TD**	λ range	0.00-0.40	0.45-0.60	0.65-0.85	0.90-0.95	1.00		
	$VoJ(\lambda)$ (%)	24.40-24.40	19.35-22.69	26.26-32.63	34.71-37.52	39.68		
Modified-2018 **R-TD**	λ range	0.00-0.35	0.40-0.55	0.60-0.80	0.85	0.90	0.95	1.00
	$VoJ(\lambda)$ (%)	24.40-24.40	18.50-21.82	24.77-31.12	32.56	34.88	37.27	39.48
2021 **TD**	λ range	0.00-0.35	0.40-0.75	0.80	0.85-0.90	0.95-1.00		
	$VoJ(\lambda)$ (%)	24.40-24.40	25.15-32.40	33.60	35.72-38.39	41.00-43.81		
2021 **R-TD**	λ range	0.00-0.30	0.35-0.70	0.75	0.80	0.85	0.90-1.00	
	$VoJ(\lambda)$ (%)	24.40-24.40	24.12-31.36	32.11	33.31	35.72	38.18-43.81	
		With COVID-19						
Modified-2018 **TD**	λ range	0.00-0.35	0.40-0.55	0.60-0.80	0.85	0.90	0.95	1.00
	VoJ(λ) (%)	14.43-14.43	8.66-12.22	15.92-22.79	24.97	26.60	31.47	34.29
Modified-2018 **R-TD**	λ range	0.00-0.35	0.40-0.55	0.60-0.85	0.90	0.95	1.00	
	VoJ(λ) (%)	0.00-0.00	(-5.23)-(-1.31)	2.91-12.67	13.71	31.54	34.09	
2021 **TD**	λ range	0.00-0.30	0.35-0.70	0.75	0.80	0.85-1.00		
	VoJ(λ) (%)	14.43-14.43	14.65-22.44	23.76	25.77	28.62-37.82		
2021 **R-TD**	λ range	0.00-0.30	0.35-0.65	0.70-0.75	0.80-1.00			
	VoJ(λ) (%)	14.43-14.43	14.65-21.33	22.14-23.76	25.56-37.82			

Mean-based versus robust designs: Based on the 2021 data, the price of robustness is very low for the modified-2018 and 2021 perfect-information designs, with the exception of the modified-2018 **R-TD** designs with COVID-19 testing (Table 6). This is mainly because, the overestimation of the COVID-19 mean, combined with higher prevalence upper limits for the other diseases (based on the modified-2018 data), leads to an overall prevalence for the robust model that exceeds the pooling threshold, making it more conservative than all other designs, which is expected based on Table 2. In particular, comparing modified-2018 **TD** and **R-TD** designs with COVID-19 testing (based on Table B.4): for $\lambda \in [0, 0.35]$, the robust design is the 18-plex $I^{(1)}$ benchmark, while the mean-based design uses a pool of 3; for $\lambda \in [0.40, 0.55]$, the robust design has a negative VoJ, unlike the mean-based design with a positive VoJ (in this case, the robust design reduces the testing cost, but not enough to compensate for the increase in the number of tests); the robust design starts improving on the $I^{(1)}$ benchmark only at $\lambda = 0.6$, and at $\lambda = 0.95$ it performs nearly as well as the mean-based design with respect to VoJ. This is because as λ increases, the robust design moves away from the $I^{(1)}$ benchmark and starts using multiple pooled assays, the cost benefit of which outweighs the increase in the number of tests.

Comparison with benchmarks: Modified-2018 **TD** designs outperform the $I^{(1)}$ benchmark on 2021 data; for the robust model, this happens mainly for the no COVID-19 testing case, as explained above.

7 Conclusions, with Limitations and Future Research Directions

We develop tools and insights for multi-disease testing design for public health screening practitioners. In the absence of practical guidelines on how multiplexing and pooling should be integrated, our study sheds important light into efficient testing practices, which can also benefit other stake-holders. For example, efficient testing enables timely and accurate diagnosis, leading to improved public health outcomes. Because the use of multiplexing and pooling does not require obtaining extra specimens from the patient, the patient does not notice any difference, but expanded testing improves patient outcomes and satisfaction [76]; assay manufacturers can also benefit from expanded testing, hence an expanded market. Quantifying such benefits for other stake-holders is an important research direction.

Limitations and Future Research Directions

To our knowledge, our model is the first mathematical model to combine multiplexing and pooling optimization in testing design for public health screening, and it is our hope that this work will spur new academic research as well as empirical explorations to further investigate the benefits of optimal testing designs. While our model considers many realistic aspects of the testing problem, any analytical model must rely on certain assumptions. Some of these assumptions, discussed below, can be considered as limitations of this research, but also present opportunities for future research.

To increase model realism, several assumptions can be relaxed. For example, while PCR assays are highly sensitive in general, they may miss a disease during the window period, when the pathogen has extremely low concentration in the specimen. Incorporating the pathogen dynamics into testing design is an important extension. We consider that the set of diseases for screening is given; adding a disease selection component to testing design (thus selecting from a set of *potential* diseases) would increase the practical impact of this research effort. Further, studying a stochastic formulation of the testing design problem, and considering correlated disease prevalences over time (e.g., due to seasonality) are worthwhile extensions. Relatedly, while the price of robustness was low in our case study, in general a mini-max type objective can be overly conservative; and it might be promising to explore other objectives, such as regret-based objectives, e.g., [31].

Testing design for respiratory diseases, considered in our case study, can be challenging; a primary reason for this challenge is seasonality. Our simple way of accounting for seasonality in testing design shows promise, and should be explored further. Our case study also suggests that optimizing the testing design infrequently, and using simple forecasting methods to deal with a rare event, such as the emergence of COVID-19, work well for testing design in the post-COVID period. This is one particular strength of multiplex assays: by bundling diseases in an assay, their combined prevalence becomes more reliable; further, small forecasting errors may not impact an optimal design as long as disease ordering is not altered much. Nevertheless, it is valuable to explore the benefits of more accurate forecasting methods

for testing design, or more frequent optimization of pool sizes than that for the assay portfolio, because pool sizes may be easier to change on a more frequent basis. It is also important to conduct case studies of other disease groups so as to quantify the benefits of optimal testing designs in other contexts.

We study the tactical testing design decision. Complementary future research directions include operational decisions, for instance, the online optimization problem [35, 43, 53] that arises in our setting when batches of specimens arrive at the laboratory in a stochastic manner. Thus, given PCR testing machine(s) and capacity, the tester needs to decide when to run the machine, i.e., below capacity, or wait for more specimens?

Acknowledgments: We are grateful to the Department Editor, Professor Özlem Ergün, the Associate Editor, and two Referees for providing excellent suggestions and comments on this manuscript, which led to significant improvements in the analysis, the insights gained, and the presentation. We would also like to thank the CDC's National Respiratory and Enteric Virus Surveillance System for providing data, and the Bureau of Clinical Laboratories at the Alabama Department of Public Health for insights on respiratory disease screening. This material is based upon work supported in part by the National Science Foundation under Grant No. # 1761842. Any opinion, findings, and conclusions or recommendations expressed in this material are those of the authors and do not necessarily reflect the views of the National Science Foundation.

References

[1] M. Al Ghounaim, Y. Xiao, C. Caya, and J. Papenburg. Diagnostic yield and clinical impact of routine cell culture for respiratory viruses among children with a negative multiplex RT-PCR result. *Journal of Clinical Virology*, 94:107–109, 2017.

[2] American Red Cross. Infectious disease, HLA and ABO donor qualification testing. `https://www.redcrossblood.org/biomedical-services/blood-diagnostic-testing/blood-testing.html`, n.d. Accessed in June 2022.

[3] S. Anily and A. Federgruen. Structured partitioning problems. *Operations Research*, 39(1):130–149, 1991.

[4] H. Aprahamian, D. R. Bish, and E. K. Bish. Optimal group testing: Structural properties and robust solutions, with application to public health screening. *INFORMS Journal on Computing*, 32(4):895–911, 2020.

[5] G. Balakrishnan, C. Landeen, E. A. Dy-Boarman, and G. C. Wall. Outcomes with multplex PCR respiratory sample testing on hospital inpatients: Outcomes and cost associated with a multiplex PCR system on nasopharyngeal swab specimens (FilmArray Respiratory Panel) in a large tertiary inpatient hospital population. *Journal of Academic Hospital Medicine*, 8(3):1–4, 2016.

[6] E. Balas and M. W. Padberg. Set partitioning: A survey. *SIAM Review*, 18(4):710–760, 1976.

[7] F. Barahona and R. Anbil. On some difficult linear programs coming from set partitioning. *Discrete Applied Mathematics*, 118(1-2):3–11, 2002.

[8] BCL-APH. Discussion with Mark Ellis of the Bureau of Clinical Laboratories - Alabama Public Health, 2022. From May 2022 discussion.

[9] C. Beckmann and H. H. Hirsch. Comparing luminex NxTAG-Respiratory Pathogen Panel and RespiFinder-22 for multiplex detection of respiratory pathogens. *Journal of Medical Virology*, 88(8):1319–1324, 2016.

[10] Biomérieux. FILMARRAY™ Respiratory Panel. `https://www.biomerieux-nordic.com/product/filmarray-respiratory-panel`, n.d. Accessed in June 2022.

[11] D. R. Bish, E. K. Bish, H. El Hajj, and H. Aprahamian. A robust pooled testing approach to expand COVID-19 screening capacity. *PLoS One*, 16(2):e0246285, 2021.

[12] C. M. Borges, P. Pathela, R. Pirillo, and S. Blank. Targeting the use of pooled HIV RNA screening to reduce cost in health department STD clinics: New York City, 2009–2011. *Public Health Reports*, 130(1):81–86, 2015.

[13] M. A. Boschetti, A. Mingozzi, and S. Ricciardelli. A dual ascent procedure for the set partitioning problem. *Discrete Optimization*, 5(4):735–747, 2008.

[14] S. P. Boyd and L. Vandenberghe. *Convex Optimization*. Cambridge University Press, New York, NY, 2004.

[15] CDC. Past weekly surveillance reports. `https://www.cdc.gov/coronavirus/2019-ncov/covid-data/covidview/covid-view-past-summaries.html`, 2021. Accessed in June 2022.

[16] CDC. Nucleic acid amplification tests (NAATs). `https://www.cdc.gov/coronavirus/2019-ncov/lab/naats.html`, 2021. Accessed in June 2022.

[17] CDC. Interim guidance for use of pooling procedures in sars-cov-2 diagnostic and screening testing. `https://www.cdc.gov/coronavirus/2019-ncov/lab/pooling-procedures.html`, 2021. Accessed in June 2022.

[18] CDC. Similarities and differences between flu and COVID-19. `https://www.cdc.gov/flu/symptoms/flu-vs-covid19.htm`, 2022. Accessed in June 2022.

[19] CDC. The National Respiratory and Enteric Virus Surveillance System (NREVSS). https://www.cdc.gov/surveillance/nrevss/, 2022. Accessed in June 2022.

[20] CDC - Influenza Division. FluView - Weekly U.S. Influenza Surveillance Report. https://www.cdc.gov/flu/weekly/#ClinicalLaboratories, 2022. Accessed in June 2022.

[21] A. K. Chakravarty, J. B. Orlin, and U. G. Rothblum. A partitioning problem with additive objective with an application to optimal inventory groupings for joint replenishment. *Operations Research*, 30(5):1018–1022, 1982.

[22] M. Chan, S. H. Koo, B. Jiang, P. Q. Lim, and T. Y. Tan. Comparison of the Biofire Film Array Respiratory Panel, Seegene AnyplexII RV16, and Argene for the detection of respiratory viruses. *Journal of Clinical Virology*, 106:13–17, 2018.

[23] T. J. Chan and C. A. Yano. A multiplier adjustment approach for the set partitioning problem. *Operations Research*, 40(1-supplement-1):S40–S47, 1992.

[24] H. Chen, H. Weng, M. Lin, P. He, et al. The clinical significance of FilmArray Respiratory Panel in diagnosing community-acquired pneumonia. *BioMed Research International*, 2017:7320859, 2017.

[25] R. M. Corless, G. H. Gonnet, D. E. Hare, D. J. Jeffrey, and D. E. Knuth. On the LambertW function. *Advances in Computational Mathematics*, 5(1):329–359, 1996.

[26] T. H. Cormen, C. E. Leiserson, R. L. Rivest, and C. Stein. *Introduction to algorithms*. MIT Press, Cambridge, MA, 2009.

[27] B. Dai, S. Ding, and G. Wahba. Multivariate Bernoulli distribution. *Bernoulli*, 19(4):1465–1483, 2013.

[28] S. Das, S. Dunbar, and Y.-W. Tang. Laboratory diagnosis of respiratory tract infections in children – the state of the art. *Frontiers in Microbiology*, 9:2478, 2018.

[29] N. Dinh and V. Jeyakumar. Farkas' lemma: three decades of generalizations for mathematical optimization. *TOP*, 22(1):1–22, 2014.

[30] R. Dorfman. The detection of defective members of large populations. *The Annals of Mathematical Statistics*, 14 (4):436–440, 1943.

[31] H. El Amine, E. K. Bish, and D. R. Bish. Robust post-donation blood screening under prevalence rate uncertainty. *Operations Research*, 66(1):1–17, 2017.

[32] H. El Hajj, D. R. Bish, and E. K. Bish. Optimal genetic screening for cystic fibrosis. *Operations Research*, 70(1): 265–287, 2022.

[33] H. El Hajj, D. R. Bish, E. K. Bish, and H. Aprahamian. Screening multi-dimensional heterogeneous populations for infectious diseases under scarce testing resources, with application to COVID-19. *Naval Research Logistics*, 69(1):3–20, 2022.

[34] H. El Hajj, D. R. Bish, E. K. Bish, and D. Kay. Novel pooling strategies for genetic testing, with application to newborn screening. *Management Science*, 68(11):7994–8014, 2022.

[35] A. N. Elmachtoub and R. Levi. Supply chain management with online customer selection. *Operations Research*, 64(2):458–473, 2016.

[36] L. Emrich and M. Piedmonte. A method for generating high-dimensional multivariate binary variates. *American Statistician*, 45:302–303, 1991.

[37] FDA. Pooled sample testing and screening testing for COVID-19. `https://www.fda.gov/medical-devices/coronavirus-covid-19-and-medical-devices/pooled-sample-testing-and-screening-testing-covid-19`, 2020. Accessed in June 2022.

[38] FDA. Nucleic acid based tests. https://www.fda.gov/medical-devices/in-vitro-diagnostics/nucleic-acid-based-tests, 2021. Accessed in June 2022.

[39] M. L. Fisher and P. Kedia. Optimal solution of set covering/partitioning problems using dual heuristics. *Management Science*, 36(6):674–688, 1990.

[40] K. E. Fleming-Dutra, A. L. Hersh, D. J. Shapiro, M. Bartoces, et al. Prevalence of inappropriate antibiotic prescriptions among US ambulatory care visits, 2010-2011. *JAMA*, 315(17):1864–1873, 2016.

[41] F. Gharabaghi, A. Hawan, S. J. Drews, and S. E. Richardson. Evaluation of multiple commercial molecular and conventional diagnostic assays for the detection of respiratory viruses in children. *Clinical Microbiology and Infection*, 17(12):1900–1906, 2011.

[42] C. C. Ginocchio and A. J. McAdam. Current best practices for respiratory virus testing. *Journal of Clinical Microbiology*, 49:S44–S48, 2011.

[43] N. Golrezaei, H. Nazerzadeh, and P. Rusmevichientong. Real-time optimization of personalized assortments. *Management Science*, 60(6):1532–1551, 2014.

[44] S. Gonsalves, J. Mahony, A. Rao, S. Dunbar, and S. Juretschko. Multiplexed detection and identification of respiratory pathogens using the NxTAG® respiratory pathogen panel. *Methods*, 158:61–68, 2019.

[45] P. R. Halmos. *Transformations and Functions*, pages 161–183. Springer New York, New York, NY, 1950.

[46] P. Hou, J. M. Tebbs, C. R. Bilder, and C. S. McMahan. Hierarchical group testing for multiple infections. *Biometrics*, 73(2):656–665, 2017.

[47] P. Hou, J. M. Tebbs, D. Wang, C. S. McMahan, and C. R. Bilder. Array testing for multiplex assays. *Biostatistics*, 21(3):417–431, 2020.

[48] F. K. Hwang. Optimal partitions. *Journal of Optimization Theory and Applications*, 34(1):1–10, 1981.

[49] F. K. Hwang, J. Sun, and E. Y. Yao. Optimal set partitioning. *SIAM Journal on Algebraic and Discrete Methods*, 6(1):163–170, 1985.

[50] Johns Hopkins University. Coronavirus Resource Center. https://coronavirus.jhu.edu/region/united-states, 2022. Accessed in June 2022.

[51] M. Johnson. PCR machines. *Materials and Methods*, 3:193, 2021.

[52] S. Kenmoe, C. Tcharnenwa, G. C. Monamele, C. N. Kengne, et al. Comparison of FTD® respiratory pathogens 33 and a singleplex CDC assay for the detection of respiratory viruses: A study from Cameroon. *Diagnostic Microbiology and Infectious Diseases*, 94(3):236–242, 2019.

[53] E. Keyvanshokooh, C. Shi, and M. P. Van Oyen. Online advance scheduling with overtime: A primal-dual approach. *Manufacturing & Service Operations Management*, 23(1):246–266, 2021.

[54] H.-Y. Kim, M. G. Hudgens, J. M. Dreyfuss, D. J. Westreich, and C. D. Pilcher. Comparison of group testing algorithms for case identification in the presence of test error. *Biometrics*, 63(4):1152–1163, 2007.

[55] M. Kuczma. *An Introduction to the Theory of Functional Equations and Inequalities: Cauchy's Equation and Jensen's Inequality*. Birkhäuser Basel, Basel, Switzerland, 2009.

[56] D. S. Leland and C. C. Ginocchio. Role of cell culture for virus detection in the age of technology. *Clinical Microbiolology Reviews*, 20(1):49–78, 2007.

[57] D. Levine. *A Parallel Genetic Algorithm for the Set Partitioning Problem*, pages 23–35. Springer US, Boston, MA, 1996.

[58] M. Lewis, G. Kochenberger, and B. Alidaee. A new modeling and solution approach for the set-partitioning problem. *Computers & Operations Research*, 35(3):807–813, 2008.

[59] C. Lindan, M. Mathur, S. Kumta, H. Jerajani, et al. Utility of pooled urine specimens for detection of Chlamydia trachomatis and Neisseria gonorrhoeae in men attending public sexually transmitted infection clinics in Mumbai, India, by PCR. *Journal of Clinical Microbiology*, 43(4):1674–1677, 2005.

[60] C. Llor and L. Bjerrum. Antimicrobial resistance: risk associated with antibiotic overuse and initiatives to reduce the problem. *Therapeutic Advances in Drug Safety*, 5(6):229–241, 2014.

[61] J. B. Mahony, G. Blackhouse, J. Babwah, M. Smieja, et al. Cost analysis of multiplex PCR testing for diagnosing respiratory virus infections. *Journal of Clinical Microbiology*, 47(9):2812–2817, 2009.

[62] F. Manne and T. Sorevik. Optimal partitioning of sequences. *Journal of Algorithms*, 19(2):235–249, 1995.

[63] P. Mastrantonio, P. Stefanelli, M. Giuliano, Y. Herrera Rojas, et al. Bordetella parapertussis infection in children: epidemiology, clinical symptoms, and molecular characteristics of isolates. *Journal of Clinical Microbiology*, 36 (4):999–1002, 1998.

[64] S. May, A. Gamst, R. Haubrich, C. Benson, and D. M. Smith. Pooled nucleic acid testing to identify antiretroviral treatment failure during HIV infection. *Journal of Acquired Immune Deficiency Syndromes*, 53(2):194, 2010.

[65] R. G. Newcombe. Two-sided confidence intervals for the single proportion: comparison of seven methods. *Statistics in Medicine*, 17(8):857–872, 1998.

[66] N. T. Nguyen, H. Aprahamian, E. K. Bish, and D. R. Bish. A methodology for deriving the sensitivity of pooled testing, based on viral load progression and pooling dilution. *Journal of Translational Medicine*, 17(1):1–10, 2019.

[67] N. T. Nguyen, E. K. Bish, and D. R. Bish. Optimal pooled testing design for prevalence estimation under resource constraints. *Omega*, 105:102504, 2021.

[68] M. Ogilvie. Molecular techniques should not now replace cell culture in diagnostic virology laboratories. *Reviews in Medical Virology*, 11(6):351–354, 2001.

[69] B. Olstad and F. Manne. Efficient partitioning of sequences. *IEEE Transactions on Computers*, 44(11):1322–1326, 1995.

[70] K. Oved, A. Cohen, O. Boico, R. Navon, et al. A novel host-proteome signature for distinguishing between acute bacterial and viral infections. *PLoS One*, 10(3):e0120012, 2015.

[71] G. Perakis and G. Roels. Regret in the newsvendor model with partial information. *Operations Research*, 56(1): 188–203, 2008.

[72] B. Pinsky and R. Hayden. Cost-effective respiratory virus testing. *Journal of Clinical Microbiology*, 57(9): e00373–19, 2019.

[73] J. Rachlin, C. Ding, C. Cantor, and S. Kasif. MuPlex: multi-objective multiplex PCR assay design. *Nucleic Acids Research*, 33(suppl_2):W544–W547, 2005.

[74] P. Ramanan, A. L. Bryson, M. J. Binnicker, B. S. Pritt, and R. Patel. Syndromic panel-based testing in clinical microbiology. *Clinical Microbiology Reviews*, 31(1):e00024–17, 2018.

[75] B. B. Rogers, P. Shankar, R. C. Jerris, D. Kotzbauer, E. J. Anderson, J. R. Watson, L. A. O'Brien, F. Uwindatwa, K. McNamara, and J. E. Bost. Impact of a rapid respiratory panel test on patient outcomes. *Archives of Pathology and Laboratory Medicine*, 139(5):636–641, 2015.

[76] P. C. Schreckenberger and A. J. McAdam. Point-counterpoint: Large multiplex PCR panels should be first-line tests for detection of respiratory and intestinal pathogens. *Journal of Clinical Microbiology*, 53(10):3110–3115, 2015.

[77] A. Subramony, P. Zachariah, A. Krones, S. Whittier, and L. Saiman. Impact of multiplex polymerase chain reaction testing for respiratory pathogens on healthcare resource utilization for pediatric inpatients. *The Journal of Pediatrics*, 173:196–201, 2016.

[78] S. M. Taylor, J. J. Juliano, P. A. Trottman, J. B. Griffin, et al. High-throughput pooling and real-time PCR-based strategy for malaria detection. *Journal of Clinical Microbiology*, 48(2):512–519, 2010.

[79] J. M. Tebbs, C. S. McMahan, and C. R. Bilder. Two-stage hierarchical group testing for multiple infections with application to the infertility prevention project. *Biometrics*, 69(4):1064–1073, 2013.

[80] K. E. Templeton. Why diagnose respiratory viral infection? *Journal of Clinical Virology*, 40:S2, 2007.

[81] E. Vallières and C. Renaud. Clinical and economical impact of multiplex respiratory virus assays. *Diagnostic Microbiology and Infectious Diseases*, 76(3):255–261, 2013.

[82] T. T. Van, J. Miller, D. M. Warshauer, E. Reisdorf, et al. Pooling nasopharyngeal/throat swab specimens to increase testing capacity for influenza viruses by PCR. *Journal of Clinical Microbiology*, 50(3):891–896, 2012.

[83] M. Van Hulst, G. A. Hubben, K. W. Sagoe, C. Promwong, et al. Web interface-supported transmission risk assessment and cost-effectiveness analysis of postdonation screening: a global model applied to Ghana, Thailand, and the Netherlands. *Transfusion*, 49(12):2729–2742, 2009.

[84] G. van Zyl, W. Preiser, S. Potschka, A. Lundershausen, et al. Pooling strategies to reduce the cost of HIV-1 RNA load monitoring in a resource-limited setting. *Clinical Infectious Diseases*, 52(2):264–270, 2011.

[85] I. Yelin, N. Aharony, E. S. Tamar, A. Argoetti, et al. Evaluation of COVID-19 RT-qPCR test in multi sample pools. *Clinical Infectious Diseases*, 71(16):2073–2078, 2020.

[86] J. Yuan, J. Yi, M. Zhan, Q. Xie, et al. The web-based multiplex PCR primer design software Ultiplex and the associated experimental workflow: up to 100-plex multiplicity. *BMC Genomics*, 22(1):1–17, 2021.

Title: Disease Bundling or Specimen Bundling? Cost- and Capacity-Efficient Strategies for Multi-disease Testing with Genetic Assays

Authors:

Douglas R. Bish: Professor, Department of Information Systems, Statistics, and Management Science, University of Alabama, Tuscaloosa, Alabama, 35487, United States, email: *drbish@cba.ua.edu*

Ebru K. Bish: Professor, Department of Information Systems, Statistics, and Management Science, University of Alabama, Tuscaloosa, Alabama, 35487, United States, email: *ekbish@cba.ua.edu*

Hussein El Hajj: Assistant Professor, Department of Information Systems and Analytics, Santa Clara University, Santa Clara, California, 95053, United States, email: *helhajj@scu.edu*

A Online Appendix

A.1 Summary of Notation

We denote vectors in boldface, random variables in upper-case and their realization in lower-case letters, use ";" for probabilistic conditioning, and provide the arguments of a function in parantheses.

The disease set $N = \{1, 2, \cdots, n\}$ is arranged in non-increasing order of disease prevalences $\pi_i, i \in N$, that is, $\pi_1 \geq \pi_2 \cdots \geq \pi_n$. The *joint* vector, $\boldsymbol{p}$, contains all mono-, co-, and no-infection probabilities for the n diseases, and the *marginal* vector $\boldsymbol{\pi} = (\pi_i)_{i \in N}$ contains the disease prevalences (Definition 1). $\boldsymbol{S} = (S^k)_{k=1,\cdots,q}$, $q = 1, \cdots, n$, denotes a q-partition of the disease set N, where each assay S^k has cardinality (size) s^k, prevalence $\pi(S^k)$, and pool size t^k, with $t^{*k}(S^k) = t^{*k}(\pi(S^k))$ denoting an optimal pool size within the domain $t \in Z^+, t \geq 1$ (with $t = 1$ denoting individual testing), which is a function of assay prevalence $\pi(S^k)$ only (Property 1). When referring to an optimal Dorfman pool size, we use the notation $t_D^{*k}(\pi(S^k))$, that is, considering the domain $t \in Z^+, t \geq 2$. We use the terms partition and assay portfolio interchangeably. In general, we use the superscripts k, k', l for assay (with a subscript added to the index in places, e.g., k_1, k_2), and the subscripts i, j, r for disease.

Functions $T(S, t)$ and $C(S, t)$ respectively denote the per subject expected number of tests ("expected tests") and per subject expected testing cost ("expected testing cost") for assay S with pool size t, and $TC(\boldsymbol{S}, \boldsymbol{t}, \lambda)$ denotes the expected total testing cost ("total cost") for partition $\boldsymbol{S}$, pool size vector $\boldsymbol{t}$, and coefficient $\lambda \in [0, 1]$, where λ (hence, $1 - \lambda$) is the weight of the expected testing cost (expected tests) in the objective function.

By Definition 3, $D^{(q)}$ and $I^{(q)}$, $q = 1, \cdots, n$, and $M^{(q)}$, $q = 2, \cdots, n$, respectively denote the *optimal* testing design when constrained to be within the q-partitioned Dorfman, individual-testing, and mixed-testing design classes (an $M^{(1)}$ design is not possible). When needed, we use the design class as a subscript to refer to the corresponding metric for the optimal design within that design class, e.g., $\boldsymbol{S}_{D^{(q)}}$, $T_{D^{(q)}}$, and $TC_{D^{(q)}}$ respectively denote the partition, the expected tests, and the total cost for an optimal $D^{(q)}$ design.

The composite cost function is given by $\tilde{c}(s, \lambda) = \lambda\ c(s) + 1 - \lambda, \forall s \in Z^+, \lambda \in [0, 1]$, where $c(.)$ is the assay cost function; by definition, any $\tilde{c}(.) \in \tilde{C}$ must satisfy Assumption ($\boldsymbol{A}$). When needed, we use the notation that composite cost functions $\tilde{c}(.)$ and $\tilde{c}'(.)$ respectively utilize assay cost functions $c(.)$ and $c'(.)$. The notation, $\tilde{c}(.) \geq_{diff} \tilde{c}'(.)$, denotes that function $\tilde{c}(.)$ has higher differences than function $\tilde{c}'(.)$ (Definition 5).

To simplify the notation, we drop the indices and function arguments when clear from context, e.g., $\tilde{c}(s)$ for $\tilde{c}(s, \lambda)$ when λ does not change, or $\tilde{c}(.)$ when referring to a generic composite cost function, $\boldsymbol{S}$ for $\boldsymbol{S}_{D^{(q)}}$ when it is clear from context that we are referring to an optimal partition for the $D^{(q)}$ design class. We also use the notation that $T^*(S) = T^*(\pi(S)) = T(\pi(S), t^*(\pi(S)))$ and $T_D^*(S) = T_D^*(\pi(S)) = T(\pi(S), t_D^*(\pi(S)))$, that is, expected tests for assay S at the (global) optimal pool size, and at the optimal Dorfman pool size, respectively.

A.2 Preliminaries

By Definition 3, optimal pool size vectors for the different design classes are given by, $\boldsymbol{t}_{I^{(q)}} = \boldsymbol{1}$, $\boldsymbol{t}_{D^{(q)}} \geq \boldsymbol{2}$, and $\boldsymbol{t}_{M^{(q)}} : \exists k, l = 1, \cdots, q : t^k_{M^{(q)}} = 1,\ t^l_{M^{(q)}} \geq 2$. Any assay with individual testing ($t = 1$) uses one test per subject for all the diseases in the assay, i.e., $T(S, 1) = 1, \forall S \subseteq N$ (Eq. (8)).

Then, by Eq. (2), the total cost of the (global) **TD** optimal solution (denoted by superscript *), and the optimal solution when constrained to be within each design class (denoted by the design class subscript), follow:

$$TC^*(\lambda) = \quad TC(\boldsymbol{S}^*, \boldsymbol{t}^*, \lambda) \ = \ \sum_{k=1}^{q^*} \tilde{c}(s^{k*}, \lambda) \times T^*(S^{k*}), \quad \text{where } q^* \in \{1, \cdots, n\} \tag{17}$$

$$TC_{I^{(q)}}(\lambda) \ = \ \sum_{k=1}^{q} \tilde{c}(s^k_{I^{(q)}}, \lambda) \times T(S^k_{I^{(q)}}, 1) = \sum_{k=1}^{q} \tilde{c}(s^k_{I^{(q)}}, \lambda) \times 1 = \sum_{k=1}^{q} \tilde{c}(s^k_{I^{(q)}}, \lambda), \quad \forall q = 1, \cdots, n \tag{18}$$

$$TC_{D^{(q)}}(\lambda) \ = \ \sum_{k=1}^{q} \tilde{c}(s^k_{D^{(q)}}, \lambda) \times T^*_D(S^k_{D^{(q)}}) = \sum_{k=1}^{q} \tilde{c}(s^k_{D^{(q)}}, \lambda) \times \left[\frac{1}{t^{k*}_{D^{(q)}}} + 1 - \left(1 - \pi(S^k_{D^{(q)}})\right)^{t^{k*}_{D^{(q)}}} \right], \quad \forall q = 1, \cdots, n \tag{19}$$

$$TC_{M^{(q)}}(\lambda) \ = \ \sum_{k=1..q : t^k_{M^{(q)}} = 1} \tilde{c}(s^k_{M^{(q)}}, \lambda) \times T(S^k_{M^{(q)}}, 1) + \sum_{l=1..q : t^l_{M^{(q)}} \geq 2} \tilde{c}(s^l_{M^{(q)}}, \lambda) \times T^*_D(S^l_{M^{(q)}}). \tag{20}$$

The following definition and properties will be used subsequently in the proofs.

Definition A1. *1. Function $f(.)$ is a subadditive real-valued function if $f(x+y) \leq f(x)+f(y)$, $\forall x, y \in \mathbb{R}$ [55]. 2. Function $f(.)$ is a subadditive set function if $f(S^1 \cup S^2) \leq f(S^1)+f(S^2)$, for any pair of sets S^1, S^2 [45].*

Property A.1. *(1) $T^*(\pi(S))$ and $T_D^*(\pi(S))$ are subadditive in $\pi(S) \in [0, \underline{p}]$. (2) Both $c(s)$ and $\tilde{c}(s,\lambda)$ are subadditive in $s \in Z^+$, $\forall \lambda \in [0,1]$. (3) $\pi(S^1 \cup S^2)$ is a subadditive set function, $\forall S^1, S^2 \subseteq N$.*

Proof. $T_D^*(\pi(S))$ is non-negative and concave increasing in $\pi(S) \in [0, \underline{p}]$, and $T^*(\pi(S)) = T_D^*(\pi(S))$ for $\pi(S) \in [0, \underline{p}]$ (Property 2). Similarly, $c(s)$ is non-negative and concave non-decreasing in $s, \forall s \in Z^+$ (Assumption ($\boldsymbol{A}$)), and $\tilde{c}(s,\lambda) = \lambda\ c(s) + 1 - \lambda$ is a linear function of $c(s)$, $\forall \lambda \in [0,1]$; and for any two sets $S^1, S^2 \subseteq N$, $\pi(S^1 \cup S^2) = \pi(S^1) + \pi(S^2) - \pi(S^1 \cap S^2) \leq \pi(S^1) + \pi(S^2)$. Then, the subadditivity results follow by Definition A1. □

Property A.2. *For the independent diseases or no co-infections cases, $T^*(S)$ is strictly concave increasing in each π_i, $\forall i \in S$, as long as $\pi(S) \leq \underline{p}$.*

Proof. For both the independent diseases and no co-infections cases, $\pi(S)$ is linear increasing in π_i, $\forall i \in S$ (Eqs. (15)-(16)), and $T^*(\pi(S))$ is strictly concave increasing in $\pi(S) \in [0, \underline{p}]$ (Property 2). Then, it follows that $T^*(\pi(S))$ is strictly concave increasing in $\pi_i, \forall i \in S$, in the region $0 \leq \pi(S) \leq \underline{p}$ [14]. □

Remark A.1. *If $\boldsymbol{\Pi}$ has an interval type uncertainty set given by,*

$$\Omega(\boldsymbol{\Pi}) = \{\boldsymbol{\pi} : \pi_i \in [\underline{\pi}_i, \overline{\pi}_i], i \in N\}, \quad \text{where } 0 \leq \underline{\pi}_i \leq \overline{\pi}_i \leq 1,\ i \in N, \tag{21}$$

then $\boldsymbol{P}$ has the following uncertainty set,

$$\Omega(\boldsymbol{P}) = \{\boldsymbol{p} \geq \boldsymbol{0} : (\boldsymbol{p}; \boldsymbol{\pi}) \text{ is a solution to (5)-(6)}, \quad \boldsymbol{\pi} \in \Omega(\boldsymbol{\Pi})\}, \tag{22}$$

where $(\boldsymbol{p}; \boldsymbol{\pi})$ (i.e., $\boldsymbol{p}$ conditional on $\boldsymbol{\pi}$) represents a solution to (5)-(6) for a given realization $\boldsymbol{\pi} \in \Omega(\boldsymbol{\Pi})$, and set $\Omega(\boldsymbol{P})$ contains all such non-negative solutions, $(\boldsymbol{p}; \boldsymbol{\pi})$, for $\boldsymbol{\pi} \in \Omega(\boldsymbol{\Pi})$. Note that for each given $\boldsymbol{\pi} \in \Omega(\boldsymbol{\Pi})$, there may be multiple solutions, $(\boldsymbol{p}; \boldsymbol{\pi})$, i.e., with different mono-/co-infection probabilities, because the linear system in (5)-(6), where $\boldsymbol{\pi}$ is given, has 2^n unknowns and $n+1$ constraints, where $2^n > n+1, \forall n \geq 2$.
Similarly, given an uncertainty set on $\boldsymbol{P}$, denoted by $\Omega(\boldsymbol{P})$, the uncertainty set on $\boldsymbol{\Pi}$ is given by,

$$\Omega(\boldsymbol{\Pi}) = \{\boldsymbol{\pi} \geq \boldsymbol{0} : (\pi_i; \boldsymbol{p}), i \in N, \text{ is the unique solution to (5)}, \quad \boldsymbol{p} \in \Omega(\boldsymbol{P})\}.$$

Letting $\underline{\pi}_i \equiv \min\{\pi_i \in \Omega(\boldsymbol{\Pi})\}$ and $\overline{\pi}_i \equiv \max\{\pi_i \in \Omega(\boldsymbol{\Pi})\}, \forall i \in N$, we can equivalently write:

$$\Omega(\boldsymbol{\Pi}) = \{\boldsymbol{\pi} : \pi_i \in [\underline{\pi}_i, \overline{\pi}_i], i \in N\}.$$

Thus, given an uncertainty set $\Omega(\boldsymbol{\Pi})$, one can obtain an uncertainty set $\Omega(\boldsymbol{P})$, and vice versa.

A.3 Supporting Results

Theorem A.1. *Consider $\Omega(\boldsymbol{\Pi}) = \{\boldsymbol{\pi} : \pi_i \in [\underline{\pi}_i, \overline{\pi}_i], i \in N\}$, where $0 \leq \underline{\pi}_i \leq \overline{\pi}_i \leq 1,\ i \in N$, and its equivalent $\Omega(\boldsymbol{P})$ from Remark A.1. For any given $\boldsymbol{x}$ and $\boldsymbol{t}$, the inner maximization in* **R-TD** *objective function (14) can be equivalently expressed as follows:*

$$\max_{\boldsymbol{p} \in \Omega(\boldsymbol{P})} \left\{ \lambda \sum_{k=1}^{n} C(\boldsymbol{x}^k, t^k; \boldsymbol{p}) + (1-\lambda) \sum_{k=1}^{n} T(\boldsymbol{x}^k, t^k; \boldsymbol{p}) \right\} = \sum_{k=1}^{n} \left[\max_{\boldsymbol{p} \in \Omega(\boldsymbol{P})} \left\{ \lambda \times C(\boldsymbol{x}^k, t^k; \boldsymbol{p}) + (1-\lambda) \times T(\boldsymbol{x}^k, t^k; \boldsymbol{p}) \right\} \right]$$

$$= \sum_{k=1}^{n} \tilde{c}\left(\sum_{i \in N} x_i^k, \lambda \right) \times \min \left\{ 1,\ \frac{1}{t^k} + 1 - \left(1 - \min \left\{ 1, \sum_{i \in N} \overline{\pi}_i x_i^k \right\} \right)^{t^k} \right\}, \tag{23}$$

where, for each $\boldsymbol{x}$, $\exists \boldsymbol{p} \in \Omega(\boldsymbol{P})$: $\pi(\boldsymbol{x}^k; \boldsymbol{p}) = \min\left\{1, \sum_{i \in N} \overline{\pi}_i x_i^k\right\}$, $\forall k = 1, \cdots, n$.

Corollary A.1. *For the special case where $\sum_{i \in N} \overline{\pi}_i \leq 1$, the worst-case solution, $\pi(\boldsymbol{x}^k; \boldsymbol{p}) = \min\left\{1, \sum_{i \in N} \overline{\pi}_i x_i^k\right\}$, $\forall k = 1, \cdots, n$, is attained at $\boldsymbol{p}$: $p_i = \overline{\pi}_i, \forall i \in N,\ p_{ij} = 0, \forall ij \in N(2),\ p_{ijr} = 0, \forall ijr \in N(3), \cdots, p_{12\ldots n} = 0,\ p_0 = 1 - \sum_{i \in N} \overline{\pi}_i$, that is, each marginal prevalence is at its upper limit and there are no co-infections.*

A.4 Proofs

Proof of Theorem A.1. From the definitions of $\Omega(\mathbf{\Pi})$ and $\Omega(\boldsymbol{P})$ (Eqs. (21), (22)), for any given assay portfolio $\boldsymbol{x} = (\boldsymbol{x}^k)_{k=1,\cdots,n}$ and pool size vector $\boldsymbol{t} = (t^k)_{k=1,\cdots,n}$, we can write:

$$\max_{\boldsymbol{p}\in\Omega(\boldsymbol{P})} \left\{ \lambda \sum_{k=1}^{n} C(\boldsymbol{x}^k, t^k; \boldsymbol{p}) + (1-\lambda) \sum_{k=1}^{n} T(\boldsymbol{x}^k, t^k; \boldsymbol{p}) \right\} \tag{24}$$

$$= \max_{\boldsymbol{p}\in\Omega(\boldsymbol{P})} \left\{ \sum_{k=1}^{n} \tilde{c}\Big(\sum_{i\in N} x_i^k, \lambda \Big) \times \min\left\{ 1,\ \frac{1}{t^k} + 1 - \Big(1 - \pi(\boldsymbol{x}^k; \boldsymbol{p})\Big)^{t^k} \right\} \right\} \tag{25}$$

$$\leq \sum_{k=1}^{n} \left[\max_{\boldsymbol{p}\in\Omega(\boldsymbol{P})} \left\{ \tilde{c}\Big(\sum_{i\in N} x_i^k, \lambda \Big) \times \min\left\{ 1,\ \frac{1}{t^k} + 1 - \Big(1 - \pi(\boldsymbol{x}^k; \boldsymbol{p})\Big)^{t^k} \right\} \right\} \right] \tag{26}$$

$$= \sum_{k=1}^{n} \tilde{c}\Big(\sum_{i\in N} x_i^k, \lambda \Big) \times \max_{\boldsymbol{p}\in\Omega(\boldsymbol{P})} \left\{ \min\left\{ 1,\ \frac{1}{t^k} + 1 - \Big(1 - \pi(\boldsymbol{x}^k; \boldsymbol{p})\Big)^{t^k} \right\} \right\} \tag{27}$$

$$\leq \sum_{k=1}^{n} \tilde{c}\Big(\sum_{i\in N} x_i^k, \lambda \Big) \times \min\left\{ 1,\ \frac{1}{t^k} + 1 - \left(1 - \min\left\{1, \sum_{i\in N} \overline{\pi}_i x_i^k\right\}\right)^{t^k} \right\}, \tag{28}$$

where (25) follows by Eqs. (2) and (8); (26) follows because, for a given assay portfolio $\boldsymbol{x} = (\boldsymbol{x}^k)_{k=1,\cdots,n}$, and pool size vector $\boldsymbol{t} = (t^k)_{k=1,\cdots,n}$, the solution to (24) requires a *common* worst-case vector, $\boldsymbol{p} \in \Omega(\boldsymbol{P})$, for *all* assays $k = 1, \cdots, n$, while (26) relaxes this restriction and allows for a potentially different worst-case vector, $\boldsymbol{p}^k \in \Omega(\boldsymbol{P})$, for *each* assay $k = 1, \cdots, n$. (27) follows because the term, $\sum_{k=1}^{n} \tilde{c}\Big(\sum_{i\in N} x_i^k, \lambda \Big)$, is a constant for a given $\boldsymbol{x}$, that is, independent of the joint vector $\boldsymbol{p}$. Finally, the upper bound in (28) follows, because for any given $\boldsymbol{x}^k$ and t^k, the term, $\frac{1}{t^k} + 1 - \big(1 - \pi(\boldsymbol{x}^k; \boldsymbol{p})\big)^{t^k}$ is strictly increasing in $\pi(\boldsymbol{x}^k; \boldsymbol{p})$, and $\pi(\boldsymbol{x}^k; \boldsymbol{p}) \leq \min\left\{1, \sum_{i\in N} \overline{\pi}_i x_i^k\right\}, \forall k = 1, \cdots, n$.

Then, to prove the equivalence of (24) and (27), and the equivalence of (27) and (28), it is sufficient to show that, for a given $\boldsymbol{x}$ and $\boldsymbol{t}$, there exists a *common* $\boldsymbol{p} \in \Omega(\boldsymbol{P})$ (for all assays $1, \cdots, n$) that corresponds to the upper bound in (28), in which case this particular $\boldsymbol{p}$ must be a worst-case solution to both (24) and (27). Equivalently, we wish to show that $\exists \boldsymbol{p} \geq \boldsymbol{0}$ that satisfies: **(i) (assay equations)** $\pi(\boldsymbol{x}^k; \boldsymbol{p}) = \min\left\{1, \sum_{i\in N} \overline{\pi}_i x_i^k\right\}, \forall k = 1, \cdots, n$; **(ii) (disease equations)** $Pr(A_i^+; \boldsymbol{p}) = \overline{\pi}_i$; and **(iii) (universal set equation)** $(\pi(N); \boldsymbol{p}) + p_0 = 1$, where (i) follows from (28), and (ii)-(iii), along with the constraint $\boldsymbol{p} \geq \boldsymbol{0}$, ensure that $\boldsymbol{p} \in \Omega(\boldsymbol{P})$.

Observe that if an assay has exactly one disease, then its assay equation reduces to the equation for its corresponding disease, and is redundant; these assay equations are omitted from further consideration. Therefore, we only consider the assay equations for assays in $Q \equiv \{k = 1, \cdots, n : s^k \geq 2\}$, with cardinality $m : 0 \leq m \leq \lfloor \frac{n}{2} \rfloor$; without loss of generality, the assays in Q are re-indexed as assays $1, \cdots, m$. Thus, we wish to show that the following system of linear equations (based on Eqs. (3)-(5)) has a non-negative solution, $\boldsymbol{p} \in \Re^{+(2^n)\times 1}$:

$$p_i + \textstyle\sum_{j:ij\in N(2)} p_{ij} + \sum_{j:ji\in N(2)} p_{ji} + \cdots + p_{12\cdots n} = \overline{\pi}_i, \quad \forall i \in N, \tag{29}$$

$$\textstyle\sum_{i\in S^k} p_i + \sum_{ij\in N(2): i\in S^k \text{ or } j\in S^k} p_{ij} + \cdots + p_{12\ldots n} = \min\left\{1, \sum_{i\in S^k} \overline{\pi}_i\right\}, \quad \forall k \in Q \tag{30}$$

$$p_0 + \textstyle\sum_{i\in N} p_i + \sum_{ij\in N(2)} p_{ij} + \sum_{ijr\in N(3)} p_{ijr} + \cdots + p_{12\ldots n} = 1. \tag{31}$$

This system has $n + m + 1$ linearly independent equations and 2^n unknowns (i.e., each element of $\boldsymbol{p}$), where $2^n \geq n + \lfloor \frac{n}{2} \rfloor + 1, \forall n \geq 2$. Let $\boldsymbol{A} \in \{0,1\}^{(n+m+1)\times(2^n)}$ and $\boldsymbol{b} \in \Re^{+(n+m+1)\times 1}$ respectively denote the binary coefficient matrix, and the non-negative RHS of this system of linear equations. By Farka's Lemma [29], exactly one of the following alternatives hold:

1. Either $\exists \boldsymbol{p} \in \Re^{(2^n)\times 1}$ that satisfies:

$$\boldsymbol{A}\boldsymbol{p} = \boldsymbol{b}, \quad \boldsymbol{p} \geq \boldsymbol{0}, \tag{F-1}$$

2. or else $\exists \boldsymbol{y} = (u_1, \cdots, u_n, v_1, \cdots, v_m, z) \in \Re^{(n+m+1)\times 1}$, where u_i corresponds to (29) for disease $i \in N$, v_k corresponds to (30) for assay $k \in Q$, and z corresponds to (31), that satisfies:

$$\boldsymbol{A}^T\boldsymbol{y} \geq \boldsymbol{0}, \tag{F-2a}$$

$$\boldsymbol{b}^T\boldsymbol{y} < 0. \tag{F-2b}$$

Then it suffices to show that $\nexists \boldsymbol{y} \in \Re^{(n+m+1)\times 1}$ that satisfies (F-2a)-(F-2b), which we prove by contradiction.

To simplify the subsequent presentation, we introduce some new notation. Denote the columns of $\boldsymbol{A}$ by $\boldsymbol{A}_x, x = 1, \cdots, 2^n$, where each column represents the constraint coefficients for an element of $\boldsymbol{p} \in \Re^{+(2^n)\times 1}$. Hence, each row of (F-2a), $\boldsymbol{A}_x^T\boldsymbol{y} \geq 0$, corresponds to an element of $\boldsymbol{p}$, which is the probability of either a mono-infection ($p_i, i \in N$), a co-infection ($p_{i\cdots j}, i, \cdots, j \in N$), or no-infection ($p_0$); in either case, it is the probability of a set of diseases $S \subseteq N$ (e.g., $S = \{i\}, S = \{i, \cdots, j\}, S = \emptyset$), and we refer to this inequality as (F-2a)(S), i.e., indexed by its disease set. As defined above, $\boldsymbol{p}, \boldsymbol{b}$, and $\boldsymbol{y}$ are all column vectors.

Suppose, to the contrary, that $\boldsymbol{y} = (u_1, \cdots, u_n, v_1, \cdots, v_m, z)$ is a solution to (F-2a)-(F-2b). Based on the signs of assay and disease variables, we decompose assay set Q into six mutually exclusive sets:

$$\begin{aligned}
&Q_{a+}^{i+} \equiv \{k \in Q : v_k \geq 0 \text{ and } \{u_i \geq 0, \forall i \in S^k\}\}, \quad Q_{a+}^{i-} \equiv \{k \in Q : v_k \geq 0 \text{ and } \{u_i < 0, \forall i \in S^k\}\},\\
&Q_{a+}^{i0} \equiv \{k \in Q : v_k \geq 0 \text{ and } \{\exists i \in S^k : u_i \geq 0, \text{ and } \exists j \in S^k : u_j < 0\}\},\\
&Q_{a-}^{i+} \equiv \{k \in Q : v_k < 0 \text{ and } \{u_i \geq 0, \forall i \in S^k\}\}, \quad Q_{a-}^{i-} \equiv \{k \in Q : v_k < 0 \text{ and } \{u_i < 0, \forall i \in S^k\}\},\\
&Q_{a+}^{i0} \equiv \{k \in Q : v_k < 0 \text{ and } \{\exists i \in S^k : u_i \geq 0, \text{ and } \exists j \in S^k : u_j < 0\}\}.
\end{aligned} \tag{32}$$

Observe that we use the indices k and i to respectively refer to assay variables and disease variables; the subscripts $a+$ and $a-$ to respectively refer to assay sets with non-negative versus negative assay variables (v_k); and the superscripts $i+$, $i-$, and $i0$ to respectively refer to assay sets whose corresponding disease variables (u_i) are all non-negative, negative, or neither. Finally, let $S^{k-} \equiv \{i \in S^k : u_i < 0\}, k \in Q$.

The proof by contradiction proceeds in two parts. First we consider a specific row of (F-2a) and perform row operations on it in order to bring it into a form that is a lower bound for the LHS of (F-2b), and show that this lower bound is non-negative, thus reaching a contradiction with the inequality in (F-2b).

To this end, consider disease set $\tilde{S} \subseteq N$:

$$\tilde{S} \equiv \bigcup_{k \in Q_{a-}^{i+}} argmin_{i \in S^k}\{u_i\} \bigcup_{k \in Q_{a+}^{i-} \cup Q_{a-}^{i-}} S^k \bigcup_{k \in Q_{a+}^{i0} \cup Q_{a-}^{i0}} S^{k-},$$

which contains the disease with the lowest u_i value (breaking ties arbitrarily) for each assay $k \in Q_{a-}^{i+}$, all the diseases in assays $k \in Q_{a+}^{i-} \cup Q_{a-}^{i-}$, and all the diseases with a negative u_i value in assays $k \in Q_{a+}^{i0} \cup Q_{a-}^{i0}$. (As will be clear in the sequel, the diseases in the assays in set Q_{a+}^{i+} are omitted, as their assay and disease variables are non-negative by definition). Consider the joint (co-infection) probability of the $\tilde{s}$ diseases in set $\tilde{S}$, and its corresponding column $\boldsymbol{A}_x$, where $\boldsymbol{A}_{i,x} = 1$, $\forall i \in \tilde{S}$, $\boldsymbol{A}_{n+k,x} = 1$ if $\tilde{S} \cap S^k \neq \emptyset$, $\forall k \in Q$, $\boldsymbol{A}_{n+m+1,x} = 1$, and $\boldsymbol{A}_{j,x} = 0$ otherwise. Then:

$$\text{(F-2a)}(\tilde{S}): \quad z + \sum_{k \in Q_{a+}^{i-}} v_k + \sum_{k \in Q_{a+}^{i0}} v_k + \sum_{k \in Q_{a-}^{i+}} v_k + \sum_{k \in Q_{a-}^{i-}} v_k + \sum_{k \in Q_{a-}^{i0}} v_k + \sum_{k \in Q_{a+}^{i-}} \sum_{i \in S^k} u_i + \sum_{k \in Q_{a+}^{i0}} \sum_{i \in S^{k-}} u_i$$

$$+ \sum_{k\in Q^{i+}_{a-}} \min_{i\in S^k}\{u_i\} + \sum_{k\in Q^{i-}_{a-}} \sum_{i\in S^k} u_i + \sum_{k\in Q^{i0}_{a-}} \sum_{i\in S^{k-}} u_i \geq 0.$$

Through a series of row operations (detailed below), (F-2a)($\tilde{S}$) can be converted into the following form:

$$\begin{aligned} z + \sum_{k\in Q^{i-}_{a+}} v_k \times \max_{i\in S^k}\{\overline{\pi}_i\} + \sum_{k\in Q^{i0}_{a+}} v_k \times \max_{i\in S^{k-}}\{\overline{\pi}_i\} + \sum_{k\in Q^{i+}_{a-}\cup Q^{i-}_{a-}\cup Q^{i0}_{a-}} v_k \times \min\{1, \sum_{i\in S^k} \overline{\pi}_i\} \\ + \sum_{k\in Q^{i+}_{a-}} \min_{i\in S^k}\{u_i\} \times \min\{1, \sum_{j\in S^k} \overline{\pi}_j\} + \sum_{k\in Q^{i-}_{a+}} \sum_{i\in S^k} u_i \times \max_{j\in S^k}\{\overline{\pi}_j\} + \sum_{k\in Q^{i-}_{a-}} \sum_{i\in S^k} u_i \times \min\{1, \sum_{j\in S^k} \overline{\pi}_j\} \\ + \sum_{k\in Q^{i0}_{a+}} \sum_{i\in S^{k-}} u_i \times \max_{j\in S^{k-}}\{\overline{\pi}_j\} + \sum_{k\in Q^{i0}_{a-}} \sum_{i\in S^{k-}} u_i \times \min\{1, \sum_{j\in S^k} \overline{\pi}_j\} \geq 0. \end{aligned} \tag{33}$$

In the remainder of the proof, we first describe the bounding of the LHS of (33), so as to reach a contradiction based on Farka's Lemma. Then we detail the specific row operations needed to convert (F-2a)($\tilde{S}$) to (33).

Bounding the LHS of (33): We bound the LHS of (33) to reach the form in (F-2b), i.e., $\boldsymbol{b}^T\boldsymbol{y}$, where each $v_k, k \in Q$, has a coefficient of $\min\{1, \sum_{i\in S^k} \overline{\pi}_i\}$, each $u_i, i \in N$, has a coefficient of $\overline{\pi}_i$, and z has a coefficient of 1. We do this through a series of upper bounds on the different terms in (33). First, because $0 \leq \overline{\pi}_i \leq 1, \forall i \in N$:

$$\overline{\pi}_j \leq \max_{i\in S}\{\overline{\pi}_i\} \leq \min\{1, \sum_{i\in S} \overline{\pi}_i\}, \quad \forall j \in S,\ S \subseteq N. \tag{34}$$

The next set of inequalities follow by (34), the definitions in (32), the definition of S^{k-}, and because $S^{k-} \subseteq S^k, \forall k \in Q$:

$$\sum_{k\in Q^{i+}_{a+}} v_k \times \min\{1, \sum_{i\in S^k} \overline{\pi}_i\} + \sum_{k\in Q^{i+}_{a+}} \sum_{i\in S^k} u_i\overline{\pi}_i \geq 0 \tag{35}$$

$$\sum_{k\in Q^{i-}_{a+}} v_k \times \max_{i\in S^k}\{\overline{\pi}_i\} \leq \sum_{k\in Q^{i-}_{a+}} v_k \times \min\{1, \sum_{i\in S^k} \overline{\pi}_i\} \tag{36}$$

$$\sum_{k\in Q^{i0}_{a+}} v_k \times \max_{i\in S^{k-}}\{\overline{\pi}_i\} \leq \sum_{k\in Q^{i0}_{a+}} v_k \times \max_{i\in S^k}\{\overline{\pi}_i\} \leq \sum_{k\in Q^{i0}_{a+}} v_k \times \min\{1, \sum_{i\in S^k} \overline{\pi}_i\} \tag{37}$$

$$\sum_{k\in Q^{i+}_{a-}} \min_{i\in S^k}\{u_i\} \times \min\{1, \sum_{j\in S^k} \overline{\pi}_j\} \leq \sum_{k\in Q^{i+}_{a-}} \min_{i\in S^k}\{u_i\} \times \sum_{j\in S^k} \overline{\pi}_j \leq \sum_{k\in Q^{i+}_{a-}} \sum_{i\in S^k} u_i\overline{\pi}_i \tag{38}$$

$$\sum_{k\in Q^{i-}_{a+}} \sum_{i\in S^k} u_i \times \max_{j\in S^k}\{\overline{\pi}_j\} \leq \sum_{k\in Q^{i-}_{a+}} \sum_{i\in S^k} u_i\overline{\pi}_i \tag{39}$$

$$\sum_{k\in Q^{i-}_{a-}} \sum_{i\in S^k} u_i \times \min\{1, \sum_{j\in S^k} \overline{\pi}_j\} \leq \sum_{k\in Q^{i-}_{a-}} \sum_{i\in S^k} u_i\overline{\pi}_i \tag{40}$$

$$\sum_{k\in Q^{i0}_{a+}} \sum_{i\in S^{k-}} u_i \times \max_{j\in S^{k-}}\{\overline{\pi}_j\} \leq \sum_{k\in Q^{i0}_{a+}} \sum_{i\in S^{k-}} u_i\overline{\pi}_i \leq \sum_{k\in Q^{i0}_{a+}} \sum_{i\in S^k} u_i\overline{\pi}_i \tag{41}$$

$$\sum_{k\in Q^{i0}_{a-}} \sum_{i\in S^{k-}} u_i \times \min\{1, \sum_{j\in S^k} \overline{\pi}_j\} \leq \sum_{k\in Q^{i0}_{a-}} \sum_{i\in S^{k-}} u_i\overline{\pi}_i \leq \sum_{k\in Q^{i0}_{a-}} \sum_{i\in S^k} u_i\overline{\pi}_i. \tag{42}$$

Using (35)-(42), we can bound the LHS of (33) as follows:

$$\text{RHS of (33)} = 0 \leq \text{ LHS of (33) } \leq z + \sum_{k\in Q} v_k \times \min\{1, \sum_{i\in S^k} \overline{\pi}_i\} + \sum_{i\in N} u_i\overline{\pi}_i = \boldsymbol{b}^T\boldsymbol{y}, \tag{43}$$

which contradicts with (F-2a):

$$\text{(F-2a)}: \ \boldsymbol{b}^T\boldsymbol{y} < 0 \Leftrightarrow z + \sum_{k\in Q} v_k \times \min\{1, \sum_{i\in S^k} \overline{\pi}_i\} + \sum_{i\in N} u_i\overline{\pi}_i < 0,$$

that is, $\nexists \boldsymbol{y} \in \Re^{(n+m+1)\times 1}$ that satisfies (F-2a) and (F-2b). Then, by Farka's Lemma, system (F-1) must have a

solution, that is, $\exists \boldsymbol{p} \in \Re^{(2^n)\times 1}$ such that $\boldsymbol{Ap} = \boldsymbol{b}$ and $\boldsymbol{p} \geq \boldsymbol{0}$. Then to complete the proof, it is sufficient to detail the row operations needed to convert (F-2a)($\tilde{S}$) to (33), which we do next.

Row operations: We define the *assay multipliers*, $\Delta_k, k \in Q \setminus Q^{i+}_{a+}$, as:

$$\Delta_k = \begin{cases} \sum_{i\in S^k} \overline{\pi}_i, & \forall k \in Q^{i+}_{a-} \cup Q^{i-}_{a-} \cup Q^{i0}_{a-} \\ \max_{i\in S^k}\{\overline{\pi}_i\}, & \forall k \in Q^{i-}_{a+} \\ \max_{i\in S^{k-}}\{\overline{\pi}_i\}, & \forall k \in Q^{i0}_{a+} \end{cases}, \tag{44}$$

and construct the **ordered vector $\boldsymbol{\Delta}$** to include any $\Delta_k < 1, k \in Q \setminus Q^{i+}_{a+}$, and the element 1, which are re-indexed following a non-decreasing order, i.e., $\Delta_1 \leq \Delta_2 \leq \cdots \leq \Delta_H < 1 = \Delta_{H+1}$, that is, $\boldsymbol{\Delta}$ includes the multipliers for all assays in $Q^{i-}_{a+} \cup Q^{i0}_{a+}$; and the multipliers for assays in $Q^{i+}_{a-} \cup Q^{i-}_{a-} \cup Q^{i0}_{a-}$ *only if* they are strictly less than 1. We use index h to refer to the elements of $\boldsymbol{\Delta}$. By construction, each $\Delta_h, h = 1, \cdots, H$, is the multiplier of at least one assay, denoted by assays $k_h, \cdots, l_h$, and $\Delta_{H+1} = 1$.

In what follows, we will conduct a series of row operations on (F-2a)($\tilde{S}$), i.e., the inequality for the joint probability of the diseases in set $\tilde{S}$. In each row operation, we will modify set $\tilde{S}$ by progressively removing a certain subset of diseases. Then we will consider the inequality in (F-2a) for the joint probability of the *remaining* diseases in this set, multiply both sides of this inequality by certain assay multipliers, and add to (F-2a)($\tilde{S}$), until we reach the desired form, (33). In the following, we describe this series of row operations first in words, then using mathematical notation.

We first multiply both sides of (F-2a)($\tilde{S}$) by Δ_1, i.e., the assay multiplier for assays $k_1, \cdots, l_1$; multiply (F-2a)($\tilde{S} \setminus \cup_{k_1,\cdots,l_1} S^k$) by $\Delta_2 - \Delta_1$; and add the two inequalities to obtain a new inequality (F-2a)($\tilde{S}$)$_{(1)}$ in which the variables for assays $k_1, \cdots, l_1$ and their diseases ($v_k, k = k_1, \cdots, l_1$, and $u_i, i \in \cup_{k=k_1,\cdots,l_1} S^k$) are multiplied by Δ_1, and all the remaining variables (in $\boldsymbol{y}$) are multiplied by Δ_2. Next, we consider Δ_2, i.e., the multiplier for assays $k_2, \cdots, l_2$; multiply (F-2a)($\tilde{S} \setminus \cup_{k_1,\cdots,l_1,k_2,\cdots,l_2} S^k$) by $(\Delta_3 - \Delta_2)$; and add to (F-2a)($\tilde{S}$)$_{(1)}$, to obtain a new inequality in which the variables for assays $k_1, \cdots, l_1$ and their diseases are multiplied by Δ_1, for assays $k_2, \cdots, l_2$ and their diseases are multiplied by Δ_2, and the remaining variables are multiplied by Δ_3. We repeat this process until H such row operations are completed, at which point we reach (33). In the following, we formally describe this series of row operations. To this end, at each iteration h, that is, when considering $\Delta_h, h = 1, \cdots, H$, we update the assay and disease sets as follows:

$$Q^{i+}_{a-}(\Delta_h) \equiv \left\{ k \in Q^{i+}_{a-} : \sum_{i\in S^k} \overline{\pi}_i > \Delta_h \right\},\ Q^{i-}_{a+}(\Delta_h) \equiv \left\{ k \in Q^{i-}_{a+} : \max_{i\in S^k}\{\overline{\pi}_i\} > \Delta_h \right\},\ Q^{i0}_{a+}(\Delta_h) \equiv \left\{ k \in Q^{i0}_{a+} : \max_{i\in S^{k-}}\{\overline{\pi}_i\} > \Delta_h \right\},$$

$$Q^{i-}_{a-}(\Delta_h) \equiv \left\{ k \in Q^{i-}_{a-} : \sum_{i\in S^k} \overline{\pi}_i > \Delta_h \right\},\ Q^{i0}_{a-}(\Delta_h) \equiv \left\{ k \in Q^{i0}_{a-} : \sum_{i\in S^k} \overline{\pi}_i > \Delta_h \right\}, \text{ and}$$

$$\tilde{S}(\Delta_h) \equiv \bigcup_{k\in Q^{i+}_{a-}(\Delta_h)} argmin_{i\in S^k}\{u_i\} \bigcup_{k\in Q^{i-}_{a+}(\Delta_h)\cup Q^{i-}_{a-}(\Delta_h)} S^k \bigcup_{k\in Q^{i0}_{a+}(\Delta_h)\cup Q^{i0}_{a-}(\Delta_h)} S^{k-},$$

that is, when considering Δ_h, we remove the diseases of assays $k_h, \cdots, l_h$ from the previous disease set $\tilde{S}(\Delta_{h-1})$. The row operations follow:

1. $\Delta_1 \times$(F-2a)($\tilde{S}$) $+(\Delta_2 - \Delta_1) \times$(F-2a)($\tilde{S}(\Delta_1)$) $\equiv$ (F-2a)($\tilde{S}$)$_{(1)}$: In the new inequality (F-2a)($\tilde{S}$)$_{(1)}$, the variables for assays $k_1, \cdots, l_1$ and their diseases ($v_k, k = k_1, \cdots, l_1$, and $u_i, i \in \cup_{k=k_1,\cdots,l_1} S^k$) are multiplied by Δ_1, and all the remaining variables (in $\boldsymbol{y}$) are multiplied by Δ_2.
2. For $h = 2, \cdots, H$: (F-2a)($\tilde{S}$)$_{(h-1)}$ $+ (\Delta_{h+1} - \Delta_h) \times$ (F-2a)($\tilde{S}(\Delta_h)$) $\equiv$ (F-2a)($\tilde{S}$)$_{(h)}$: In the new inequality (F-2a)($\tilde{S}$)$_{(h)}$, the variables for assays $k_1, \cdots, l_1$ and their diseases are multiplied by Δ_1, for assays $k_2, \cdots, l_2$ and their diseases are multiplied by Δ_2, and so on, and for assays $k_h, \cdots, l_h$ and their diseases are multiplied by Δ_h, and all the remaining variables are multiplied by Δ_{h+1}.

3. At the conclusion of row operation H, the final inequality (F-2a)$(\tilde{S})_{(H)}$ is such that the variables for assays $k_1, \cdots, l_1$ and their diseases are multiplied by Δ_1, for assays $k_2, \cdots, l_2$ and their diseases are multiplied by Δ_2, for assays $k_3, \cdots, l_3$ and their diseases are multiplied by Δ_3, and so on, for assays $k_H, \cdots, l_H$ and their diseases multiplied by Δ_H, and all the remaining variables are multiplied by 1, that is, we reach (33). This completes the proof. □

Proof of Corollary A.1. The result follows directly from Theorem A.1 because $\pi(\boldsymbol{x}^k; \boldsymbol{p}) = \sum_{i \in N} \overline{\pi}_i x_i^k \leq \pi(N) = \sum_{i \in N} \overline{\pi}_i \leq 1$, $\forall k = 1, \cdots, n$. Hence, to conserve $\pi(\boldsymbol{x}^k; \boldsymbol{p}) = \sum_{i \in N} \overline{\pi}_i x_i^k$, $\forall k = 1, \cdots, n$, and $\pi(N) = \sum_{i \in N} \overline{\pi}_i$, we have that $p_i = \overline{\pi}_i, \forall i \in N,\ p_{ij} = 0, \forall ij \in N(2),\ p_{ijr} = 0, \forall ijr \in N(3), \cdots, p_{12\ldots n} = 0,\ p_0 = 1 - \sum_{i \in N} \overline{\pi}_i$. □

Proof of Property 2. Part 1. For any assay $S \subseteq N$, from Eq. (8):

$$T(S,t) = \frac{1}{t} + 1 - (1 - \pi(S))^t \leq T(S,1) = 1 \Leftrightarrow \pi(S) \leq 1 - \sqrt[t]{\frac{1}{t}}, \qquad \text{where } \frac{\partial \left(1 - \sqrt[t]{\frac{1}{t}}\right)}{\partial t} = -t^{\left(\frac{-2t-1}{t}\right)} \left[ln(t) - 1\right] > 0 \Leftrightarrow t < e,$$

that is, function $1 - \sqrt[t]{\frac{1}{t}}$ is strictly increasing for $t \leq 2$, and strictly decreasing for $t \geq 3$. Therefore, the maximum value of $\pi(S)$ for which pooled testing, with integer pool sizes, outperforms individual testing is attained at $t = 2$ or $t = 3$. Then, the prevalence threshold, $\underline{p}$, follows because $1 - \sqrt[2]{\frac{1}{2}} = 0.292893 < 1 - \sqrt[3]{\frac{1}{3}} = 0.306639 \approx 0.31$. □

Proof of Theorem 1. The following relationships hold $\forall \lambda \in [0,1]$, hence we drop λ as an argument.

By Property A.1, $\tilde{c}(s)$ is subadditive in s, that is, $\tilde{c}(s) \leq \sum_{k=1}^{q} \tilde{c}(s^k),\ \forall s^k \in Z^+ : \sum_{k=1}^{q} s^k = s, \forall q = 2, \cdots, s, \forall s \in Z^+$ (Definition A1). Then, from Eq. (18), $TC_{I^{(1)}} = \tilde{c}(n) \leq \sum_{k=1}^{q} \tilde{c}(s^k_{I^{(q)}}) = TC_{I^{(q)}},\ \forall q = 2, \cdots, n$, hence $I^{(1)} \preceq I^{(q)},\ \forall q = 2, \cdots, n$. Let $S \subseteq N$ denote the set of diseases that are individually tested in an optimal $M^{(q)}$ design. For set S, $TC_{I^{(1)}}(S) = \tilde{c}(s) \leq \sum_{k=1}^{q} \tilde{c}(s^k_{I^{(q)}}) = TC_{I^{(q)}}(S),\ \forall q = 2, \cdots, s, S \subseteq N$, hence, it is optimal to bundle all the diseases in set S into one multiplex and individually test.

Part 1. Case where $\pi(N) \leq \underline{p}$: Then, $\pi(S) \leq \pi(N) \leq \underline{p}, \forall S \subseteq N \Rightarrow T^*_D(S) \leq T(S,1) = 1, \forall S \subseteq N$ (Property 2). Hence by Eqs. (18)-(19), $TC_{D^{(1)}} = \tilde{c}(n) \times T^*_D(N) \ \leq\ \tilde{c}(n) \times T(N,1) = TC_{I^{(1)}}$, hence $D^{(1)} \preceq I^{(1)} \Rightarrow D^{(1)} \preceq I^{(q)}$, $\forall q = 1, \cdots, n$, because $I^{(1)} \preceq I^{(q)}$, $\forall q = 2, \cdots, n$, as shown above.

Next, consider an $M^{(q)}$ design, which, by definition and as shown above, must contain exactly one assay with individual testing, say assay $k' \in \{1, \cdots, q\} : T(S^{k'}_{M^{(q)}}, t^{k'}_{M^{(q)}} = 1) = 1$. Construct an alternative design that uses the $M^{(q)}$ partition, $\boldsymbol{S}_{M^{(q)}}$, but with pool size vector $\boldsymbol{t}^*_D(\boldsymbol{S}_{M^{(q)}}) \geq \boldsymbol{2}$, that is, each assay in the $M^{(q)}$ partition is now pooled with the optimal pool size. Because $\pi(S) \leq \underline{p}, \forall S \subseteq N$, we have that $T^*_D(S^k_{M^{(q)}}) \leq T(S^k_{M^{(q)}}, 1)$, $\forall k = 1, \cdots, q$ (Property 2), that is, this new design, where all assays are pooled, is a feasible design for the $D^{(q)}$ class, and has a total cost less than or equal to that of the optimal $M^{(q)}$ design. This inequality continues to hold for the optimal $D^{(q)}$ design, and we have that $D^{(q)} \preceq M^{(q)}, \forall q = 2, \cdots, n$. Therefore, the optimal design class is $D^{(q)}$, for some $q = 1, \cdots, n$.

Part 2. Case where $\pi_1 \leq \underline{p} < \pi(N)$: By Property 2, $1 = T(N,1) \leq T^*_D(N) \Rightarrow I^{(1)} \preceq D^{(1)}$; and from Eq. (7), $\pi_1 \leq \underline{p} \Rightarrow \pi_i \leq \underline{p}, \forall i \in N \Rightarrow T^*_D(\{i\}) \leq T(\{i\}, 1) = 1,\ \forall i \in N$. Then, because $M^{(n)}$ is an all-singleton design, i.e., $\boldsymbol{S} = (\{i\})_{i \in N}$, it must have exactly one assay that is individually tested, and the total cost of this design can be improved by pooling this particular assay (with optimal pool size), hence converting the design into a feasible $D^{(n)}$ design with a total cost less than or equal to the optimal $M^{(n)}$ design. This inequality continues to hold for the optimal $D^{(n)}$ design, and we have that $D^{(n)} \preceq M^{(n)}$. Therefore, the optimal design class is either $I^{(1)}$, or $D^{(q)}$ for some $q = 2, \cdots, n$, or $M^{(q)}$ for some $q = 2, \cdots, n-1$.

Part 3. Case where $\pi_n \geq \underline{p}$: Then, $\underline{p} \leq \pi_n \leq \pi(S), \forall S \subseteq N \Rightarrow T(S,1) = 1 \leq T^*_D(S), \forall S \subseteq N$ (Property 2). Therefore, we can show that $I^{(q)} \preceq D^{(q)}, \forall q = 1, \cdots, n$, and $I^{(q)} \preceq M^{(q)}, \forall q = 2, \cdots, n$. Further, $I^{(1)} \preceq I^{(q)}, \forall q = 2, \cdots, n$ as shown above. Then, the optimal design class is $I^{(1)}$.

Part 4. Case where $\exists i \in \{1,\cdots,n-1\} : \pi_{i+1} < \underline{p} < \pi_i$: Then, $\pi(N) \geq \pi_1 \geq \pi_2 \cdots \geq \pi_i > \underline{p}$. Hence, by Property 2, $1 = T(N,1) \leq T_D^*(N) \Rightarrow I^{(1)} \preceq D^{(1)}$. Consider any $D^{(q)}$, $q = 2,\cdots,n$, which must contain at least one assay $k' \in \{1,\cdots,q\} : \pi(S^{k'}_{D^{(q)}}) > \underline{p} \Rightarrow T_D^*(S^{k'}_{D^{(q)}}) > T(S^{k'}_{D^{(q)}},1) = 1$ (Property 2). Construct an alternative design that uses the $D^{(q)}$ partition, $\boldsymbol{S}_{D^{(q)}}$, but with $t^{k'}_{D^{(q)}} = 1$, which is a feasible design for the $M^{(q)}$ class, and has a total cost less than or equal to that of the optimal $D^{(q)}$ design. This inequality continues to hold for the optimal $M^{(q)}$ design, and we have that $M^{(q)} \preceq D^{(q)}, \forall q = 2,\cdots,n$.

Next consider set $S = \{1,\cdots i\} \subset N$, where $\pi(S) \geq \pi_i > \underline{p}$. Then, by part 3 of this theorem, $I^{(1)}$ is optimal for set S, that is, in an optimal design, all the diseases in set S are bundled into one multiplex and individually tested. Because the total cost is additive over assay sets; the set of remaining diseases, $N \setminus S = \{i+1,\cdots,n\}$, has cardinality $n-i$; and all the i diseases in set S are bundled into one multiplex assay, an optimal design can have at most $n-i+1$ assays, exactly one of which is individually tested. That is, the optimal design class is either $I^{(1)}$, or $M^{(q)}$ for some $q = 2,\cdots,n-i+1$. □

Proof of Property 3. The first part follows from Definition 5 because $\tilde{c}(s,\lambda) = \lambda\ c(s) + 1 - \lambda$ is a linear function of $c(s), s \in Z^+$. For the second part, for any $\epsilon \in (0,\lambda)$, we have:

$$\tilde{c}(s+1,\lambda-\epsilon) - \tilde{c}(s,\lambda-\epsilon) = (\lambda-\epsilon)\ [c(s+1)-c(s)] \quad \leq \quad \lambda\ [c(s+1)-c(s)] = \tilde{c}(s+1,\lambda) - \tilde{c}(s,\lambda),\ \forall s \in Z^+,$$

and it follows, by Definition 5, that $\tilde{c}(s,\lambda) \geq_{diff} \tilde{c}(s,\lambda-\epsilon)$. □

Proof of Theorem 2. Consider the smallest-difference composite cost function in $\tilde{C}$, that is, $\lambda = 0$ or $c(s) = \gamma, \forall s \in Z^+$, where the objective reduces to the minimization of the expected tests function, $T(.)$. By Theorem 1, $I^{(1)} \preceq I^{(q)}, \forall q = 2,\cdots,n$, and an $M^{(q)}$ design contains exactly one assay with individual testing, that is, $T(S^{k'}_{M^{(q)}}, t^{k'}_{M^{(q)}} = 1) = 1$, for some $k' \in \{1,\cdots,q\}$, and $q-1$ assays are pooled. Then, $T_{M^{(q)}} > 1 = T_{I^{(1)}}$, hence $I^{(1)} \preceq M^{(q)}, \forall q = 2,\cdots,n$. Next we characterize an optimal design class.

Part 1. Case where $\pi(N) \leq \underline{p}$: By Theorem 1, the optimal design class is $D^{(q)}$, for some $q = 1,\cdots,n$. Consider a $D^{(q)}$ design, with partition $\boldsymbol{S}_{D^{(q)}}$, for any $q = 2,\cdots,n$. We construct a feasible $D^{(q-1)}$ design by combining any two sets, $S^{k_1}_{D^{(q)}}$ and $S^{k_2}_{D^{(q)}}$, $k_1, k_2 \in \{1,\cdots,q\}, k_1 \neq k_2$, into a new set, $S^k \equiv S^{k_1}_{D^{(q)}} \cup S^{k_2}_{D^{(q)}}$. Because $T_D^*(S)$ is subadditive in $\pi(S) \in [0,\underline{p}]$, and $\pi(S)$ is subadditive in set S (Property A.1), it follows that $\sum_{r=1}^{2} T_D^*(S^{k_r}) \geq T_D^*(S^k)$. Because this result holds for a feasible $D^{(q-1)}$ design, it continues to hold for an optimal $D^{(q-1)}$ design, hence $D^{(q-1)} \preceq D^{(q)}$, for all $q = 2,\cdots,n$. Consequently, $D^{(1)} \preceq D^{(2)} \preceq \cdots \preceq D^{(n)}$, and the optimal design class is $D^{(1)}$.

Part 2. Case where $\pi(N) > \underline{p}$: Because $I^{(1)} \preceq I^{(q)}$ and $I^{(1)} \preceq M^{(q)}, \forall q = 2,\cdots,n$, it is sufficient to show that $I^{(1)} \preceq D^{(q)}$, that is, $T_{I^{(1)}} \leq T_{D^{(q)}}, \forall q = 1,\cdots,n$. By Property 2, $1 = T_{I^{(1)}} < T_D^*(N) = T_{D^{(1)}}$, hence $I^{(1)} \preceq D^{(1)}$. Next consider any Dorfman design, $D^{(q)}, q = 2,\cdots,n$, with partition $\boldsymbol{S}_{D^{(q)}}$. There are two possible cases:

(a) Case where $\exists k' \in \{1,\cdots,q\} : \pi(S^{k'}_{D^{(q)}}) > \underline{p}$: Then, we have that $T_D^*(S^{k'}_{D^{(q)}}) > T(S^{k'}_{D^{(q)}},1) = 1$ (Property 2), and it trivially follows that $1 = T_{I^{(1)}} < \sum_{k=1}^{q} T_D^*(S^k_{D^{(q)}})$, hence $I^{(1)} \preceq D^{(q)}, \forall q = 2,\cdots,n$.

(b) Case where $\pi(S^k_{D^{(q)}}) \leq \underline{p}$, $\forall k = 1,\cdots,q$: Because $\pi(S^k_{D^{(q)}}) \leq \underline{p} < \pi(N), \forall k = 1,\cdots,q$, $\exists k' \in \{1,\cdots,q\} : \pi(\cup_{k=1}^{k'-1} S^k_{D^{(q)}}) \leq \underline{p} < \pi(\cup_{k=1}^{k'} S^k_{D^{(q)}})$.

Define some dummy set $\tilde{S} :\ \pi\left(\left(\cup_{k=1}^{k'-1} S^k_{D^{(q)}}\right) \cup \tilde{S}\right) = \pi\left(\cup_{k=1}^{k'-1} S^k_{D^{(q)}}\right) + \pi\left(\tilde{S}\right) = \underline{p}$, and let $S' \equiv \left(\cup_{k=1}^{k'-1} S^k_{D^{(q)}}\right) \cup \tilde{S}$. By construction, $\pi(S') = \underline{p} \Rightarrow T_D^*(S') = 1$, and we can write:

$$T_{I^{(1)}} = 1 \ = \ T_D^*(S') \ \leq \ T_D^*(\tilde{S}) + \sum_{k=1}^{k'-1} T_D^*(S^k_{D^{(q)}}) \ < \ \sum_{k=1}^{k'} T_D^*(S^k_{D^{(q)}}) \ \leq \ \sum_{k=1}^{q} T_D^*(S^k_{D^{(q)}}),$$

where the first two equalities follow by Property 2, the first inequality follows because $T_D^*(S)$ is subadditive in $\pi(S)$, the second inequality follows because $T_D^*(S)$ is strictly increasing in $\pi(S)$, and the last inequality follows because $k' \leq q$. Hence $I^{(1)} \preceq D^{(q)}$, $q = 2,\cdots,n$.

In each case the optimal design class is $I^{(1)}$, completing the proof. □

Proof of Theorem 3. Consider the highest-difference composite cost function in $\tilde{C}$, that is, $\lambda = 1$ and $c(s) = \gamma \times s \Rightarrow \tilde{c}(s) = \gamma \times s, \forall s \in Z^+$, where the objective reduces to the minimization of $\sum_{k=1}^{q} s^k \times T^*(S^k)$.

First, we show that if $\pi(N) \leq \underline{p}$, then $D^{(n)} \preceq D^{(n-1)} \preceq \cdots \preceq D^{(1)}$. Consider a $D^{(q)}$ design, with partition $\boldsymbol{S}_{D^{(q)}}$, for any $q = 1, \cdots, n-1$. Then, $\exists k' \in \{1, \cdots, q\} : s^{k'}_{D^{(q)}} \geq 2$. We construct a feasible $D^{(q+1)}$ design by splitting set $S^{k'}_{D^{(q)}}$ into mutually exclusive sets, $S^{k'_1}$ and $S^{k'_2} : \cup_{r=1}^{2} S^{k'_r} = S^{k'}_{D^{(q)}}$ and $\cap_{r=1}^{2} S^{k'_r} = \emptyset$. Then:

$$\sum_{r=1}^{2} s^{k'_r} \times T^*_D(S^{k'_r}) \leq \sum_{r=1}^{2} s^{k'_r} \times T^*_D(S^{k'}_{D^{(q)}}) = s^{k'}_{D^{(q)}} \times T^*_D(S^{k'}_{D^{(q)}}),$$

where the inequality follows because, by construction $\pi(S^{k'_r}) \leq \pi(S^{k'}_{D^{(q)}}), r = 1, 2$, and $\sum_{r=1}^{2} s^{k'_r} = s^{k'}_{D^{(q)}}$, and $T^*_D(\pi(S))$ is increasing in $\pi(S) \in [0, \underline{p}]$ (Property 2). Because this result holds for a feasible $D^{(q+1)}$ design, it must hold for an optimal $D^{(q+1)}$ design, and we have that $D^{(q+1)} \preceq D^{(q)}, \forall q = 1, \cdots, n-1$.
We are ready to characterize an optimal design class.

<u>*Part 1.*</u> Case where $\pi_1 \leq \underline{p}$:

(a) Case where $\pi(N) \leq \underline{p}$: By Theorem 1, the optimal design class is $D^{(q)}$ for some $q = 1, \cdots, n$. Further, as shown above, $D^{(n)} \preceq D^{(n-1)} \preceq \cdots \preceq D^{(1)}$, hence the optimal design class is $D^{(n)}$.

(b) Case where $\pi(N) > \underline{p}$: By Theorem 1, the optimal design class is either $I^{(1)}$, or $D^{(q)}$ for some $q = 2, \cdots, n$, or $M^{(q)}$ for some $q = 2, \cdots, n-1$. From Eq. (7), $\pi_1 \leq \underline{p} \Rightarrow \pi_i \leq \underline{p}, \forall i \in N \Rightarrow T^*_D(\{i\}) \leq 1, \forall i \in N$. Further, $T^*_D(\pi(S))$ is increasing in $\pi(S) \in [0, \underline{p}]$, with $T^*_D(\underline{p}) = 1$, hence $T^*_D(\{i\}) \leq T^*_D(S), \forall i \in S, S \subseteq N$. Then:

$$T^*_D(\{i\}) \leq \min\{1, T^*_D(S)\}, \forall i \in S, S \subseteq N \Rightarrow \sum_{i \in S} T^*_D(\{i\}) \leq s \times \min\{1, T^*_D(S)\} \leq s \times T^*_D(S), \forall S \subseteq N, \quad (45)$$

and the result that $D^{(n)} \preceq D^{(q)}$, for any $q = 1, \cdots, n-1$, follows. Also, from Eq. (45), $TC_{D^{(n)}} = \sum_{i \in N} 1 \times T^*_D(\{i\}) \leq n = TC_{I^{(1)}}$. Hence, $D^{(n)} \preceq I^{(1)}$.

Finally, in an $M^{(q)}$ design, $T(S^{k'}_{M^{(q)}}, t^{k'}_{M^{(q)}} = 1) = 1$ for some $k' \in \{1, \cdots, q\}$, hence, by Eq. (45), $D^{(n)} \preceq M^{(q)}$, for any $q = 2, \cdots, n-1$. Hence, the optimal design class is $D^{(n)}$.

<u>*Part 2.*</u> Case where $\pi_n \geq \underline{p}$: By Theorem 1, the optimal design class is $I^{(1)}$. Next we show that the total cost of *any* individual-testing design $I^{(q)}, q = 2, \cdots, n$, is the same:

$$TC_{I^{(q)}} = \sum_{k=1}^{q} s^k_{I^{(q)}} \times T(S^k_{I^{(q)}}, 1) = \sum_{k=1}^{q} s^k_{I^{(q)}} = n = n \times T(N, 1) = TC_{I^{(1)}}.$$

Hence any individual-testing design, $I^{(q)}, q = 1, \cdots, n$, is optimal.

<u>*Part 3.*</u> Case where $\exists i \in N : \pi_{i+1} < \underline{p} < \pi_i$: By Theorem 1, the optimal design class is either $I^{(1)}$, or $M^{(q)}$ for some $q = 2, \cdots, n-i+1$. Decompose set N into two mutually exclusive and exhaustive sets, $S^1 = \{1, \cdots, i\}$ and $S^2 = \{i+1, \cdots, n\}$, that is, $\pi_j > \underline{p}, \forall j \in S^1$, and $\pi_j \leq \underline{p}, \forall j \in S^2$. Then, by part 2 of this theorem, any $I^{(q)}, q = 1, \cdots, i$, is optimal for set $S^1 = \{1, \cdots, i\}$; and by part 1 of this theorem, $D^{(n-i)}$ is optimal for set $S^2 = \{i+1, \cdots, n\}$. Because the total cost is additive over assay sets, an optimal design is the combination of the optimal designs for sets S^1 and S^2, that is, any $M^{(q)}$ for $q = n-i+1, \cdots, n$. □

Proof of Theorem 4. Because $\pi(N) \leq \underline{p}$, by Theorem 1, the optimal design class is $D^{(q)}$, with partition $\boldsymbol{S}_{D^{(q)}}$ for some $q = 1, \cdots, n$. Because $T^*_D(S)$ is subadditive in $\pi(S) \in [0, \underline{p}]$, we have that:

$$T_{D^{(1)}} = T^*_D(N) \leq \sum_{k=1}^{q} T^*_D(S^k_{D^{(q)}}), \forall q = 2, \cdots, n. \quad (46)$$

Recall that an optimal pool size $t^*(\pi(S))$ depends only on $\pi(S)$ (Property 2), that is, it does not change with λ; and $T^*_D(S)$ denotes the expected tests for set $S \subseteq N$ at the optimal pool size for set S. The proof is three-fold: First we show that $\exists \overline{\lambda}^{(1)} \leq 1$ such that $D^{(1)}(\lambda)$ is optimal if and only if $\lambda \leq \overline{\lambda}^{(1)}$, then we show that $\exists \overline{\lambda}^{(n-1)} \leq 1$ such that $D^{(n)}(\lambda)$ is optimal if and only if $\lambda > \max\left\{\overline{\lambda}^{(1)}, \overline{\lambda}^{(n-1)}\right\}$; finally we show that $\exists \overline{\lambda}^{(q)} \leq 1, q = 2, \cdots, n-1$, such that $D^{(r)}(\lambda)$, for some $r = 2, \cdots, q$, is optimal if and only if $\lambda \in \left(\max\left\{\overline{\lambda}^{(1)}, \overline{\lambda}^{(q-1)}\right\}, \overline{\lambda}^{(q)}\right]$.

We first prove that $\exists \overline{\lambda}^{(1)}: \quad D^{(1)}(\lambda) \preceq D^{(q)}(\lambda), \forall q = 2, \cdots, n \Leftrightarrow \lambda \leq \overline{\lambda}^{(1)}$.

(a) We first show that, if for some λ, $D^{(1)}(\lambda) \preceq D^{(q)}(\lambda), \forall q = 2, \cdots, n$, then $D^{(1)}(\lambda - \epsilon) \preceq D^{(q)}(\lambda - \epsilon), \forall \epsilon \in [0, \lambda]$:

$$D^{(1)}(\lambda) \preceq D^{(q)}(\lambda), \forall q = 2, \cdots, n$$

$$\Leftrightarrow \tilde{c}(n) \times T_D^*(N) \leq \sum_{k=1}^{q} \tilde{c}(s_{D^{(q)}}^k) \times T_D^*(S_{D^{(q)}}^k), \forall q = 2, \cdots, n$$

$$\Leftrightarrow [\lambda\ c(n) + 1 - \lambda] \times T_D^*(N) \leq \sum_{k=1}^{q} [\lambda\ c(s_{D^{(q)}}^k) + 1 - \lambda] \times T_D^*(S_{D^{(q)}}^k), \forall q = 2, \cdots, n. \tag{47}$$

There are two possible cases:

(i) Case where $c(n) \times T_D^*(N) \leq \sum_{k=1}^{q} c(s_{D^{(q)}}^k) \times T_D^*(S_{D^{(q)}}^k), \forall q = 2, \cdots, n$: Then, the result trivially follows by (46) and the condition stated for this case, because we have, $\forall q = 2, \cdots, n$, and any $\epsilon \in [0, \lambda]$:

$$(\lambda - \epsilon)\ c(n) \times T_D^*(N) \leq (\lambda - \epsilon) \sum_{k=1}^{q} c(s_{D^{(q)}}^k) \times T_D^*(S_{D^{(q)}}^k), \quad \text{and} \quad [1 - (\lambda - \epsilon)] \times T_D^*(N) \leq [1 - (\lambda - \epsilon)] \times \sum_{k=1}^{q} T_D^*(S_{D^{(q)}}^k)$$

$$\Rightarrow TC_{D^{(1)}}(\lambda - \epsilon) \leq TC_{D^{(q)}}(\lambda - \epsilon).$$

(ii) Case where $c(n) \times T_D^*(N) > \sum_{k=1}^{q} c(s_{D^{(q)}}^k) \times T_D^*(S_{D^{(q)}}^k)$, for some $q = 2, \cdots, n$: It is sufficient to show that,

$$-\epsilon\ c(n) \times T_D^*(N) + \epsilon \times T_D^*(N) \leq -\epsilon \sum_{k=1}^{q} c(s_{D^{(q)}}^k) \times T_D^*(S_{D^{(q)}}^k) + \epsilon\ \sum_{k=1}^{q} T_D^*(S_{D^{(q)}}^k),$$

which holds, because by (46) and the condition stated for this case, we have that, for any $\epsilon \in [0, \lambda]$:

$$-\epsilon\ c(n) \times T_D^*(N) < -\epsilon \sum_{k=1}^{q} c(s_{D^{(q)}}^k) \times T_D^*(S_{D^{(q)}}^k), \quad \text{and} \quad \epsilon \times T_D^*(N) \leq \epsilon\ \sum_{k=1}^{q} T_D^*(S_{D^{(q)}}^k) \quad \Rightarrow \quad TC_{D^{(1)}}(\lambda - \epsilon) \leq TC_{D^{(q)}}(\lambda - \epsilon).$$

Thus, in both cases, $D^{(1)}(\lambda - \epsilon) \preceq D^{(q)}(\lambda - \epsilon), \forall q = 2, \cdots, n, \forall \epsilon \in [0, \lambda]$.

(b) To complete the proof, we now show that, if for some λ, $D^{(q)}(\lambda) \preceq D^{(1)}(\lambda)$, for some $q = 2, \cdots, n$, then $D^{(q)}(\lambda + \epsilon) \preceq D^{(1)}(\lambda + \epsilon), \forall \epsilon \in [0, 1 - \lambda]$. It is sufficient to show that,

$$\epsilon\ c(n) \times T_D^*(N) - \epsilon \times T_D^*(N) \geq \epsilon\ \sum_{k=1}^{q} c(s_{D^{(q)}}^k) \times T_D^*(S_{D^{(q)}}^k) - \epsilon\ \sum_{k=1}^{q} T_D^*(S_{D^{(q)}}^k).$$

Because $D^{(q)}(\lambda) \preceq D^{(1)}(\lambda)$ and by the inequality in (46), it must be true that,

$$c(n) \times T_D^*(N) \geq \sum_{k=1}^{q} c(s_{D^{(q)}}^k) \times T_D^*(S_{D^{(q)}}^k).$$

Then, for any $\epsilon \in [0, 1 - \lambda]$:

$$\epsilon \sum_{k=1}^{q} c(s_{D^{(q)}}^k) \times T_D^*(S_{D^{(q)}}^k) \leq \epsilon\ c(n) \times T_D^*(N), \quad \text{and} \quad -\epsilon \sum_{k=1}^{q} T_D^*(S_{D^{(q)}}^k) \quad \leq -\epsilon \times T_D^*(N) \quad \Rightarrow \quad TC_{D^{(q)}}(\lambda + \epsilon) \leq TC_{D^{(1)}}(\lambda + \epsilon).$$

That is, $D^{(q)}(\lambda + \epsilon) \preceq D^{(1)}(\lambda + \epsilon), \forall \epsilon \in [0, 1 - \lambda]$, and the result follows.

Next, we prove that $\exists \overline{\lambda}^{(n-1)}: \ D^{(n)} \preceq D^{(q)}, \forall q = 1, \cdots, n-1 \Leftrightarrow \lambda > \max\left\{\overline{\lambda}^{(1)}, \overline{\lambda}^{(n-1)}\right\}$.

(a) We first show that, if for some λ, $D^{(q)}(\lambda) \preceq D^{(n)}(\lambda)$, for some $q = 1, \cdots, n-1$, then $D^{(q)}(\lambda - \epsilon) \preceq D^{(n)}(\lambda - \epsilon), \forall \epsilon \in [0, \lambda]$:

$$D^{(q)}(\lambda) \preceq D^{(n)}(\lambda)$$

$$\Leftrightarrow \sum_{k=1}^{q} \tilde{c}(s_{D^{(q)}}^k) \times T_D^*(S_{D^{(q)}}^k) \leq \sum_{k=1}^{n} \tilde{c}(1) \times T_D^*(\{k\})$$

$$\Leftrightarrow \sum_{k=1}^{q} [\lambda\ c(s_{D^{(q)}}^k) + 1 - \lambda] \times T_D^*(S_{D^{(q)}}^k) \leq \sum_{k=1}^{n} [\lambda\ c(1) + 1 - \lambda] \times T_D^*(\{k\}). \tag{48}$$

There are two possible cases:

(i) Case where $\sum_{k=1}^{q} c(s_{D^{(q)}}^k) \times T_D^*(S_{D^{(q)}}^k) \leq \sum_{k=1}^{n} c(1) \times T_D^*(\{k\})$: Then, the result trivially follows by (46)

and the condition stated for this case, because for any $\epsilon \in [0, \lambda]$:

$$(\lambda-\epsilon)\sum_{k=1}^{q} c(s^k_{D^{(q)}}) \times T^*_D(S^k_{D^{(q)}}) \leq (\lambda-\epsilon)\sum_{k=1}^{n} c(1) \times T^*_D(\{k\}), \quad \text{and} \quad (1-(\lambda-\epsilon))\sum_{k=1}^{q} T^*_D(S^k_{D^{(q)}}) \leq (1-(\lambda-\epsilon))\sum_{k=1}^{n} T^*_D(\{k\})$$

$$\Rightarrow TC_{D^{(q)}}(\lambda-\epsilon) \leq TC_{D^{(n)}}(\lambda-\epsilon).$$

(ii) Case where $\sum_{k=1}^{q} c(s^k_{D^{(q)}}) \times T^*_D(S^k_{D^{(q)}}) > \sum_{k=1}^{n} c(1) \times T^*_D(\{k\})$: It is sufficient to show that,

$$-\epsilon \sum_{k=1}^{n} c(1) \times T^*_D(\{k\}) + \epsilon \sum_{k=1}^{n} T^*_D(\{k\}) \leq -\epsilon \sum_{k=1}^{q} c(s^k_{D^{(q)}}) \times T^*_D(S^k_{D^{(q)}}) + \epsilon \sum_{k=1}^{q} T^*_D(S^k_{D^{(q)}}),$$

which holds, because by (46) and the condition stated for this case, we have that, for any $\epsilon \in [0, \lambda]$:

$$-\epsilon\sum_{k=1}^{q} c(s^k_{D^{(q)}}) \times T^*_D(S^k_{D^{(q)}}) < -\epsilon\sum_{k=1}^{n} c(1) \times T^*_D(\{k\}), \quad \text{and} \quad \epsilon\sum_{k=1}^{q} T^*_D(S^k_{D^{(q)}}) \leq \epsilon\sum_{k=1}^{n} T^*_D(\{k\})$$

$$\Rightarrow TC_{D^{(q)}}(\lambda-\epsilon) \leq TC_{D^{(n)}}(\lambda-\epsilon).$$

Thus, in both cases, $D^{(q)}(\lambda-\epsilon) \preceq D^{(n)}(\lambda-\epsilon), \forall \epsilon \in [0, \lambda]$.

(b) To complete the proof, we now show that, if for some λ, $D^{(n)}(\lambda) \preceq D^{(q)}(\lambda), \forall q = 1, \cdots, n-1$, then $D^{(n)}(\lambda+\epsilon) \preceq D^{(q)}(\lambda+\epsilon), \forall \epsilon \in [0, 1-\lambda]$. It is sufficient to show that,

$$\epsilon \sum_{k=1}^{q} c(s^k_{D^{(q)}}) \times T^*_D(S^k_{D^{(q)}}) - \epsilon \sum_{k=1}^{q} T^*_D(S^k_{D^{(q)}}) \geq \epsilon \sum_{k=1}^{n} c(1) \times T^*_D(\{k\}) - \epsilon \sum_{k=1}^{n} T^*_D(\{k\}).$$

Because of the optimality of $D^{(n)}(\lambda)$ and the inequality in (46), it must be true that,

$$\sum_{k=1}^{n} c(1) \times T^*_D(\{k\}) \leq \sum_{k=1}^{q} c(s^k_{D^{(q)}}) \times T^*_D(S^k_{D^{(q)}}).$$

Then, for any $\epsilon \in [0, 1-\lambda]$:

$$\epsilon\sum_{k=1}^{n} c(1) \times T^*_D(\{k\}) \leq \epsilon\sum_{k=1}^{q} c(s^k_{D^{(q)}}) \times T^*_D(S^k_{D^{(q)}}), \quad \text{and} \quad -\epsilon\sum_{k=1}^{n} T^*_D(\{k\}) \leq -\epsilon\sum_{k=1}^{q} T^*_D(S^k_{D^{(q)}})$$

$$\Rightarrow TC_{D^{(n)}}(\lambda+\epsilon) \leq TC_{D^{(q)}}(\lambda+\epsilon).$$

That is, $D^{(n)}(\lambda+\epsilon) \preceq D^{(q)}(\lambda+\epsilon), q = 1, \cdots, n-1, \forall \epsilon \in [0, 1-\lambda]$, and the result follows.

Finally, we show that $\exists \overline{\lambda}^{(q)} \leq 1, q = 2, \cdots, n-1$, such that if $\lambda \in \left(\max\left\{\overline{\lambda}^{(1)}, \overline{\lambda}^{(q-1)}\right\}, \overline{\lambda}^{(q)}\right]$, then the optimal solution is $D^{(r)}(\lambda)$, for some $r = 2, \cdots, q$. To this end, we first show that $\exists \lambda^q \leq 1, q = 3, \cdots, n$, such that $D^{(q-1)}(\lambda) \preceq D^{(q)}(\lambda), \forall \lambda \leq \lambda^q$.

Consider any $D^{(q)}$ design for $q \geq 2$. We construct a feasible $D^{(q-1)}$ design by combining any two assay sets, $k_1, k_2 \in \{1, \cdots, q\} : k_1 \neq k_2$, in the $D^{(q)}$ design, while keeping all remaining assays intact. We show that, if for some λ, $D^{(q-1)}(\lambda) \preceq D^{(q)}(\lambda)$, then $D^{(q-1)}(\lambda-\epsilon) \preceq D^{(q)}(\lambda-\epsilon), \forall \epsilon \in [0, \lambda]$. Because all assays other than k_1 and k_2 remain the same, it is sufficient to show that, given:

$$[\lambda\ c(s^{k_1} + s^{k_2}) + 1 - \lambda] \times T^*_D(\pi(S^{k_1} \cup S^{k_2})) \leq \sum_{r=1}^{2} [\lambda\ c(s^{k_r}) + 1 - \lambda]\ \times\ T^*_D(\pi(S^{k_r})), \tag{49}$$

the following inequality holds:

$$[(\lambda-\epsilon)\ c(s^{k_1} + s^{k_2}) + 1 - (\lambda-\epsilon)] \times T^*_D(\pi(S^{k_1} \cup S^{k_2})) \leq \sum_{r=1}^{2} [(\lambda-\epsilon)\ c(s^{k_r}) + 1 - (\lambda-\epsilon)] \times\ T^*_D(\pi(S^{k_r})), \tag{50}$$

equivalently, the following inequality holds:

$$\left(\epsilon c(s^{k_1}+s^{k_2})-\epsilon\right)\times T_D^*(\pi(S^{k_1}\cup S^{k_2}))\geq \sum_{r=1}^{2}\left(\epsilon c(s^{k_r})-\epsilon\right)\times\ T_D^*(\pi(S^{k_r})). \tag{51}$$

Because $T_D^*(\pi(S))$ is subadditive in $\pi(S)$, and $\pi(S)$ is subadditive in set S (Property A.1), for any $k_1,k_2\in\{1,\cdots,q\}: k_1\neq k_2$:

$$\pi(S^{k_1})+\pi(S^{k_2})\geq \pi(S^{k_1}\cup S^{k_2}),\text{ and} \tag{52}$$

$$\sum_{r=1}^{2}T_D^*(\pi(S^{k_r}))\geq T_D^*(\sum_{r=1}^{2}\pi(S^{k_r}))\geq T_D^*(\pi(S^{k_1}\cup S^{k_2})). \tag{53}$$

There are two possible cases:

(i) Case where $c(s^{k_1}+s^{k_2})\times T_D^*(\pi(S^{k_1}\cup S^{k_2}))\geq\sum_{r=1}^{2}c(s^{k_r})\times\ T_D^*(\pi(S^{k_r}))$: Then, for any $\epsilon>0$:

$$\epsilon\ c(s^{k_1}+s^{k_2})\times T_D^*(\pi(S^{k_1}\cup S^{k_2}))\geq \epsilon\ \sum_{r=1}^{2}c(s^{k_r})\times\ T_D^*(\pi(S^{k_r})), \tag{54}$$

and from Eq. (53),

$$-\epsilon\ T_D^*(\pi(S^{k_1}\cup S^{k_2}))\geq -\epsilon\ \sum_{r=1}^{2}T_D^*(\pi(S^{k_r})), \tag{55}$$

hence adding (54) and (55) leads to:

$$\left(\epsilon c(s^{k_1}+s^{k_2})-\epsilon\right)\times T_D^*(\pi(S^{k_1}\cup S^{k_2}))\geq \sum_{r=1}^{2}\left(\epsilon c(s^{k_r})-\epsilon\right)\times\ T_D^*(\pi(S^{k_r})), \tag{56}$$

that is, (51) is satisfied, and this feasible $D^{(q-1)}$ design dominates the optimal $D^{(q)}$ design, and this result continues to hold for the optimal $D^{(q-1)}$ design, that is, $D^{(q-1)}(\lambda-\epsilon)\preceq D^{(q)}(\lambda-\epsilon),\forall\epsilon\in[0,\lambda]$.

(ii) Case where $c(s^{k_1}+s^{k_2})\times T_D^*(\pi(S^{k_1}\cup S^{k_2}))<\sum_{r=1}^{2}c(s^{k_r})\times\ T_D^*(\pi(S^{k_r}))$: Then, we have that

$$\left(\lambda c(s^{k_1}+s^{k_2})+1-\lambda\right)\times T_D^*(\pi(S^{k_1}\cup S^{k_2}))<\sum_{r=1}^{2}\left(\lambda c(s^{k_r})+1-\lambda\right)\times\ T_D^*(\pi(S^{k_r})),\ \forall\lambda\in[0,1], \tag{57}$$

that is, $D^{(q-1)}(\lambda)\preceq D^{(q)}(\lambda),\forall\lambda\in[0,1]$.

Then, it follows that $\exists\lambda^q\leq 1, q=3,\cdots,n$, such that $D^{(q-1)}\preceq D^{(q)},\forall\lambda\leq\lambda^q$. Therefore, the result follows by setting $\overline{\lambda}^{(q-1)}=\min_{k=q,\cdots,n}\{\lambda^k\}$, for $q=3,\cdots,n$.

Note that only the existence of the $D^{(1)}$ optimal-region, $\lambda\in[0,\overline{\lambda}^{(1)}]$, is guaranteed. In other words, $D^{(n)}$-optimal region may be empty if $\max\left\{\overline{\lambda}^{(1)},\overline{\lambda}^{(n-1)}\right\}=1\Rightarrow\left(\max\left\{\overline{\lambda}^{(1)},\overline{\lambda}^{(n-1)}\right\},1\right]=\emptyset$; and the region where $D^{(r)}$, for some $r=1,\cdots,q$, is optimal may be empty if $\overline{\lambda}^{(q)}\leq\overline{\lambda}^{(1)}\Rightarrow\left(\max\left\{\overline{\lambda}^{(1)},\overline{\lambda}^{(q-1)}\right\},\overline{\lambda}^{(q)}\right]=\emptyset$. □

Proof of Lemma 1. From Theorem 4, $D^{(n)}\preceq D^{(q)},\forall q=1,\cdots,n-1\Leftrightarrow\lambda>\max\left\{\overline{\lambda}^{(1)},\overline{\lambda}^{(n-1)}\right\}$, equivalently,

$$\sum_{k=1}^{n}\tilde{c}(1,\lambda)\times T_D^*\big(\pi(\{k\};\boldsymbol{p})\big)\leq\sum_{k=1}^{q}\tilde{c}(s^k_{D^{(q)}},\lambda)\times T_D^*\big(\pi(S^k_{D^{(q)}};\boldsymbol{p})\big),\quad\forall q=1,\cdots,n-1\Leftrightarrow\lambda>\max\left\{\overline{\lambda}^{(1)},\overline{\lambda}^{(n-1)}\right\}. \tag{58}$$

By Definition 6, for any $\boldsymbol{p}'$ that is more correlated than $\boldsymbol{p}$, $\pi(S;\boldsymbol{p}')\leq\pi(S;\boldsymbol{p}),\forall S\subseteq N: s\geq 2$, and $\pi(S;\boldsymbol{p}')=\pi(S;\boldsymbol{p}),\forall S\subseteq N: s=1$, and $T_D^*(\pi(S))$ is increasing in $\pi(S)\in[0,\underline{p}]$ (Property 2), that is, as $\boldsymbol{p}$ becomes more correlated, for each given λ, the LHS of (58) remains the same, while the RHS is non-increasing. Therefore, the range of λ values for which the condition in (58) is satisfied either remains the same or shrinks. Then due to the $D^{(n)}$-optimality region delineated in Theorem 4, $\overline{\lambda}^{(n-1)}$ must be non-decreasing as $\boldsymbol{p}$ gets more correlated. □

Proof of Theorem 5.

Part 1. We first prove the result for the Dorfman design class.

(a) Independent diseases case: Consider that the prevalences of the diseases in set N are mutually independent. Consider any assay $S \subseteq N$, and swap any two diseases $i \in S,\ j \in N \backslash S$. The difference between the prevalences of the new assay $S\backslash\{i\} \cup \{j\}$, and the original assay S, can be expressed as follows:

$$\pi(S\backslash\{i\} \cup \{j\}) - \pi(S) = \frac{(\pi_j - \pi_i)[1 - \pi(S)]}{1 - \pi_i} = (\pi_j - \pi_i) \prod_{r \in S\backslash\{i\}} (1 - \pi_r). \tag{59}$$

Consider any unordered partition $\boldsymbol{S} = (S^1, S^2)$, where $S^1 = \{i_1, \cdots, i_{s^1}\}$ and $S^2 = \{j_1, \cdots, j_{s^2}\}$, with cardinality vector $\boldsymbol{s} = (s^1, s^2)$, where the diseases in each set $S^k, k = 1, 2$, are arranged following a non-increasing order of disease prevalences, that is, $\pi_{i_1} \geq \pi_{i_2} \geq \cdots \geq \pi_{i_{s^1}}$ and $\pi_{j_1} \geq \pi_{j_2} \geq \cdots \geq \pi_{j_{s^2}}$. Because $\mathbf{S}$ is not an ordered partition, we must have that, either $\pi_{i_1} > \pi_{j_1} > \pi_{i_{s^1}}$, or $\pi_{j_1} > \pi_{i_1} > \pi_{j_{s^2}}$, and in both cases, it follows that:

$$\pi_{i_1} > \pi_{j_{s^2}} \text{ and } \pi_{j_1} > \pi_{i_{s^1}}. \tag{60}$$

For each disease $r \in N$, define two dummy diseases, $r^{(\epsilon)}$ and $r^{(-\epsilon)}$, with respective prevalences, $\pi_{r^{(\epsilon)}} = \pi_r + \epsilon$ and $\pi_{r^{(-\epsilon)}} = \pi_r - \epsilon$, for any $\epsilon > 0$ such that $\pi_{r^{(\epsilon)}}, \pi_{r^{(-\epsilon)}} \in [0, 1]$. Then, from Eq. (59), we have that:

$$\pi(S^1\backslash\{i_{s^1}\} \cup \{i_{s^1}{}^{(\epsilon)}\}) - \pi(S^1) = \epsilon \prod_{r \in S^1\backslash\{i_{s^1}\}} (1 - \pi_r) \ \leq \ \epsilon \prod_{r \in S^1\backslash\{i_1\}} (1 - \pi_r) = \pi(S^1) - \pi(S^1\backslash\{i_1\} \cup \{i_1{}^{(-\epsilon)}\}), \tag{61}$$

and a similar inequality can be derived for set S^2.

In the following, we show that swapping diseases between sets S^1 and S^2, as many times as needed so that set S^1 ends up containing either the s^1 highest prevalence diseases, or the s^1 lowest prevalence diseases in set N (depending on the cost structure), and hence S^2 ends up containing the remaining diseases, either reduces, or does not change, the total cost. Thus we conclude that there exists an optimal partition that is ordered. There are two possible cases:

(i) Case where Condition **(C1)** holds, where

Condition **(C1)**: $\tilde{c}(s^1) \times [T_D^*(S^1\backslash\{i_{s^1}\} \cup \{i_{s^1}{}^{(\epsilon)}\}) - T_D^*(S^1)] \geq \tilde{c}(s^2) \times [T_D^*(S^2) - T_D^*(S^2\backslash\{j_1\} \cup \{j_1{}^{(-\epsilon)}\})]$.

Then, by Eq. (61), because $T_D^*(S)$ is concave increasing in any $\pi_r, r \in S$ (Property A.2), we have that:

$$T_D^*(S^1\backslash\{i_{s^1}\} \cup \{i_{s^1}{}^{(\epsilon)}\}) - T_D^*(S^1) \leq T_D^*(S^1) - T_D^*(S^1\backslash\{i_1\} \cup \{i_1{}^{(-\epsilon)}\}). \tag{62}$$

Similarly,

$$T_D^*(S^2\backslash\{j_{s^2}\} \cup \{j_{s^2}{}^{(\epsilon)}\}) - T_D^*(S^2) \leq T_D^*(S^2) - T_D^*(S^2\backslash\{j_1\} \cup \{j_1{}^{(-\epsilon)}\}). \tag{63}$$

Then, Condition **(C1)** and Eqs. (62)-(63) lead to:

$$\begin{aligned}
\tilde{c}(s^1) \times [T_D^*(S^1) - T_D^*(S^1\backslash\{i_1\} \cup \{i_1{}^{(-\epsilon)}\})] \geq & \tilde{c}(s^1) \times [T_D^*(S^1\backslash\{i_{s^1}\} \cup \{i_{s^1}{}^{(\epsilon)}\}) - T_D^*(S^1)] \\
\geq & \tilde{c}(s^2) \times [T_D^*(S^2) - T_D^*(S^2\backslash\{j_1\} \cup \{j_1{}^{(-\epsilon)}\})] \\
\geq & \tilde{c}(s^2) \times [T_D^*(S^2\backslash\{j_{s^2}\} \cup \{j_{s^2}{}^{(\epsilon)}\}) - T_D^*(S^2)] \\
\Leftrightarrow \tilde{c}(s^1) \times T_D^*(S^1) + \tilde{c}(s^2) \times T_D^*(S^2) \geq & \tilde{c}(s^1) \times T_D^*(S^1\backslash\{i_1\} \cup \{i_1{}^{(-\epsilon)}\}) + \tilde{c}(s^2) \times T_D^*(S^2\backslash\{j_{s^2}\} \cup \{j_{s^2}{}^{(\epsilon)}\}),
\end{aligned}$$

and letting $\epsilon = \pi_{i_1} - \pi_{j_{s^2}} (> 0)$ yields a partition $\boldsymbol{S'} = (S^{1'}, S^{2'})$, where $S^{1'} = S^1\backslash\{i_1\} \cup \{j_{s^2}\}$ and $S^{2'} = S^2\backslash\{j_{s^2}\} \cup \{i_1\}$, and $TC(\boldsymbol{S'}, \boldsymbol{t}^*(\boldsymbol{S'})) \leq TC(\boldsymbol{S}, \boldsymbol{t}^*(\boldsymbol{S}))$.
Observe that by Eqs. (59)-(60), we have that:

$$\pi(S^{1'}) - \pi(S^1) = \pi(S^1\backslash\{i_1\} \cup \{j_{s^2}\}) - \pi(S^1) = (\pi_{j_{s^2}} - \pi_{i_1}) \frac{[1 - \pi(S^1)]}{1 - \pi_{i_1}} < 0 \quad \Leftrightarrow \quad \pi(S^{1'}) < \pi(S^1), \text{ and} \tag{64}$$

$$\pi(S^{2'}) - \pi(S^2) = \pi(S^2\backslash\{j_{s^2}\} \cup \{i_1\}) - \pi(S^2) = (\pi_{i_1} - \pi_{j_{s^2}}) \frac{[1 - \pi(S^2)]}{1 - \pi_{j_{s^2}}} > 0 \quad \Leftrightarrow \quad \pi(S^{2'}) > \pi(S^2). \tag{65}$$

Then, it is sufficient to show that if the new $\boldsymbol{S'} = (S^{1'}, S^{2'})$ is not an ordered partition, then Condition **(C1)** is still satisfied, and hence, starting with the new unordered partition $\boldsymbol{S'}$, one can swap the highest prevalence disease in set $S^{1'}$ with the lowest prevalence disease in set $S^{2'}$, in order to either reduce or keep the same total cost. Then one can repeat this argument to swap as many times as needed so that the revised set S^1 contains the s^1 lowest prevalence diseases, hence the revised set S^2 contains the s^2 highest prevalence diseases, resulting in an ordered

partition that is optimal.
To this end, we wish to show that:

$$\tilde{c}(s^1) \times [T_D^*(S^{1'} \backslash \{i_{s^1}\} \cup \{i_{s^1}{}^{(\epsilon)}\}) - T_D^*(S^{1'})] \geq \tilde{c}(s^2) \times [T_D^*(S^{2'}) - T_D^*(S^{2'} \backslash \{j_1\} \cup \{j_1{}^{(-\epsilon)}\})],$$

that is, Condition **(C1)** continues to be satisfied by the new partition $\boldsymbol{S'} = (S^{1'}, S^{2'})$.
By Eqs. (59), (64), and (65), we have that:

$$\pi(S^1 \backslash \{i_{s^1}\} \cup \{i_{s^1}{}^{(\epsilon)}\}) = \frac{\epsilon[1-\pi(S^1)]}{1-\pi_{i_{s^1}}} \quad < \quad \frac{\epsilon[1-\pi(S^{1'})]}{1-\pi_{i_{s^1}}} = \pi(S^{1'} \backslash \{i_{s^1}\} \cup \{i_{s^1}{}^{(\epsilon)}\}), \text{ and} \tag{66}$$

$$\pi(S^2) - \pi(S^2 \backslash \{j_1\} \cup \{j_1{}^{(-\epsilon)}\}) = \frac{\epsilon[1-\pi(S^2)]}{1-\pi_{j_1}} \quad > \quad \frac{\epsilon[1-\pi(S^{2'})]}{1-\pi_{j_1}} = \pi(S^{2'} - \pi(S^{2'} \backslash \{j_1\} \cup \{j_1{}^{(-\epsilon)}\}). \tag{67}$$

By Eqs. (66)-(67), and because $T_D^*(S)$ is concave increasing in any $\pi_r, r \in S$ (Property A.2), we can write:

$$T_D^*(S^{1'} \backslash \{i_{s^1}\} \cup \{i_{s^1}{}^{(\epsilon)}\}) - T_D^*(S^{1'}) \geq T_D^*(S^1 \backslash \{i_{s^1}\} \cup \{i_{s^1}{}^{(\epsilon)}\}) - T_D^*(S^1), \text{ and} \tag{68}$$

$$T_D^*(S^2) - T_D^*(S^2 \backslash \{j_1\} \cup \{j_1{}^{(-\epsilon)}\}) \geq T_D^*(S^{2'}) - T_D^*(S^{2'} \backslash \{j_1\} \cup \{j_1{}^{(-\epsilon)}\}), \tag{69}$$

and we have that:

$$\begin{aligned}
\tilde{c}(s^1) \times [T_D^*(S^{1'} \backslash \{i_{s^1}\} \cup \{i_{s^1}{}^{(\epsilon)}\}) - T_D^*(S^{1'})] \geq & \tilde{c}(s^1) \times [T_D^*(S^1 \backslash \{i_{s^1}\} \cup \{i_{s^1}{}^{(\epsilon)}\}) - T_D^*(S^1)] \\
\geq & \tilde{c}(s^2) \times [T_D^*(S^2) - T_D^*(S^2 \backslash \{j_1\} \cup \{j_1{}^{(-\epsilon)}\})] \\
\geq & \tilde{c}(s^2) \times [T_D^*(S^{2'}) - T_D^*(S^{2'} \backslash \{j_1\} \cup \{j_1{}^{(-\epsilon)}\})],
\end{aligned}$$

where the first and third inequalities follow by Eqs. (68)-(69), and the second inequality follows by Condition **(C1)**. That is, Condition **(C1)** continues to hold for partition $\boldsymbol{S'} = (S^{1'}, S^{2'})$.

Hence, if $\boldsymbol{S'}$ is an ordered partition, then we have attained an ordered partition $\boldsymbol{S'}$ for which $TC(\boldsymbol{S'}, \boldsymbol{t^*}(\boldsymbol{S'})) \leq TC(\boldsymbol{S}, \boldsymbol{t^*}(\boldsymbol{S}))$; and if $\boldsymbol{S'}$ is not an ordered partition, then we can repeat the same process by swapping the highest prevalence disease in set $S^{1'}$ with the lowest prevalence in set $S^{2'}$, thus either reducing or keeping the same total cost until an ordered partition in which the revised set S^1 contains the s^1 lowest prevalence diseases and the revised set S^2 contains the s^2 highest prevalence diseases is attained, establishing the desired result.

(ii) Case where Condition **(C1)** does not hold, that is,

$$\tilde{c}(s^1) \times [T_D^*(S^1 \backslash \{i_{s^1}\} \cup \{i_{s^1}{}^{(\epsilon)}\}) - T_D^*(S^1)] < \tilde{c}(s^2) \times [T_D^*(S^2) - T_D^*(S^2 \backslash \{j_1\} \cup \{j_1{}^{(-\epsilon)}\})]$$

The proof of this case follows similarly to the proof of Case 1, by repeatedly swapping the lowest prevalence disease in set S^1 with the highest prevalence disease in set S^2 (i.e., starting with swapping $i_{s^1} \in S^1$ with $j_1 \in S^2$) until an ordered partition in which the revised set S^1 contains the s^1 highest prevalence diseases and the revised set S^2 contains the s^2 lowest prevalence diseases is attained, and it can be shown that this ordered partition incurs a total cost that is less than or equal to the cost of the original partition.

(b) <u>No co-infections case:</u> Consider that the prevalences of the diseases in set N are mutually exclusive. Then, $\pi(S) = \sum_{i \in S} \pi_i, \forall S \subseteq N$ (Eq. (4)). Consider any $D^{(q)}$ design, $q = 2, \cdots, n$, with partition $\boldsymbol{S} = (S^k)_{k=1,\cdots,q}$, and a fixed cardinality vector $\boldsymbol{s} = (s^k)_{k=1,\cdots,q}$. Because the size of each assay, $s^k, k = 1, \cdots, q$, is fixed for all possible partitions, $\tilde{c}(s^k)$ becomes a constant, hence $\tilde{c}(s^k) \times T_D^*(S^k)$ is concave increasing in $\pi(S^k : |S^k| = s^k), k = 1, \cdots, q$ (Property 2), that is, considering all sets S^k with cardinality $|S^k| = s^k$. Hence, the total cost, $TC_{D^{(q)}}(\boldsymbol{S} : |\boldsymbol{S}| = \boldsymbol{s})$, is minimized by an ordered q-partition [3, 21].

<u>*Part 2.*</u> We next prove the result for the mixed-testing design class. Consider any $M^{(q)}$ design, $q = 2, \cdots, n$, and let N^I and N^D respectively denote the set of diseases that are tested (in any number of assays) individually, and via pooling, with respective cardinalities, $n^I, n^D \in Z^+ : n^I + n^D = n$. Then, $N^I \cup N^D = N$ and $N^I \cap N^D = \emptyset$. By Theorem 4, $M^{(q)}$ contains one assay, comprised of all diseases in set N^I, that is individually tested, and $q-1$ assays (i.e., subsets of set N^D) that are pooled.

Next, we turn our attention to those diseases that are tested via pooling, i.e., set N^D, and study the optimal partition of set N^D, which, by definition of $M^{(q)}$, needs to be a $q-1$-partition, with each assay using pooling. Let $\boldsymbol{S}(N^D) = (S^k(N^D))_{k=1,\cdots,q-1}$ denote any $q-1$-partition of set N^D. Then, by Eq. (19), we have that

$$TC(\boldsymbol{S}(N^D), \boldsymbol{t}_D^*(\boldsymbol{S}(N^D))) = \sum_{k=1}^{q-1} \tilde{c}(s^k(N^D)) \times T_D^*(S^k(N^D)) = \sum_{k=1}^{q-1} \tilde{c}(s^k(N^D)) \times \left[\frac{1}{t_D^*(S^k(N^D))} + 1 - \left(1 - \pi(S^k(N^D))\right)^{t_D^*(S^k(N^D))} \right].$$

First, we show that there exists an optimal $M^{(q)}$ design in which set N^I contains the n^I highest prevalence diseases in set N. Assume, to the contrary, that this is not the case. Then, $\exists i_1 \in N^I, i_2 \in N^D : \pi_{i_1} < \pi_{i_2}$. Assume, without loss of generality, that $i_2 \in S^{k'}(N^D) \subseteq N^D$, for some $k' = 1, \cdots, q-1$. Then, swapping diseases i_1 and i_2 will not affect the total cost of individual testing, because $TC(N^I, t=1) = TC(N^I \cup \{i_2\} \setminus \{i_1\}, 1) = \tilde{c}(n^I)$, but it will alter the total cost of pooled testing by $TC(\boldsymbol{S}(N^D \cup \{i_1\} \setminus \{i_2\})) - TC(\boldsymbol{S}(N^D)) = \tilde{c}(s^{k'}(N^D)) \times T_D^*(S^{k'}(N^D) \cup \{i_1\} \setminus \{i_2\})) - \tilde{c}(s^{k'}(N^D)) \times T_D^*(S^{k'}(N^D)) < 0$, where the inequality follows because $T_D^*(S)$ is strictly increasing in $\pi(S)$ (Property 2); and for both the independent diseases and no co-infections cases, $\pi(S)$ is linear increasing in π_i, $\forall i \in S$ (Eqs. (15)-(16)), hence, $\pi(S^{k'}(N^D)) > \pi(S^{k'}(N^D) \cup \{i_1\} \setminus \{i_2\})$, that is, we have identified a q-partitioned mixed-testing design with a lower total cost. Thus, there exists an optimal mixed-testing design in which set N^I contains $\{1, \cdots, n^I\}$. The second part of the result, that the diseases in set N^D are tested via pooling following an ordered $q-1$-partition, follows directly from part 1 of this theorem, completing the proof. □

Proof of Corollary 1.

Part 1. The reduction, of the problem of finding an optimal partition of set N, to a Shortest Path Problem follows from Theorem 5, which states the existence of an optimal design that uses an ordered partition under the assumptions stated in this corollary, in light of Lemma 1 in [21].

Part 2. The construction of graph $G(V(N), E(N))$ requires the computation of all edge weights, $w_{i,j} = \tilde{c}(s, \lambda) \times T^*(S)$, where $S = \{i, i+1, \cdots, j-1\}$, $\forall i, j \in V(N) : i < j$. Hence, $n+1-i$ computations are needed for each $w_{i,j}, i < j \leq n+1$, $i \in N$, for a total of $\sum_{i=1}^{n}(n+1-i) = \frac{1}{2}n(n+1)$ computations, leading to polynomial complexity in the order of $O(n^2)$. Solving the Shortest Path Problem by a topological sorting algorithm also has polynomial complexity, $O(n^2)$ [26], establishing the desired result. □

B Case Study: Details and Supporting Results

Assay cost function: Based on [76], which reports the per test cost for 2-plex and 20-plex PCR respiratory assays as \$42 and \$114.8, respectively, we explore various concave cost functions that satisfy, $21 \leq c(1) \leq 42$ and $c(20) = 114.8$. We consider a functional form that has a fixed cost per assay, and a variable cost per disease bundled. For the two extreme values for $c(1)$ (along with the given value of $c(20)$), at $c(1) = 21$, $c(s) = 16.06 + 4.94 \times s$; and at $c(1) = 42$, $c(s) = 38.17 + 3.83 \times s$. In §6, we provide the results for the $c(s) = 25.54 + 4.46 \times s$ function, yielding $c(1) = 30$; sensitivity analysis on cost parameters indicate similar qualitative findings.

CI for R-TD: For each year in the study period, we use the 52 weekly prevalence data for each disease to construct a 95% CI for each $\Pi_i, i \in N$, based on the Wald's method, e.g., [65], which utilizes the normal distribution approximation invoked by the Central Limit Theorem: $\hat{\pi}_i \pm \frac{z \times \hat{\sigma}_i}{\sqrt{52}}$, where $\hat{\pi}_i$ and $\hat{\sigma}_i$ respectively represent the average and standard deviation for the 52 weeks, and z is the corresponding standard normal CDF.

Price of robustness ratio (PoR) (%): $\frac{[TC^{\mathbf{R\text{-}TD}^*}(\lambda) - TC^{\mathbf{TD}^*}(\lambda)]}{TC^{\mathbf{TD}^*}(\lambda)} \times 100$.

Table B.1: PoR for 2018 and 2021 perfect-information **R-TD** designs, based on 2018 and 2021 data, resp.

λ range	0.00-0.55	0.60	0.65	0.70	0.75	0.80	0.85	0.90	0.95	1.00
2018-PoR (%)	0.000	0.232	0.020	0.022	0.024	0.026	0.037	1.600	2.395	1.203
2021-PoR (%)	0.000	0.000	0.000	-2.392	0.000	0.030	0.000	0.000	0.000	0.000

Table B.2: VoJ for 2018 **TD** designs (with and without seasonality) based on 2018 data - without COVID-19 testing

λ range	0-0.15	0.20-0.40	0.45	0.50	0.55	0.60	0.65	0.70	0.75	0.80	0.85	0.90	0.95	1.00
$VoJ(\lambda)$ (%) - Without seasonality	0.0	0.0	0.4	1.0	1.6	2.4	3.9	5.5	7.0	8.5	10.2	13.4	16.7	20.5
$VoJ(\lambda)$ (%) - With seasonality	5.3	5.2	5.4	6.2	7.2	8.3	9.7	11.3	13.0	14.6	16.7	19.4	22.2	25.2

Table B.3: The metrics for 2018 **TD** and **R-TD** designs based on 2019-2021 data - without COVID-19 testing

Model ($n = 17$)	Range of λ Values	Testing Cost Mean (Min-Max)	Number of Tests Mean (Min-Max)
TD	0.00-0.40	1.00 (1.00-1.00)	1.00 (1.00-1.00)
	0.45-0.55	0.93 (0.93-0.93)	1.05 (1.05-1.06)
	0.60-0.80	0.88 (0.83-1.07)	1.21 (1.11-1.62)
	0.85	0.86 (0.82-1.03)	1.25 (1.17-1.57)
	0.90	0.81 (0.74-0.94)	1.39 (1.26-1.63)
	0.95-1.00	0.79 (0.69-0.97)	1.56 (1.34-1.93)
R-TD	0.00-0.40	1.00 (1.00-1.00)	1.00 (1.00-1.00)
	0.45-0.55	0.93 (0.93-0.93)	1.05 (1.05-1.06)
	0.60-0.80	0.88 (0.83-1.06)	1.21 (1.11-1.59)
	0.85	0.86 (0.82-1.02)	1.25 (1.17-1.55)
	0.90	0.84 (0.79-0.98)	1.32 (1.22-1.63)
	0.95-1.00	0.82 (0.72-0.99)	1.54 (1.34-1.90)

Table B.4: The metrics for modified 2018 **TD** and **R-TD** designs based on 2021 data

	Modified 2018 design			2021 perfect-information design		
Model ($n = 17$)	Range of λ Values	Testing Cost Mean (Min-Max)	Number of Tests Mean (Min-Max)	Range of λ Values	Testing Cost Mean (Min-Max)	Number of Tests Mean (Min-Max)
Without COVID-19 Testing						
TD	0.00-0.40	0.76 (0.42-0.94)	0.76 (0.42-0.94)	0.00-0.35	0.76 (0.42-0.94)	0.76 (0.42-0.94)
	0.45-0.60	0.68 (0.37-1.03)	0.91 (0.49-1.60)	0.40-0.75	0.62 (0.36-0.77)	0.83 (0.49-1.02)
	0.65-0.85	0.63 (0.35-0.91)	0.94 (0.54-1.42)	0.80	0.60 (0.35-0.75)	0.90 (0.53-1.12)
	0.90-0.95	0.60 (0.36-0.93)	1.16 (0.69-1.89)	0.85-0.90	0.56 (0.34-0.75)	1.10 (0.67-1.47)
	1.00	0.60 (0.36-0.94)	1.35 (0.81-2.13)	0.95-1.00	0.56 (0.34-0.74)	1.12 (0.69-1.47)
R-TD	0.00-0.35	0.76 (0.42-0.94)	0.76 (0.42-0.94)	0.00-0.30	0.76 (0.42-0.94)	0.76 (0.42-0.94)
	0.40-0.55	0.68 (0.37-1.02)	0.90 (0.49-1.57)	0.35-0.70	0.62 (0.36-0.77)	0.83 (0.49-1.02)
	0.60-0.80	0.63 (0.36-0.90)	0.94 (0.54-1.40)	0.75	0.60 (0.35-0.75)	0.90 (0.53-1.12)
	0.85	0.62 (0.37-0.87)	0.98 (0.58-1.38)	0.80	0.57 (0.34-0.78)	1.07 (0.65-1.49)
	0.90	0.60 (0.36-0.92)	1.16 (0.69-1.87)	0.85	0.56 (0.34-0.75)	1.10 (0.67-1.47)
	0.95	0.59 (0.36-0.86)	1.25 (0.76-1.75)	0.90-1.00	0.56 (0.34-0.74)	1.12 (0.69-1.47)
	1.00	0.61 (0.37-0.93)	1.38 (0.85-2.13)			
With COVID-19 Testing						
TD	0.00-0.35	0.86 (0.59-1.02)	0.86 (0.59-1.02)	0.00-0.30	0.86 (0.59-1.02)	0.86 (0.59-1.02)
	0.40-0.55	0.77 (0.51-1.11)	1.01 (0.65-1.70)	0.35-0.70	0.71 (0.49-0.84)	0.93 (0.66-1.10)
	0.60-0.80	0.70 (0.48-0.98)	1.05 (0.72-1.53)	0.75	0.68 (0.48-0.82)	1.00 (0.71-1.21)
	0.85	0.66 (0.47-0.98)	1.27 (0.88-2.01)	0.80	0.63 (0.45-0.81)	1.21 (0.87-1.57)
	0.90	0.66 (0.46-0.97)	1.36 (0.93-2.02)	0.85-1.00	0.62 (0.45-0.80)	1.23 (0.89-1.57)
	0.95	0.65 (0.46-0.92)	1.36 (0.97-1.89)			
	1.00	0.66 (0.46-0.99)	1.46 (1.01-2.25)			
R-TD	0.00-0.35	1.00 (1.00-1.00)	1.00 (1.00-1.00)	0.00-0.30	0.86 (0.59-1.02)	0.86 (0.59-1.02)
	0.40-0.55	0.90 (0.86-1.12)	1.16 (1.06-1.70)	0.35-0.65	0.71 (0.49-0.84)	0.93 (0.66-1.10)
	0.60-0.85	0.81 (0.77-0.99)	1.20 (1.13-1.54)	0.70-0.75	0.68 (0.48-0.82)	1.00 (0.71-1.21)
	0.90	0.81 (0.76-1.04)	1.36 (1.24-1.93)	0.80-1.00	0.62 (0.45-0.80)	1.23 (0.89-1.57)
	0.95	0.65 (0.46-0.91)	1.36 (0.97-1.87)			
	1.00	0.66 (0.46-0.98)	1.49 (1.05-2.25)			